Dissertation

VTT PUBLICATIONS 730

Sami Koskinen

Sensor Data Fusion Based Estimation of Tyre-Road Friction to Enhance Collision Avoidance

VTT PUBLICATIONS 730

Sensor Data Fusion Based Estimation of Tyre–Road Friction to Enhance Collision Avoidance

Sami Koskinen

A dissertation for the degree of Doctor of Science in Technology is to be presented by permission of the Faculty of Automation, Mechanical and Materials Engineering, the Tampere University of Technology, for public examination and debate in lecture hall K1702 in Konetalo (Korkeakoulunkatu 6) on Friday, 12 March 2010, at 12 noon.

ISBN 978-951-38-7382-0 (soft back ed.)
ISSN 1235-0621 (soft back ed.)

ISBN 978-951-38-7383-7 (URL: http://www.vtt.fi/publications/index.jsp)
ISSN 1455-0849 (URL: http://www.vtt.fi/publications/index.jsp)

JULKAISIJA – UTGIVARE – PUBLISHER

VTT, Vuorimiehentie 5, PL 1000, 02044 VTT
puh. vaihde 020 722 111, faksi 020 722 4374

VTT, Bergsmansvägen 5, PB 1000, 02044 VTT
tel. växel 020 722 111, fax 020 722 4374

VTT Technical Research Centre of Finland, Vuorimiehentie 5, P. O. Box 1000, FI-02044 VTT, Finland
phone internat. +358 20 722 111, fax +358 20 722 4374

Textual editing Mark Phillips
Technical editing Mirjami Pullinen

Edita Prima Oy, Helsinki 2010

Sami Koskinen. Sensor Data Fusion Based Estimation of Tyre–Road Friction to Enhance Collision Avoidance [Anturidatafuusioon perustuva renkaan ja tien välisen kitkan estimointi ja tulosten hyödyntäminen törmäyksenestossa]. Espoo 2010. VTT Publications 730. 188 p. + app. 12 p.

Keywords friction, sensor, data fusion, collision avoidance, collision mitigation, environmental sensing, tyre, road, conditions, trajectory, curvature-velocity, ADAS

Abstract

Vehicle steering, braking and acceleration are subject to friction forces arising from contact of the tyres with the road surface. The contact force is both enabling and limiting. The ratio of the contact friction to the force of the tyres pressing on the road surface is described as the coefficient of friction. The maximum coefficient of friction for different surfaces characterizes the extent of tyre grip.

Collision avoidance and collision mitigation systems require information on tyre grip so as to accurately calculate braking distances and evasive manoeuvres. Estimating road slipperiness (skid resistance) during driving has however proven difficult.

This dissertation discusses estimating the maximum coefficient of friction (herein referred to as the friction potential) together with determining road conditions. Both estimations are based on multi-sensor data fusion; that is, combining data from several sensors. The presented sensor data fusion utilizes various sensors from three main classes: 1) environmental sensors, 2) sensors measuring vehicle dynamics and 3) experimental tyre sensors. This work concentrates particularly on methods for combining measurements of vehicle dynamics with environmental sensor readings; for example, wheel speed signals are linked to readings about ice, snow or water on the road.

The methods were incorporated into a prototype passenger car implementation, where testing yielded a reliable estimate of friction potential for approximately 90% of driving time. The estimate of friction potential was then within 0.2 of reference values measured in braking tests. These results encapsulate a proof of concept on asphalt roads in some wet, snowy, icy and dry road conditions.

The advantages of friction estimation for collision avoidance and collision mitigation systems are analysed using mainly simulations. A correct initial estimate of the friction potential enables the systems to improve traffic safety efficiently also in slippery road conditions. However, the range of available environmental sensors does not cover long braking distances.

Together with the simulations, the work introduces a new method for collision avoidance calculations and timing the activation of collision mitigation. The method is based on a large number of pre-calculated vehicle trajectories.

Sami Koskinen. Sensor Data Fusion Based Estimation of Tyre–Road Friction to Enhance Collision Avoidance [Anturidatafuusioon perustuva renkaan ja tien välisen kitkan estimointi ja tulosten hyödyntäminen törmäyksenestossa]. Espoo 2010. VTT Publications 730. 188 s. + liitt. 12 s.

Keywords friction, sensor, data fusion, collision avoidance, collision mitigation, environmental sensing, tyre, road, conditions, trajectory, curvature-velocity, ADAS

Tiivistelmä

Renkaiden ja tien välinen liikettä vastustava voima, kitka, asettaa rajat ajoneuvon ohjaukselle, jarrutukselle ja kiihdytykselle. Se on samalla sekä mahdollistava että rajoittava kontaktivoima. Kitkan ja renkaita tietä vasten puristavan voiman suhde ilmaistaan kitkakertoimella. Kitkakertoimen maksimiarvo eri pinnoilla kuvaa renkaiden pitävyyttä.

Kehitteillä oleviin törmäyksiä estäviin ja törmäysenergiaa lieventäviin kuljettajan tukijärjestelmiin tarvitaan tietoa renkaiden pitävyydestä, jotta jarrutusmatkoja ja väistömahdollisuuksia voidaan arvioida entistä tarkemmin. Tien liukkauden määrittäminen ennalta ajon aikana, ilman renkaiden selkeää luistoa, on kuitenkin osoittautunut hankalaksi.

Tämä väitöstyö käsittelee kitkakertoimen maksimiarvon, tässä kitkapotentiaalin, ja kelitietojen määrittämistä. Tutkimuksessa hyödynnetään anturidatafuusiota eli useiden antureiden tuottamien tietojen yhdistämistä. Anturidatafuusiossa käytetyt anturit edustavat kolmea päätyyppiä: 1) ympäristöä havainnoivat anturit, 2) auton liiketilaa mittaavat anturit ja 3) rengasantureiden prototyypit. Työssä keskitytään erityisesti menetelmiin, joilla voidaan yhdistää ajoneuvon liiketilan mittaustietoja ympäristöä havainnoivien antureiden tuottamiin tietoihin. Esimerkiksi renkaiden pyörimisnopeuksista saatuja tietoja yhdistetään tietoihin tiellä olevasta jäästä, lumesta tai vedestä.

Esitellyillä menetelmillä ja henkilöautoon toteutetulla prototyyppijärjestelmällä on testeissä kyetty arvioimaan kitkapotentiaalia luotettavasti noin 90 prosenttia ajoajasta. Tällöin kitkapotentiaalin arvio poikkeaa enintään 0,2 jarrutustesteillä mitatuista referenssiarvoista. Järjestelmää on testattu asfalttiteillä. Menetelmien toimivuus on todennettu joukolla märkiä, lumisia, jäisiä ja kuivia kelejä.

Kitka-arvion hyötyjä on analysoitu törmäyksiä estävissä ja törmäysenergiaa lieventävissä järjestelmissä pääasiassa simulaatiotuloksia käyttäen. Arvio kitka-

potentiaalista auttaa näitä järjestelmiä parantamaan liikenneturvallisuutta tehokkaasti myös liukkailla keleillä. Kuitenkaan saatavilla olevien keliantureiden mittauskantama ei vielä kata pitkiä jarrutusmatkoja.

Tämä työ esittelee simulaatioiden yhteydessä uuden, lukuisiin ennalta lasketuihin liikeratoihin perustuvan nopean laskentamenetelmän törmäystilanteiden arviointiin ja esteiden väistöön.

Preface

The research for this thesis was mainly carried out in the FRICTI@N EU project, funded by the European Commission as part of the 6th Framework Programme. The project concentrated on measuring and estimating tyre–road friction with several vehicle-mounted sensors. I am grateful to the whole consortium (10 partners) for their co-operation and insight into the friction phenomenon and all the different ways to detect it.

The project was initiated by Dr Tapani Mäkinen (VTT), who saw the need for a dedicated project aimed at providing more information that would be useful for vehicle safety systems. He has also guided us young scientists at VTT into the networks of automotive research in the EU. Thank you for the opportunity!

The author's main responsibility in the FRICTI@N project was the high-level sensor data fusion architecture and implementation. Several people have helped to improve the initial designs and I want to express my total gratitude especially to the project co-ordinator Pertti Peussa (VTT), Dr Liang Nanying, who was visiting VTT from Singapore Technological University at the time, Thomas Haas from VDO Automotive AG, who pushed forward especially the vehicle dynamics based algorithms, and Dr Matti Kutila (VTT) for discussions on environmental sensing.

This research would not have been possible without Christian Hartweg and Thomas Hüsemann from RWTH Aachen University, who integrated the project components into the development vehicle and among other things, provided driving data and validation results.

In my earlier studies on collision avoidance, it was Ari Virtanen (VTT) who first introduced me to the topic during my diploma thesis on a robotic wheelchair in 1999–2000. Recently I have had the possibility to develop our algorithms further to cover moving objects, vehicle dynamics and friction information in more detail. In addition to Ari, I wish to thank Michael Köhler and Dr Kay Fürstenberg

from Ibeo Automobile Sensor GmbH for clarifying the automotive requirements and for pushing me in a new direction with the algorithm development.

I want to express my gratitude to the supervisor of this thesis on the university side, Professor Kalevi Huhtala from the Tampere University of Technology, for his good comments on publishing the results and improving the analysis.

The final editing has been very educational. I am grateful to the pre-reviewers Professor Matti Juhala (Helsinki University of Technology) and Professor András Várhelyi (Lund University) for their constructive criticisms and invaluable advice. My gratitude goes to Professor Juhala and Dr Kay Fürstenberg also for agreeing to act as opponents for my dissertation.

Finally, I express my love and gratitude to my family, who also motivate me to drive safely.

Tampere, January 2010

Contents

Abbreviations

4WD	Four-Wheel Drive
ABS	Anti-lock Braking System
AEB	Automatic Emergency Braking
ACC	Adaptive Cruise Control
ADAS	Advanced Driver Assistance Systems
CA	Collision Avoidance
CAN	Controller Area Network
CMbB	Collision Mitigation by Braking
CMS	Collision Mitigation (Brake) System
CPU	Central Processing Unit
CRF	Centro Ricerche Fiat S.C.p.A.
CVM	Curvature-Velocity Method
DARPA	Defense Advanced Research Projects Agency
DB	Database
EFF	Environmental Feature Fusion
EPAS	Electric Power Assisted Steering
ESC	Electronic Stability Control
EU	European Union
FCD	Floating Car Data

FEA	Finite Element Analysis
GPS	Global Positioning System
HMI	Human-Machine Interface
HPAS	Hydraulic Power Assisted Steering
IKA	Institut für Kraftfahrzeuge Aachen, RWTH Aachen University
IMU	Inertial Measurement Unit
IP	Integrated Project
IR	Infrared
ISM	Industrial, Scientific and Medical
LED	Light Emitting Diode
NIR	Near Infrared
PSD	Position Sensitive Detector
ROI	Region of Interest
RPU	Rapid Prototyping Unit
SAW	Surface Acoustic Wave
TCS	Traction Control System
TFF	Tyre Feature Fusion
T-CVM	Target Curvature-Velocity Method
TTC	Time To Collision
V2I	Vehicle-to-Infrastructure
V2V	Vehicle-to-Vehicle
VDO	VDO Automotive AG, Continental Corporation
VFF	Vehicle Feature Fusion
VTT	VTT Technical Research Centre of Finland

List of symbols

a	Acceleration
C_d	Drag coefficient
F	Force, e.g. F_y for lateral force and F_d for air resistance (drag)
g	Acceleration due to gravity
I	Intensity
K_{us}	Understeer coefficient
L	Wheelbase
m	Mass
M_z	Self-aligning torque
r	Radius
s	Distance
t	Time
v	Speed, e.g. v_0 for initial speed. Also used for velocity, when the value includes a direction.
α	Angle
δ_f	Steer angle of front tyre
λ	Slip
μ	Coefficient of friction
ω	Angular velocity

1. Introduction

1.1 Background

The European transport policy for 2010 sets new targets for road safety as well as for the introduction of active safety systems in new vehicles. One of the most ambitious and key goals is to halve the number of road fatalities [1]. Albeit that responsibility will fall mainly on the national authorities, the European Union can contribute through several actions, such as harmonising regulations and promoting technologies to improve road safety.

In 2005, VTT proposed a three-year EU project named FRICTI@N [2], that concentrated on measuring friction and road slipperiness using on-board sensors and data fusion. It was envisaged that information on friction and road conditions can be used to enhance the performance of several integrated and co-operative safety systems, such as automatic emergency braking and vehicle-to-vehicle communication around accident black spots. The project obtained funding from the 6th Framework Programme. It belonged to the Commission's Intelligent Car Initiative, which supports the development and deployment of systems helping drivers to prevent or avoid traffic accidents. The FRICTI@N project has provided the main framework for this thesis.

In a preceding EU project, APOLLO [3], which pioneered intelligent tyre systems, tyre deformation sensing was seen as a promising technology for detecting friction levels and aquaplaning. The FRICTI@N project utilized results and also tyre sensors from the APOLLO project, but concentrated purely on friction rather than on constructing intelligent tyres.

Friction is a force between tyres and a road that are in contact. The key variable to be measured or estimated during driving is the maximum coefficient of

friction between the tyres and the road surface. It characterizes the extent of tyre grip on a road. A detailed description is given in 1.2.

In a state of the art study that was carried out during preparations for the FRICTI@N project, it was seen that no available single sensor was able to continuously estimate the maximum coefficient of friction of a moving vehicle. Continuous estimation would be required by several active safety systems and moreover, they would need information from tens of meters ahead of the vehicle. Some environmental sensor types did show potential for estimating weather and road conditions. Based on the previous research it was also known that both tyre and vehicle sensors that measure forces and accelerations can be used to estimate the maximum friction coefficient during certain driving manoeuvres. It seemed likely that a fusion of this sensor data would be the most promising method for obtaining friction information to serve various applications.

1.1.1 Motivation

The tyre–road contact area is where all steering, acceleration and braking manoeuvres are put into action; contact forces between the vehicle and road surface interact at tyre–road contact patches of varying size and shape. The other forces acting continuously on the vehicle are gravity and aerodynamic forces.

Even if friction has an obvious role in vehicle control, drivers may sometimes forget the basic limits it sets. After all, on dry asphalt, maximum friction forces are seldom reached in normal driving.

In a Finnish empirical field study [4], travel speeds on snow-covered roads were only about 4 km/h lower than in good driving conditions. The speed reduction on icy roads was 3–7 km/h. This suggests that drivers do not adapt their driving behaviour sufficiently in changing conditions and view the speed limits as guidance, not restrictions.

In a recent study also from Finland, it was found that drivers had difficulties in estimating road slipperiness, shown by comparing their estimates with road weather station measurements [5]. There is even a Finnish anecdote that the first day of winter surprises drivers every year.

The lowering of winter-time speed limits has been used for several years in the Nordic countries, especially in Finland, and this has had a positive effect on traffic safety [6, 7]. It is young and inexperienced drivers as well as older drivers who have the highest risk of a fatal accident during winter-time [8]. When comparing winter-time and summer-time accidents, a considerably higher percentage

of fatal accidents occurs in winter as a result of overtaking (indicating loss of control), head-on collisions and accidents involving pedestrians. Truck drivers also experience difficulties in winter driving conditions more often than average [6]. The increased risks are similar in Finnish and Swedish data [7].

A look at London's recent accident statistics shows that drivers' misjudgement of appropriate driving speeds is a major factor in speed-related accidents. For example, they fail to realize that wet road conditions increase the likelihood of skidding, or misjudge the sharpness of a bend. For male drivers, speed-related accidents constitute 57% of all at-fault accidents, and of these, 16% were considered as misjudgements. For women, the percentage of speed-related accidents was smaller, at 31%, but of these, 64% were considered as misjudgements [9].

Currently vehicle systems do not especially support the driver in estimating road slipperiness. Electronic control systems like ABS and ESC participate in the vehicle control only when the maximum friction is exceeded. Future safety systems such as collision mitigation (the main method of mitigation is automated emergency braking right before a collision) and co-operative driving applications (applications based on vehicle radio communication) would benefit from a more continuous friction estimation system. Also some of the existing systems could be supported with advance information that is of sufficiently high quality. The information would enable, for example, ABS to start braking with the optimal brake pressure based on the current maximum coefficient of friction, meaning the early cycles of operation are more efficient.

Collision Mitigation Systems (CMS), which apply the brakes a moment before an accident to reduce speed, are less effective on snow if a high friction coefficient is assumed – braking will begin too late given the low friction. In early collision mitigation prototypes the maximum coefficient of friction has been a static value based on ordinary driving conditions, i.e. dry asphalt.

Slippery road conditions can also affect safety systems' calculations in cases where the vehicle is trying to join the traffic flow or drive through an intersection, or when generally estimating safety margins for driving.

Along with driver behaviour and alertness, which are not measured in current vehicles, the *maximum coefficient of friction remains one of the key unknowns* in the algorithms of future ADAS (Advanced Driver Assistance Systems) that calculate e.g. the risk of collision or safe speed.

1.2 Tyre–road friction

Tyre–road friction is a complex phenomenon and several models have been created to describe it. The variety of materials used in tyres, their deformations, the changing properties of the road and unknown foreign materials in the tyre–road contact patch make it difficult to derive friction values from the physical properties of the rubber and road surface. Also, the tyre–road interaction is usually modelled for hard surfaces (roads) and the models may not apply if the tyres sink deep.

The friction coefficient (μ) is defined, regardless of the acting surfaces, as the ratio of the normal (N) and tangential contact force (F) between two bodies:

$$\mu = \frac{F}{N} \tag{1}$$

A useful simplification of this equation can be derived when an object is moving on an even surface and only gravitation is acting as the normal force. The tangential force of Equation 1 can then be written as mass multiplied by acceleration, where the acceleration results from all tangential (in this case, horizontal) forces. The normal force becomes the mass multiplied by acceleration due to gravity (g). This simplification gives the following equation, which presents the friction coefficient as the acceleration (a) of an object on an even surface:

$$\mu = \left|\frac{a}{g}\right|, \text{ considering simplifications} \tag{2}$$

From this equation, it is easy to see that the friction coefficient varies, and that the maximum would be reached with maximum acceleration.

Traditionally the force transfer between a tyre and a road is modelled using tyre slip, which is measured as the speed difference of the surfaces in percentage terms (definitions in Chapter 4.3.1). The viscoelastic behaviour of tyre materials causes the coefficient of friction to increase with sliding velocity until a maximum value is reached at a certain speed. The effect is easy to understand by imagining a brush against a surface: the force increases when the bristles bend. At higher sliding velocities and tyre slip, the friction coefficient decreases.

Figure 1 shows an example of slip-force curves with different vertical load. The effect of vertical load on friction forces is depicted as almost linear. Depending on the hardness of rubber compounds, it can, however, cause a larger true area of contact and change the friction coefficient [10].

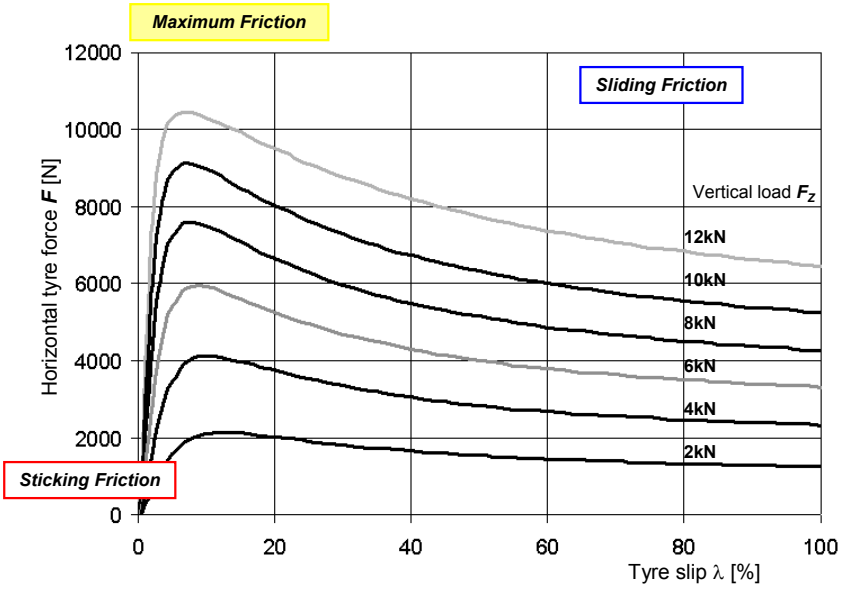

Figure 1. Friction characteristics example [11].

The slip ratio describes the point of operation and is used for example in optimising braking. The maximum friction is reached near 10–15% slip but this depends on the tyres and the road conditions. Pure sliding friction is experienced with 100% slip.

Usually the maximum friction coefficient reached with a passenger car on dry asphalt is between 1.0–1.2. On wet asphalt the coefficient depends on several factors such as the water depth, tyre tread pattern and also on vehicle speed due to the rising hydrodynamic pressure. A variation between 0.5–0.9 can be expected at slow speeds. On snow, a maximum friction coefficient of 0.4 would be the preliminary estimate, using winter tyres, but e.g. 0.25 using summer tyres. There are several types of ice, such as smooth, wet and sanded ice, but a range 0.05–0.25 covers many of these cases. Tyre manufacturer measurements for friction profiles of different tyres can give more accurate estimates of the values than the ones in the literature, which have been collected for average car tyres. [12, 13 (p. 27)]

The simplified Equation 2 described the maximum friction coefficient as equivalent to the maximum acceleration of a car on different horizontal road surfaces; a maximum acceleration of 1 *g* would indicate a maximum friction coefficient of 1.0. This simplification disregards air resistance and assumes a perfect contact to the road, with all four tyres acting. Further, when a vehicle is

moving on an inclined road, a gravity component affects the acceleration. The relationship between vehicle acceleration and friction is discussed in more detail in Chapter 4.3.1. However, in horizontal braking tests with moderate speeds, the error components in the simplification are small when compared to the maximum friction coefficient.

Figure 1 uses the traditional sticking/static and sliding/kinetic friction terms to describe the value ranges of low and high slip. Several theories exist that describe exactly the different aspects of friction force, including the effects of tyre deformation (e.g. rolling friction due to energy dissipated as rubber is compressed and released), molecular bonds causing adhesive forces and traction forces by means of tearing and wear. [14]

The curve describing the relation between slip and force is likewise not fully static; rather, a hysteresis effect occurs when comparing acceleration with braking. Additional dynamic parameters such as effects from steering angle rate and camber can also be identified. [15]

Due to the many variables involved in tyre–road friction modelling, many models have a basis in empirical studies. The most famous semi-empirical model is Pacejka's model [16], also known as the "Magic Formula". This model has been shown to suitably match experimental data and is widely used in simulations. The several parameters of this model can be identified for a tyre by matching experimental data.

A friction estimation system has typically to take into account several parameters that influence the maximum friction coefficient and the forces that can be applied. The parameters can be categorized to

1. tyre parameters (e.g. tyre pressure and stiffness)
2. vehicle parameters (suspension, load, …)
3. driving manoeuvres (acceleration, braking, cornering, …)
4. road surface parameters (asphalt microtexture, gravel, …)
5. road conditions (dry, icy, snowy, slushy, …).

Inaccuracy in identifying contributing factors of this kind can cause large errors in friction estimation. On the other hand, there are applications where considerable improvements can be achieved even with a 3-level classification of maximum road friction: high, medium, low. A number of vehicle safety applications and their requirements are discussed in Chapter 2.

A more straightforward method for estimating or rather measuring the maximum coefficient of friction is naturally by hard braking or using maximum friction while cornering. However, the goal of on-board friction estimation systems is usually to be able to detect slipperiness with low excitation from normal driving. This is also one of the main goals of this study.

This thesis uses the following terminology, originating from the APOLLO and FRICTI@N projects, in measuring different types of friction:

1. Friction used – the friction coefficient currently in use, corresponding to the magnitude of relative tangential forces acting in tyre–road contact. The term can be used when discussing single tyres or the vehicle as a whole.
2. Friction potential – the maximum tyre–road friction coefficient that can be used.
3. Friction available – the remaining potential to use higher forces; the difference between the friction potential and friction used.
4. Upcoming friction potential – the future friction potential in the direction of movement.

Figure 2 gives a graphical representation of these terms:

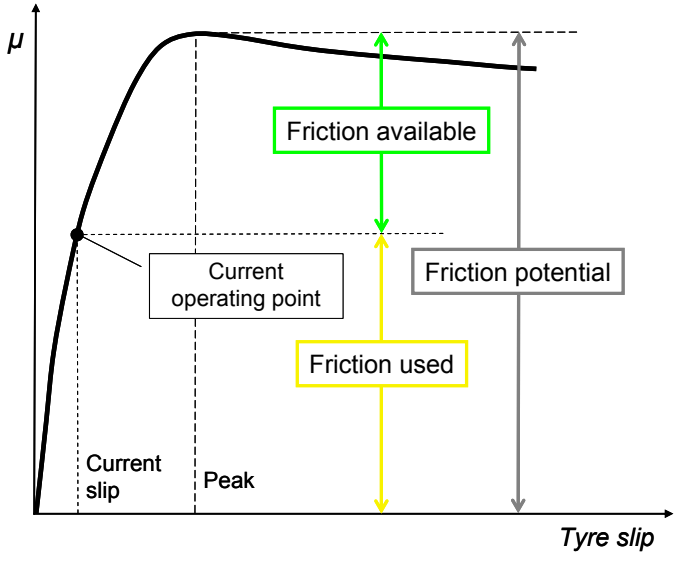

Figure 2. Representation of friction potential, used and available.

The *friction used* is usually determined by using standard vehicle-driving-dynamics sensors like accelerometers and wheel speed sensors. The forces could also be measured directly from the tyres. Often friction used is calculated as a lumped value for the whole vehicle, depending on the required accuracy. Although the calculation is accurate compared to estimations of friction potential and upcoming friction, it does have several error sources: wind speed is usually unknown, road bumps cause momentary variations and the force and load distribution between tyres may not be accurately estimated. When measuring the friction used for example from longitudinal acceleration in a vehicle's co-ordinate system, changes in vehicle pitch rate and resulting pitch angle also cause variations in accelerometer measurements. Friction used will be discussed in more detail in Chapter 4.3.1.

The *friction potential*, the maximum coefficient of friction, is a theoretic estimate if not experienced as friction used. The potential can be estimated using friction models and measuring tyre and vehicle behaviour. The changes caused by impaired friction can indicate the friction potential. Additionally, information from environmental sensors and road weather stations can be used. Environmental sensors (non-contacting measurement) are, however, unable to truly test the potential since the potential exists only between a tyre and a road.

Vehicle dynamics sensors do not tell about the *upcoming friction potential*. Rather the processing for friction used and potential can take time and the values are actually past values. To get information about the friction potential values ahead, environmental sensors measuring road surface type and conditions have the key role. Co-operative systems that communicate information between road users can also be taken into consideration.

The *friction available* is useful when considering the vehicle dynamics and e.g. driver information systems for how much unused potential still remains before there is a risk of uncontrolled sliding.

1.3 Hypothesis, objectives and constraints

The aim of this study is to test the research hypothesis:

Environmental sensing combined with information from existing vehicle dynamics sensors – and optionally from a tyre sensor – enables the estimation of tyre–road friction potential with an accuracy and reliability high enough to enhance collision mitigation and avoidance.

A data fusion approach and architecture are presented along with test results. The advantages of friction estimation are presented in a novel algorithm for collision avoidance.

The major objectives of this thesis are:

- To study an architecture for sensor data fusion from three different types of sensors: (I) existing in-vehicle sensors for vehicle dynamics, (II) environmental sensors, and (III) tyre-based sensors.
- To examine the quality of friction information achieved through sensor data fusion and generally the potential of estimating the maximum coefficient of friction with the selected sensors. An instrumented research vehicle has been used in the validation of the concepts.
- To simulate and discuss the advantages of friction estimation in collision mitigation and collision avoidance. A new collision avoidance algorithm is presented before the simulations. The method uses pre-calculated look-up tables for the vehicle to quickly assess the safety of optional trajectories. Besides friction information, the algorithm takes into account both static and dynamic obstacles, vehicle dimensions, kinematics and partially also dynamics.

Minor contributions are also focused on:

- Discussing the use of friction related information in current and future vehicle safety systems, including co-operative applications.
- Review requirements for measuring key variables for maximum friction coefficient estimation with environmental sensors.
- The practical difficulties of collision avoidance and high classification requirements for environmental sensing.

This thesis covers research work that was subject to particular constraints:

- The measurements and data collection have been limited to test vehicles, sensors and tracks available during the FRICTI@N project.
- The algorithm for collision mitigation and avoidance has been tested in simulations only, for safety reasons, and as the required components for detection of dynamic obstacles and friction have not yet been integrated into an autonomous vehicle. The results are, however, compared to

existing collision mitigation systems. An early development version of the algorithm has been previously used in a robot application.

Since the main parts of this research were carried out in the EU project FRICTI@N, involving several partners, it is important to outline the author's central contributions also from this perspective. The contribution of this thesis is in data fusion architecture and its detailed implementation, using sensors developed by other partners (Figure 3). In particular, the work concentrates on the benefits of environmental sensing in combination with traditional vehicle-dynamics-based algorithms. While collision mitigation had a role also in the FRICTI@N project, the simulation and algorithm concepts presented here have been completed later as a separate work.

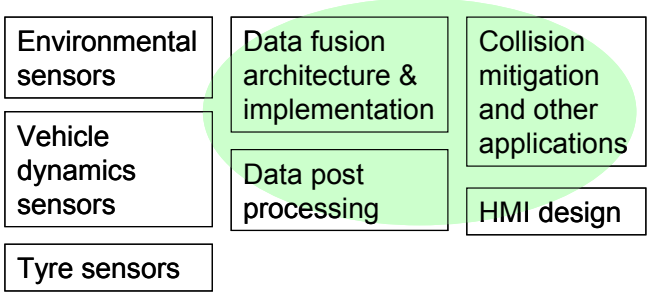

Figure 3. Thesis central contributions.

1.4 Structure of the thesis

The thesis began (Chapter 1) by discussing the advantages of friction estimation from the perspective of promoting traffic safety. Then the research hypothesis, aims and limitations of the work were declared.

Chapter 2 explores users and requirements for friction information. Especially the benefits to various Advanced Driver Assistance Systems are considered based on collected views and tests made within research organizations.

Chapter 3 describes state-of-the-art techniques and implementations for measuring tyre–road friction. This section also presents the sensor systems used in the study.

The friction estimation system and data fusion approach of this study are discussed in detail in Chapter 4.

Chapter 5 presents the test vehicle integration of the friction estimation system as well as HMI aspects.

Chapter 6 explains the procedure used for algorithm validation and the main test sessions during the study. It discusses in detail several tests conducted with the estimation system.

The benefits to be gained from friction estimation are presented in Chapter 7, which deals with collision avoidance and mitigation. The chapter introduces a novel algorithm for calculating the times to a collision (TTC values) for millions of steering, braking and acceleration options using different coefficients of friction. The method has its origin in autonomous mobile robot research but it is not limited to any particular type of vehicle. The use of the collision avoidance algorithms in future driver assistance applications is an actual topic of European research.

Chapters 8 and 9 outline the major achievements and consider the future development work necessary for building real commercial products that would likely be incorporated into vehicles by car manufacturers.

2. Users and Requirements for Friction Information

The higher the accuracy and frequency of friction potential estimation, the more applications that can be supported. A visual driver information system may require only one estimate per second (1 Hz) and not many decimals for friction potential, while ABS brake systems can apply and release brakes more than ten times a second, requiring fast and accurate estimation to operate near the maximum friction.

A driver may wish for a warning several seconds before e.g. entering black ice, whereas ABS mainly requires the current friction potential and maybe advance information of some split seconds only.

Most needs would be satisfied by a measuring frequency of e.g. 100 Hz for each tyre, a friction coefficient accuracy of 0.01, and advance information about an area in front of the vehicle up to the maximum braking distance. However, getting even close to this would require improvements in sensing technology, as will be discussed in Chapter 3, and maybe even require the introduction of a so-called 5^{th} wheel to vehicles, simply to measure friction potential continuously. Alternatively, the vehicle could perform braking periodically either using longitudinal forces or slightly turning wheels. The approaches where extra braking or other manoeuvres are used to determine friction have not received much attention in studies. Such suggested modifications have so far been rejected by the automotive industry.

The requirements for a friction potential estimation system in production vehicles rather deal with finding an optimal price/performance ratio and optimal information quality for different applications. New expensive sensors are to be avoided unless the benefit would be clearly evident. Some existing sensors can be modified to also provide information on road conditions.

Figure 4 gives an overview of how friction information can be provided to several applications and bring benefits at different levels, including traffic safety on a societal level.

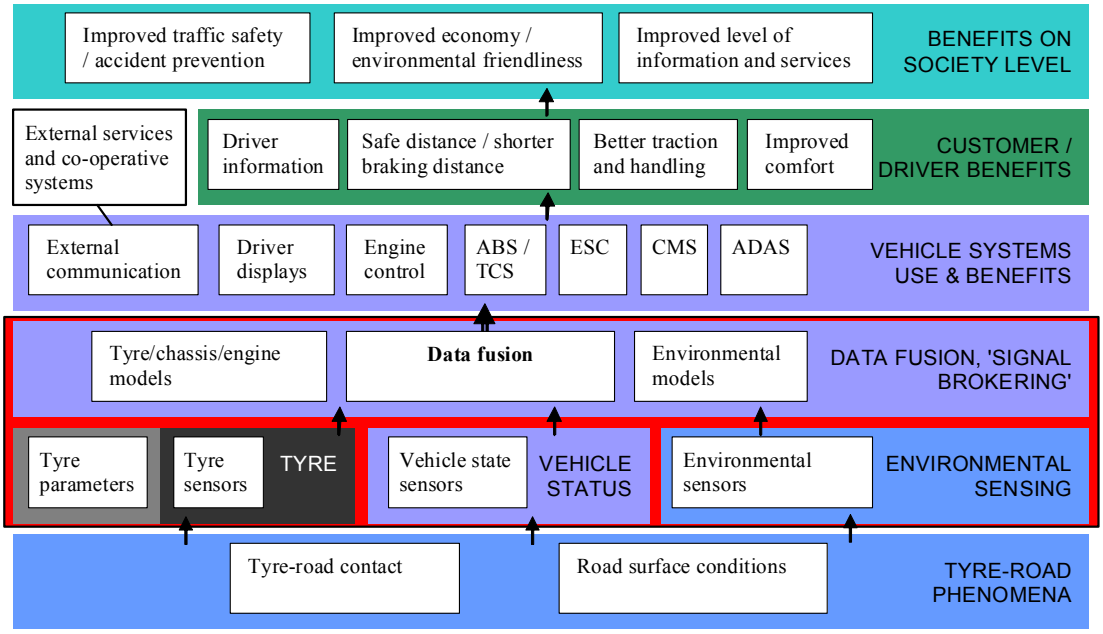

Figure 4. Collecting and distributing friction information to benefit several applications. The friction estimation system is marked with red.

The term ‘signal brokering’ in the figure describes an idea from the FRICTI@N project that the friction estimation system should be the collector and distributor of all information related to road conditions as well as tyres.

The key users of the friction estimation system could be categorized into

- driver information systems
- vehicle dynamic control systems
- advanced driver assistance systems
- co-operative applications.

For each of these categories, different functions can be identified which will benefit from tyre–road friction information.

2.1 Driver information

Drivers are generally good at interpreting the actions of other road users, such as observing a pedestrian looking around before crossing the road, their own driving performance, and also road weather conditions. Computers and sensor systems on the other hand excel at measuring distances, velocities and vehicle state, continuously. In some situations the vehicle can correct and warn about errors made by the driver.

A driver may for example have little experience in driving on a slippery road. Most northern drivers gain experience in driving on snow and ice, but even in the north, gaining experience with some difficult conditions, such as thick slush on an unploughed road, can take longer. Drivers may also have problems in estimating the vehicle behaviour and remaining friction potential during hard manoeuvres such as fast cornering on a wet road.

The estimates for friction used/potential and upcoming friction could be provided directly to a driver. However, there are difficulties:

- Friction used can be felt as acceleration of the vehicle by a driver and therefore the driver generally has a good idea about it. Telling something the driver already "knows" is usually not beneficial. Overloading the driver with information and flashing displays should be avoided.
- The cases where the friction used is close to the friction potential are more interesting and this information could improve a driver's understanding of driving limits. Estimation of friction potential on the other hand may not be fully continuous and it easily contains larger errors than the friction used. The feasibility of continuously displaying friction levels comes down to the performance of the friction estimation system. Some cases where the friction used is close to the potential might also go undetected and the driver would not receive a warning.
- The friction potential in front of the vehicle can vary a lot according to the vehicle trajectory. On a road with fresh snow the vehicle track may still be clean but the potential can change rapidly within centimetres. This type of accurate information, giving a map of the vehicle surroundings, might be difficult to show to the driver.

The road conditions and friction potential can also be condensed into simple symbols and warnings such as the snowflake icon used by several automotive

brands to remind the driver of slippery conditions. By averaging friction potential estimates over e.g. the length of road segments in digital maps might make it possible to provide a driver with a rough classification of a road segment slipperiness in a manner similar to the snowflake icon.

If a driver information system does not need frequent updates, rather just once per second or less, this would give an opportunity to filter out momentary errors in friction estimation. The frequency of false warnings in a driver warning system generally needs to be low to ensure user acceptance of the system.

On the other hand, averaging friction potential even over a period of one second can lead to the loss of valuable information. Even if the weather and tyre performance were not to change so rapidly, the tyre–road friction potential can. The effects of averaging should be evaluated against the shortest slippery sections that alter the vehicle dynamics during different manoeuvres. When driving straight, a slippery spot can go unnoticed, but the same spot could cause difficulties for a motorcyclist intending to turn.

Advance warning icons, when there is for example black ice (the friction drops suddenly) or when the driver is close to the friction limits, could be interesting topics for HMI development. The HMI concepts are discussed further in Chapter 5.2.

Considering the discussed difficulties in continuously presenting friction potential to drivers, it currently seems likely that friction estimates will have a bigger role indirectly, through operation of other driver assistance systems.

2.2 Vehicle dynamic control

Modern passenger cars are equipped with several control systems that monitor vehicle dynamics and stability. These systems improve the vehicle handling and safety by e.g. detecting and preventing skid. Currently the most important systems linked with friction potential are:

- Tyre slip control systems:
    - Antilock Braking System (ABS)
    - Traction Control System (TCS), also known as Anti-Slip Regulation (ASR)
- Electronic Stability Control (ESC) and rollover stability control.

ABS, TCS and ESC already contain friction estimation algorithms and generally their performance is difficult to improve. Only an optimal friction potential estimation system could considerably improve the performance while braking. A more likely approach is to provide these systems with an initial value for friction potential, which they do not have, and in that way aid the operation during the first cycles. Generally this would help to avoid overshooting brake pressures or motor torque on slippery surfaces such as ice, and to find optimal levels quicker. If the slip is allowed to grow too large, the transmitted forces do not reach maximum.

Another input to improve the operation of ABS could theoretically be the detection of gravel or deep snow. On these surfaces, locked wheels dig in and the build-up of material in front of the tyre stops the vehicle more quickly than ABS. However, locking tyres sacrifices the possibility to steer the vehicle and can cause a loss of control [17].

A friction estimation system would rather be better at preventing dangerous manoeuvres than later helping to correct them. There has been discussion on friction estimation "giving eyes to ESC", referring to advance information from environmental sensing.

2.3 Advanced Driver Assistance Systems

Advanced Driver Assistance Systems (ADAS) are in-vehicle technologies designed to improve safety by aiding the driver. The systems enhance the driver's perception of hazards and in some cases partly automate the driving task. Examples of ADAS are lane departure warning, collision mitigation, intelligent speed adaptation and automatic parking. The term is still new and there is a need to clearly define what ADAS constitute. [18]

One definition is that the systems use environmental sensing to create a view of the vehicle surroundings. A vision system to track pavement markings or a radar to detect obstacles in front of the vehicle are examples of the sensors used. A digital map can also be considered as a sensor. [18]

The potential safety impacts of different ADAS have recently been evaluated in several European projects such as PReVAL and eImpact. The effects on injuries and fatalities, at 100% fleet penetration, have been estimated as being in excess of 10% for future systems like active lane keeping support and map-based warnings of dangerous locations and speeding. Also collision mitigation has been estimated to have high impacts on safety, depending on the implementation details (detects

pedestrians or not) and assumptions made in the evaluation. The expectations are generally high for the introduction of these systems. [19, 20]

Environmental sensing with cameras, radars and laser scanners is new for production vehicles, and many ADAS are still at prototype phase, with a targeted entry into the market some time beyond 2010. This was the case for example in the recent large European Integrated Project (IP) PReVENT, which showcased several new systems. Several questions still remain about the systems' reliability, performance and interaction with the driver. In particular, system performance tests conducted in adverse weather conditions are required to estimate market readiness. [19]

Systems designed for analysing natural signals such as a camera image or speech are not generally expected to perform error-free. Changing weather and lighting conditions, noisy signals and numerous types of real-world situations challenge the algorithms and even humans who try to interpret the signals. In machine vision, changing light is a classic problem. Further, trying to teach computers to recognize objects such as pedestrians requires the most advanced algorithms; the pedestrians can vary from a pregnant woman to removers carrying a sofa. Similar problem cases occur in speech recognition when trying to recognize speech during high background noise (e.g. in a crowd) or when the speaker does not formulate his words or sentences clearly.

It is generally not reasonable to expect 100% reliability for systems based on environmental sensing! However, this is nevertheless the goal for safety systems.

Reliability can be increased by limiting the operating range of a system, e.g. only activating it at high speeds. This makes further assumptions possible but still may not bring full reliability.

To avoid potential liability issues, the first ADAS implementations have concentrated on driver warnings instead of actuation. The vehicle might be allowed to take control for example to mitigate unavoidable collisions, or according to other carefully defined limits. Occasional false warnings have not been considered to be as critical as the vehicle making a wrong manoeuvre.

False warnings will likely negatively affect the user acceptance of the system and, depending on the application and HMI design, can also cause dangerous situations. Even not getting a warning signal can be dangerous if the driver learns to trust the system too much [19].

At least the following basic uncertainties are present in ADAS algorithms as well as in semi-autonomous driving:

- the intentions of other road users (if they are about to turn, brake etc).
- inaccuracy of digital maps with e.g. traffic signs and road works
- detection of driver alertness and performance (falling asleep, talking on the phone, reaction time)
- environmental sensing accuracy and reliability, especially in adverse weather conditions
- tyre–road friction potential not known accurately.

The unknown intentions of other road users can be handled partly by estimating the maximum acceleration (affected by friction potential) and therefore the change in their location. The greater the acceleration, the greater the safety margins that are needed when calculating potential collisions. Also future co-operative systems communicating e.g. that the driver in front may be turning left according to his navigator could relay some intentions. This topic will be addressed also in Chapter 7, which deals with collision avoidance.

Detecting driver alertness and activity has been studied using e.g. cameras to detect eye movement, sensors in the seat to measure stance and heart rate and also Bluetooth communication between mobile phones and the vehicle.

Finally in the list, the maximum tyre–road friction coefficient is commonly a static variable for many current ADAS implementations such as for the prototypes for collision mitigation. What the static value should be is a matter of lengthy discussion, but any value causes error during changing conditions. The value is often set high in prototypes based on the average friction levels available throughout the year. Therefore the biggest errors in calculation are seen on snow and ice.

Table 1 describes briefly the problems that certain ADAS without friction estimation face on slippery surfaces:

Table 1. ADAS types and difficulties from having no friction estimation.

ADAS type	**Problems from assuming a static high friction potential**
Collision mitigation	The system applies the brakes too late on low friction surfaces. Does not warn when the risk is already high.
Collision avoidance	Not able to avoid collision, calculates wrong safety margins and potentially even dangerous manoeuvres.
Lane departure warning	Minor; the effect is via curve speed warning.
Curve speed warning	Does not warn in dangerous curves or alternatively is set to warn too easily.
Adaptive cruise control and systems informing/warning of safe distance	Too short distance to vehicle in front.
Intersection safety	Wrong calculations for other road user movement and ego vehicle acceleration.
Park assistance	In extreme cases unable to perform the manoeuvre.

Due to the varying nature of friction potential, tuning the applications may be problematic even if a friction estimate would be available: For example in curve speed warning, the vehicle trajectory can vary a lot within tens of meters and so can friction. The capabilities of environmental perception can also drop with distance. When driving close to the limits of friction, and where there are alternating patches of ice, snow and dry surface, calculating maximum curve speed becomes difficult. A safety margin is required to compensate for the uncertainties. High risk level and clear speeding cases can, however, be calculated more easily.

As a conclusion, friction estimation could help several ADAS to reach their full potential also in difficult road conditions.

2.4 Co-operative applications

The co-operative approach for improving traffic safety is based on communicating information and measurements between road users and also from and to infrastructure. The information can be used e.g. to extend the driver's view by creating an "electronic horizon" where advance and extra information is shown on a map, even projected onto the windscreen or used otherwise in vehicle systems [21]. The vehicle's own measurements are supported by the communicated data. Generally the communication can help to disseminate warnings and traffic information, and bring situational awareness to several systems.

There is ongoing development to standardize communication and several projects are piloting applications.

The standardization of communication is led by the IEEE working group for Wireless Access in Vehicular Environments (WAVE). A WLAN variant 802.11p, communicating at 5.9 GHz (the exact frequency ranges are different for the U.S. and Europe), is expected to be finalized during the first half of 2010 [22].

The largest EU projects in the field of co-operative traffic are at the moment SAFESPOT and CVIS with a budget each of approximately EUR 40 million. Their results in 2010 will provide insight also into how close the technology is to market introduction.

The co-operative applications are commonly divided into vehicle-to-vehicle (V2V) and vehicle-to-infrastructure (V2I) according to the type of communication used. Both communication methods can be used for distributing friction-related information such as warnings about dangerous road conditions.

A key challenge in using friction information in co-operative applications is that the friction potential is different for each vehicle and its tyres. On dry asphalt the differences could be considered small, but in adverse weather conditions the performance differences between tyres grow (especially winter tyres vs. summer tyres). This might mean that only the road weather information or rough category values can be transferred to other vehicles and not the friction potential directly. This study later discusses (see Chapter 4) an approach based on recording the tyre performance on different road conditions detected by environmental sensors as an attempt to normalize the friction potential.

Another challenge is the high variance of friction even over short stretches of road. When GPS positioning accuracy is considered to be 5 meters, even for "same" co-ordinates, the experienced friction can be different. Recording the

minimum and maximum friction potential (fluctuation range) for a road segment might provide a useful reference.

Finally, as friction can change rapidly due to e.g. spilled oil on the street, the aging of measurements and therefore the coverage over the road network are challenges for co-operative applications.

2.4.1 Vehicle-to-vehicle

A vehicle-to-vehicle (V2V) scenario using friction data could be that a car detects a big change in road conditions at a road segment and then passes on this information to the following and nearby vehicles. This information would be shown to the other drivers to make them more aware of the changing road conditions or a potentially dangerous location.

The V2V applications include improved versions of stand-alone ADAS, where e.g. the safety margin calculation is improved with information from other vehicles. Friction estimation also yields extra information that could be broadcasted. Table 2 suggests a classification for V2V applications using friction information:

Table 2. Vehicle-to-vehicle co-operative applications that benefit from friction information.

V2V application type	Use of friction information
Safety margin Using a co-operative systems approach, it will be possible to calculate and suggest safety margins to the driver.	The dynamic capabilities of the vehicle, road conditions, driver status and a dynamic map including other road users would be used in the calculations. The safety margin calculation can be used in enhanced ACC, collision mitigation systems, calculating safe distance to the vehicle in front, intersection safety and curve speed warning.
Local danger warning Local warnings are sent to other vehicles in case of a danger, e.g. accident, breakdown, driving off the road, stopping at a dangerous place, fire or bad road weather conditions.	Warning of an especially slippery road segment could include environmental measurements, measured friction during high slip, co-ordinates, road segment ID and time. The information could be shown on a navigator screen for example.
Enhanced map data for the road segments ahead of the vehicle PReVENT EU project used a term “electronic horizon” for advance map information combined from several sources [21]. SAFESPOT project used the term “Local Dynamic Map”, emphasizing the dynamic content [23].	To improve the range, accuracy and reliability of road weather information in other vehicles and their applications.

2.4.2 Vehicle-to-infrastructure

The second communication type is defined as vehicle-to-infrastructure (V2I) communication. In this case the information is picked up by an individual car and transferred to the infrastructure. The infrastructure could process the data and deliver it to other road users or radio stations. An infrastructural system

would be able to control traffic signs, provide data for traffic management or inform authorities about road surfaces.

V2I applications are a clear example of using friction measurement and estimation systems as part of *probe vehicle* concepts. The main purpose is to collect information about dangerous locations and statistical friction information to be processed further. The main applications are presented in the following table:

Table 3. V2I applications using friction information.

V2I application type	**Use of friction information**
Real time measurements of weather and road conditions	Vehicle systems will collect and transmit real time weather information to all road users and to road operators' and public authorities' traffic information servers. The information can be presented statistically and used in vehicle safety applications.
Local danger warning	Co-ordinates and classification of a black spot that caused problems.
Curve speed warning based on statistical friction information	The curve speed warning application aids the driver in choosing an appropriate speed. On-board information is used to determine if the driver needs to be alerted.

2.5 Requirements

The application categories and examples discussed above present many requirements for a friction estimation system. In summary, the system should be able to

1. determine the current friction used – to estimate how close the vehicle is to limits and to collect friction used levels
2. determine the friction potential and the rate of changes – to estimate e.g. the maximum accelerations for safety margin calculations and warn of sudden large changes

3. predict the upcoming friction potential (with environmental sensors) – for use in different driver assistance systems
4. classify road conditions (snow, icy, slushy, wet, dry…) to be used e.g. in driver information systems and co-operative applications
5. record the co-ordinates (location reference) and time for friction potential estimates
6. provide a validity for friction estimates and preferably metadata on estimation errors and tyre type
7. produce a high enough sample rate for driver information systems (approximately >1 Hz) or also ADAS (>10 Hz).

Preferably the system design should not include large design changes to current vehicles (e.g. 5th wheel) or expensive sensors.

Additionally, as several standard vehicle sensors are available for measuring friction related variables such as acceleration and temperature, a friction estimation system should utilize these sensors.

3. Sensors and Methods for Estimating Friction

3.1 Overview on measuring road conditions

Technology for observing road parameters and tyre–road contact has figured as a topic in a number of projects internationally – both EU-funded and others. The existing systems and prototypes can be divided into

- fixed roadside monitoring systems (road-segment specific)
- road monitoring with probe vehicles
- environmental sensors
- in-vehicle sensors for vehicle control systems
- tyre sensors and tyre modelling.

3.1.1 Fixed roadside monitoring systems

Fixed roadside weather monitoring stations are mainly for winter maintenance management, supervision, planning and optimization. Road weather stations can have different sensors (e.g. temperature, wind speed, surface water depth) and weather cameras based on visual information.

The Vaisala Remote Road Surface State Sensor DSC111 monitors the presence of water, ice, slush and snow/frost using spectroscopy. It also estimates the level of grip based on the road conditions. The integration time is several seconds to filter out passing vehicles. [24]

A weather warning system for drivers of heavy vehicles based on mobile phone positioning was introduced in Finland in 2005. The warning system is

based on already existing road weather services, weather radars, weather cameras and road weather stations. With mobile phone positioning and the mobile phone network, weather information and warnings can be delivered to the drivers entering the critical area [25].

3.1.2 Road monitoring with probe vehicles

Probe vehicles are used to automatically gather road condition information while driving in the traffic flow. Existing systems usually employ public transport. The collected information is transmitted to processing centres and the processed information is then distributed to other road users. Also the term Floating Car Data (FCD) is commonly used for data collection with probe vehicles.

Finnra's (Finnish National Road Administration) mobile road condition monitoring system utilizes buses on regular routes to gather information about driving conditions. The monitoring equipment measures air temperature and humidity, tyre–road friction, road surface temperature and GPS co-ordinates. The friction measurement is based on a fifth wheel. The information, also containing images, is transmitted in real time to Finnra's road weather monitoring system via GSM. [26]

VTT's RASTU project (2006–2008) demonstrated road slipperiness measurements with trailer lorries using the vehicle bus information on wheel speeds and engine thrust: Especially when climbing uphill with a heavy load, there is noticeable speed difference between the tractive wheels and front wheels. This information on tyre slip was used to classify the slipperiness (not directly the friction coefficient) of a road segment, with no additional sensors. [27]

3.1.3 Environmental sensors

Optical, acoustic and radio frequency based environmental sensors utilize changes in the signal reflectance, polarization and absorption properties caused by the road surface. The contactless environmental sensors cannot be used for direct force measurement but can detect road conditions. The existing vehicle rain sensors and outdoor temperature sensors can be used to support friction measurements.

Swedish company Sensice (http://www.sensice.com/) has since 2007 acquired European and U.S. patents for their ice detector based on infrared spectroscopy and a novel cheap design. The system is able to detect several surface states: dry, wet, icy, black ice and ice/sleet covered with a layer of water. Localized ice de-

tection is mentioned as of particular value in areas prone to icing, such as bridges. The system could also help to prevent pedestrian accidents when used to detect ice e.g. at entrances to public buildings. [28]

The results of the research called “Discrimination of the road condition toward understanding of vehicle driving environments” showed that the road condition discrimination accuracy could be improved by using additional knowledge, such as information regarding snowfall, rainfall, and the time-related continuity of the change in road conditions. [29]

3.1.4 In-vehicle sensors for vehicle control systems

In-vehicle sensors provide information about the driving state of the vehicle, such as wheel lock-up or turning. These sensors can be used to measure changes caused by impaired friction and uneven road surface. They do not directly measure road conditions or the friction potential ahead.

The possibilities to detect friction potential with standard vehicle sensors have been widely analysed (see [14] for a good overview). The friction potential can be measured during hard braking, though generally the research concentrates on early detection and friction classification during normal driving.

Measuring longitudinal slip and the slip slope (curve shape before maximum forces are reached) from the difference in wheel speeds (as proposed in [30]) is one of the traditional methods. Many advanced models add e.g. tyre, suspension, engine torque and steering parameters for improved modelling accuracy.

Lateral forces have also received wide interest as turning generates forces for friction estimation. For example the methods based on steering torque and tyre self-aligning torque rely on the evidence that the self-aligning torque saturates at lower values of slip angle than the lateral force (e.g. [31]). This feature (Figure 5) allows the estimation of friction potential at low values of side slip angle. Two existing algorithms based on self-aligning torque were used in this study and are further discussed in Chapter 4.3.1.

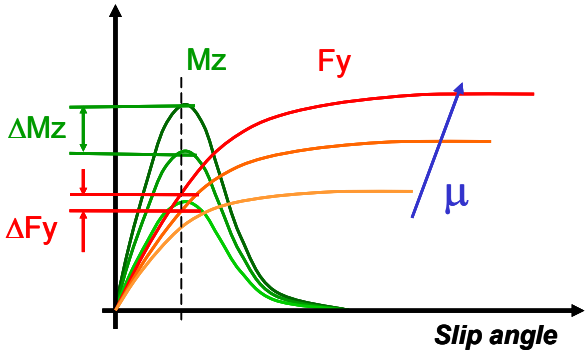

Figure 5. Qualitative comparison of self-aligning torque (M_z) and lateral force (F_y). [2]

Dynamical friction models (including e.g. hysteresis effects and dependence on velocity) such as LuGre have also been used in friction estimation. The road conditions are characterized with a single parameter in the model and it can even be estimated using only wheel angular velocity. The classification is possible only during slip. [32]

"The estimation of tyre–road friction by [the] tyre rotational vibration model" required only ABS's wheel speed sensors. The estimation was based on the fact that the resonance characteristics of wheel angular velocity vary by tyre–road friction. The presented method could detect changes in friction potential during normal driving. The weakness of this system is that the resonance characteristics change when braking, accelerating or cornering, and the method cannot then be used. This method could detect friction potential changes and derive some road condition categories, but cannot estimate the actual friction value. The method was patented by Toyota in 2004 [33]. The approach was tested also in the FRICTI@N project by VTT (Dr Liang Nanying) in co-operation with Nokian Tyres Plc, though unsuccessfully, as it was not possible to fully reproduce the results. The power spectrum density of wheel angular velocity near the suggested 40 Hz region was found to be somewhat different on asphalt vs. ice only for one type of tyre out of three. A relatively high wheel-speed-sampling frequency (> 100 Hz) would be required for completing the assessment and studying in what cases and with what equipment differences were appearing or not.

3.1.5 Tyre sensors

During the past few years, tyre sensors have figured as a topic of R&D to estimate tyre–road contact. The first prototypes have already been demonstrated. Several sensor technologies have been used in the development of intelligent tyre systems, such as acoustic (noise), optical, acceleration and deformation sensors. Mathematical tyre models are being developed and used together with force and deformation sensing to estimate friction coefficient, slip, aquaplaning, tyre pressures etc.

Today, only laboratory prototypes of advanced tyre sensors with limited performance exist. These include

- a magnetic side wall torsion sensor by Continental [34]
- a position sensor based on a magnet and a Hall sensor by the University of Darmstadt [35]
- Surface Acoustic Wave (SAW) sensors, e.g. [36]
- the APOLLO/FRICTI@N project prototypes using optical and strain sensors.

The APOLLO project (2002–2005) pioneered an intelligent tyre system with integrated deformation sensing, batteryless power generation and wireless data transfer. Acceleration, strain and optical sensors were used and tested for deformation measurements. Sensor durability inside the tyre was a major problem. Tests showed that acceleration sensors can quite accurately determine the contact length of the tyre from the radial velocity and tangential position signal. On snowy surfaces, the tangential deflection signal was different on high and low friction surfaces. On asphalt, bitumen and concrete, the friction potential could not be estimated because of high signal variation. Tentative results of the project also suggested that the detection of nascent aquaplaning would be possible. [3]

3.1.6 Conclusions

A state of the art review performed in the beginning of this study suggested the following conclusions concerning the use of friction information for advanced driver support systems:

- The importance of tyre–road contact information for enhanced driver assistance is widely recognized.

- A number of activities to develop a system for determining friction and/or road slipperiness are underway.
- Previous studies have been successful in classifying road conditions roughly and detecting changes in friction potential when certain conditions (driving situations and environmental conditions) are fulfilled.
- It seems evident that using a one-sensor approach is not successful in determining friction potential and/or road slipperiness with sufficient accuracy to benefit several applications.
- The performance of a number of vehicle control systems could be enhanced by means of classifiable friction or road slipperiness information.
- Drivers, infrastructure owners and other external systems as well as co-operative driving could benefit from friction information.
- Current EU Integrated Projects for ADAS and co-operative systems require information on road slipperiness in order to demonstrate more convincingly the benefits of the applications under development.
- The number of relevant patents in the field is not yet large (based on reviews made twice during the FRICTI@N project, in 2005 and in 2007), and these patents do not include systems using a multiple sensor approach (other than multiple vehicle state sensors) to determine friction or road slipperiness.

At the time of planning this study, in 2005, Audi demonstrated with their All-road Quattro concept car an environmental sensor called Audi Road Vision [37]. The sensor combined laser and infrared spectroscopy to distinguish between road conditions and to recognize various types of road surfaces, including gravel. It also should give feedback to ESC and ACC. The product has still not entered the market, but it serves as one of the first examples of how friction estimation with environmental sensing has been an expanding topic in the automotive field.

The FRICTI@N project was not the only project that began to study friction estimation using multi-sensor data fusion. A smaller Swedish study [31] started around the same time. Currently no other similar friction studies are underway but the advent of environmental sensors has widely inspired sensor data fusion projects.

Moreover, in what can already be considered as the de facto approach, road operators are combining information from several measurement systems and advanced probe vehicles, using cameras and special friction-measuring equipment.

3.2 Sensors used in the development

The principle idea behind using sensors in this study, and in the FRICTI@N project, was to combine information from "look under the car" tyre-based sensors and vehicle-dynamics sensors with forward-looking sensors that monitor the road surface. The project aimed to use sensor clustering, which yields tyre–road friction potential with a minimum number of sensors. Most of the sensors used for friction estimation were either commercially available or prototypes of upcoming sensors. New sensor development was not a key goal.

A specially instrumented Audi A6 was used as the development vehicle (Figure 6). It is owned by RWTH Aachen University, Institut für Kraftfahrzeuge Aachen (IKA). The vehicle details will be further discussed in Chapter 5, System Integration.

Figure 6. Audi in Aachen wet track tests August 2008.

The vehicle-dynamics sensors were commercial sensors already existing in the development vehicle, including wheel speed measurement sensors, an Inertial Measurement Unit (IMU, measuring accelerations and rotations), brake pressure sensors, steering angle sensors etc. The exact requirements are set by the selected vehicle feature fusion algorithms (Chapter 4).

Concerning environmental sensors, the FRICTI@N project selected the following state-of-the-art sensors to be installed on the development vehicle (Table 4):

Table 4. Environmental sensors used in the study.

Environmental sensor	**Measurement distance**
Road Eye, a laser/infrared spectroscopy based road condition sensor developed by a Swedish company, Optical Sensors	~1 meter
Ibeo's LUX laser scanner. The outputs used in this study were precipitation and true ground speed.	Precipitation is measured from an area up to 10 meters in front. True ground speed and heading measurements are based on detection of static objects in sensor range (200 meters).
VTT's prototype stereo camera measuring polarization differences	Region of interest in the tests approximately 10–30 meters in front.
Ordinary road and air temperature sensors	The vicinity of the vehicle.

Additionally the vehicle was instrumented with a Correvit ground speed camera to be used as an accurate reference sensor when studying vehicle dynamics and velocity estimations with IMU, wheel speeds and laser scanner. True ground speed measurements are used to calculate slip from wheel speed readings.

Commercial infrared cameras were used to record reference data especially during the development phase of the VTT's camera prototype. The FRICTI@N project also studied the use of modified radar technology to detect road conditions [38]. These sensors were not, however, included in this data fusion study.

The tyre sensor was an upgraded version of an APOLLO project prototype: an optical position sensor that is capable of providing information on the motion and deformation of the inner liner of the tyre.

The following gives a more detailed description of the sensors used in the development of sensor data fusion.

3.2.1 Road Eye

Absorption spectroscopy is widely used as an analytical technique for identifying different chemical compounds and also their concentrations in samples. The compounds have a specific absorption spectrum for electromagnetic radiation, so giving them a fingerprint.

The technique can also be used for the classification of road surfaces. In particular, the different absorptions of infrared wavelengths by water and ice (Figure 7) have been useful in detecting different road conditions.

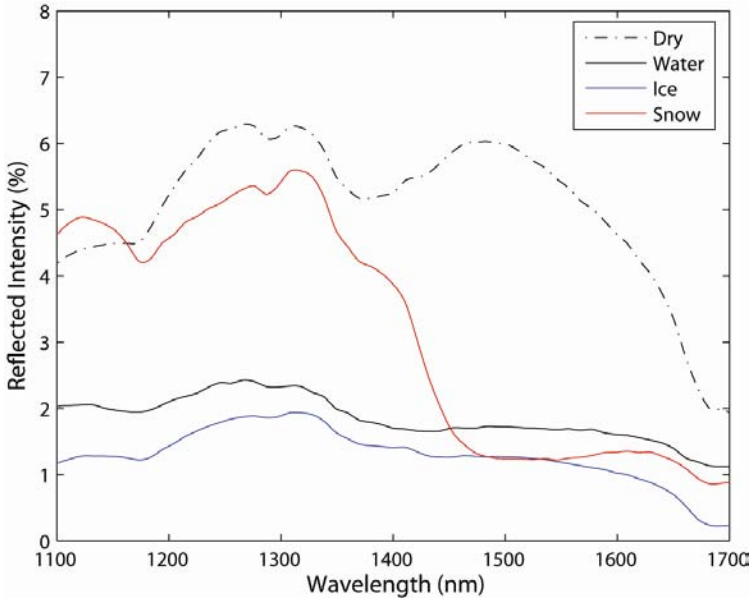

Figure 7. Spectral response for dry, wet icy and snowy asphalt [39].

The Road Eye sensor (Swedish patent nr 9904665-8) is based on measuring the absorption of infrared light at wavelengths 1320 and 1570 nm. The wavelengths are produced with two laser diodes. A focusing optic in front of the diodes produces an illuminated spot of around 10 mm on the road surface. The sensor is designed for short distance (500–1500 mm) measurement and classification of road conditions for vehicle use. The active lighting ensures the sensor's operation in both night and day conditions.

The sensor, shown in Figure 8, is developed by Optical Sensors (http://www.opticalsensors.se/), which is a small Swedish company. It has been previously investigated in several road research projects, such as the IVSS pro-

ject (www.ivss.se), and is one of the most interesting environmental sensors currently available. The sensor detects ice on the road and also water films, but with a lower sensitivity. A clear indication can be given for ice that is typically 0.5 mm or thicker, compared to a minimum water film thickness of about 2 mm or thicker. [31]

Figure 8. Road Eye sensor (http://www.opticalsensors.se/roadeye.htm). The dimensions of the casing are 51 × 53 × 45 mm.

The sensor output is an intensity measurement for both of the used wavelengths. Figure 9 shows an exemplar classification from a test track measurement with four road conditions: dry asphalt, water, ice and snow. Each measurement is marked with an ‘x’ and the coloured polygons represent the classification boundaries for the road conditions. The boundaries for water and ice are close to each other, hence their classification is difficult.

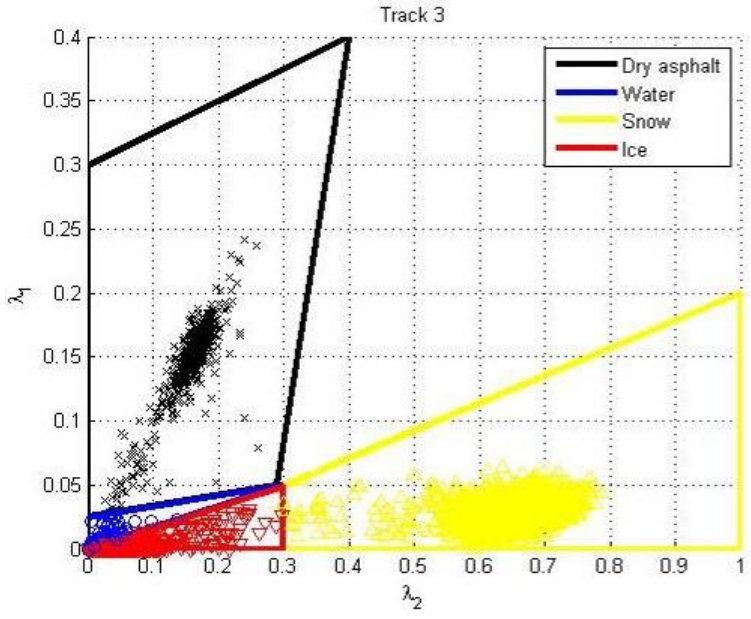

Figure 9. Classification boundaries depicted in a 2-dimensional plane with the two wavelengths as axis [2].

The boundary areas between classes are where the road surfaces are easily mistaken. More classification examples with the sensor are given in [40].

The classification results obtained with Road Eye were the main environmental sensor input in this study, along with basic temperature measurements. The classification's robustness was further improved by supporting the calculation with temperature measurements and the friction used. This will be discussed in Chapter 4 under environmental data fusion.

The limited measurement distance and area meant, however, that only "road conditions under the right front tyre" were measured. The installation on the development vehicle is later shown in Figure 10, together with the laser scanner installation.

3.2.2 Ibeo LUX

Laser scanners operate on the time of flight principle by sending short laser pulses and measuring the time taken for the reflected light to return to the sensor. The travel time tells the distance to an object.

In the LUX laser scanner, manufactured by Ibeo Automobile Sensor GmbH (Germany), a semiconductor laser diode emits pulses that last a few nanoseconds. The sensing beam is guided over a rotating mirror, scanning a horizontal angle of 100° with a resolution down to 0.1°. The scan frequency is 12.5 Hz and the measurement range is up to 200 meters. [41]

In Figure 10, the LUX is temporarily mounted immediately to the right of the number plate. The Road Eye, with a metal housing and the Correvit reference sensor, uses the same mounting.

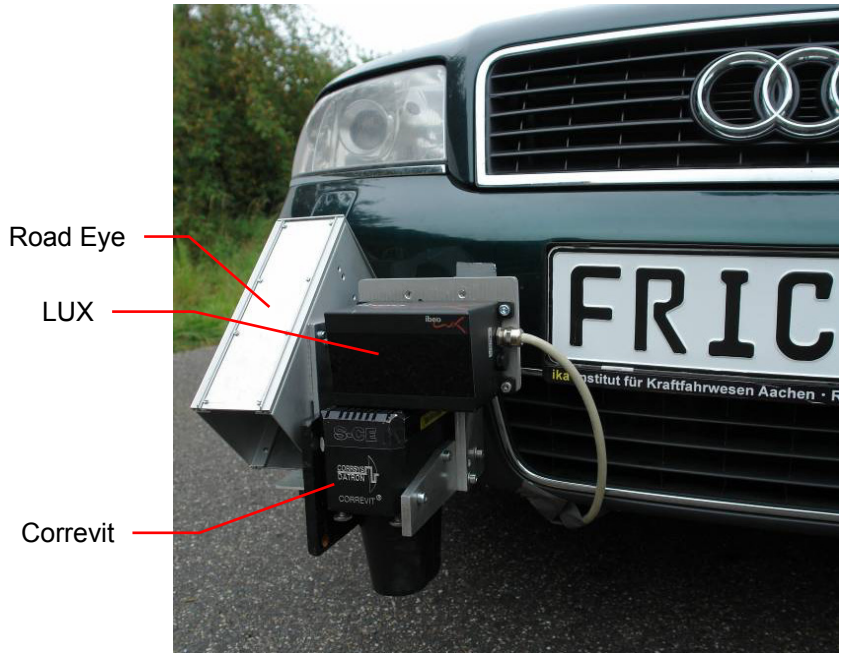

Figure 10. LUX and Road Eye sensors installed on the development vehicle: The Road Eye housing is on the left, LUX on the right, while the Correvit reference sensor points downwards.

Ibeo has developed their laser scanners for ADAS applications such as ACC Stop & Go, Automatic Emergency Braking, Pedestrian Protection and Lane Departure Warning. These applications require accurate detection and robustness against adverse weather conditions. The robustness has been achieved with multi-echo technology and by splitting each laser pulse into four layers. The layers have an aperture angle of 3.2°, also allowing for compensation of the vehicle pitch. The sensors evaluate and filter data from up to 16 reflections per

measurement. Reflections coming from rain, dirty cover or fog can therefore be filtered out [42, 43].

During the FRICTI@N project, Ibeo developed the LUX sensor so as to not only filter out cluttered echoes, but *to use this information to detect rain and snowfall*. The following Figure 11 shows a laser scanner recording during snowfall. No objects are present, thus the points represent falling snow flakes.

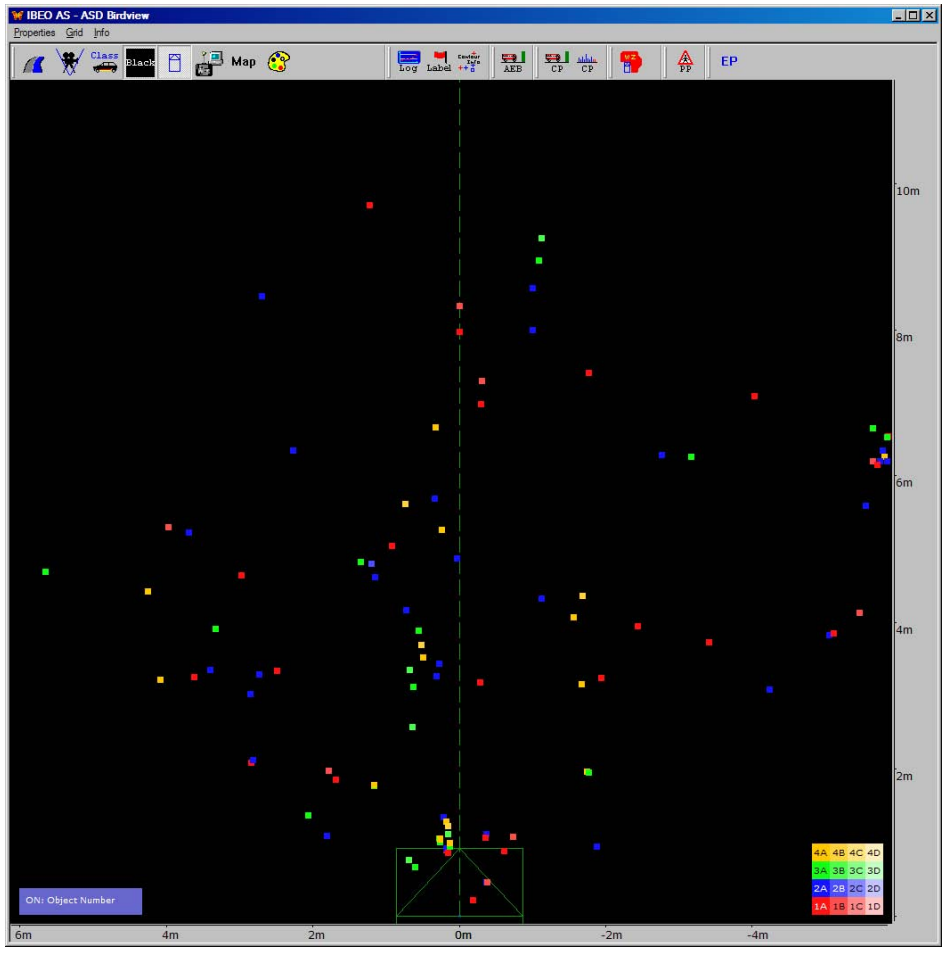

Figure 11. A laser scanner measurement during snowfall. Image courtesy of Ibeo.

The amount of snowfall is related to the number and distribution of measurements in the sensor's field of view. Similar results are found during rain. The scanner's precipitation output was included in the data fusion of this study and fused with air temperature measurements to classify rain and snowfall.

Additionally the sensor provides true ground speed and vehicle heading. This is based on detection of stationary objects and their movement in consecutive sensor scans. The estimate is available when static objects are present.

3.2.3 VTT's IcOR polarization camera prototype

VTT developed the IcOR polarization camera prototype (Figure 12) in the FRICTI@N and SAFESPOT projects, which ran simultaneously. The SAFESPOT is an EU Integrated Project (IP) concentrating in co-operative applications [23].

Figure 12. IcOR camera prototype with dedicated polarization filters.

The IcOR's advantage is to be able to detect ice and water approximately 10–70 m in front of the vehicle, which provides the driver or vehicle with time to react to changing conditions.

In the beginning of the FRICTI@N project, VTT's team collected test data in Ivalo, northern Finland, using a commercial infrared camera by Xenics and additional band pass and polarization filters. The camera was sensitive in the short wavelength band 900–1700 nm. The results showed enough potential to continue the development. Figure 13 gives an example of ice detection.

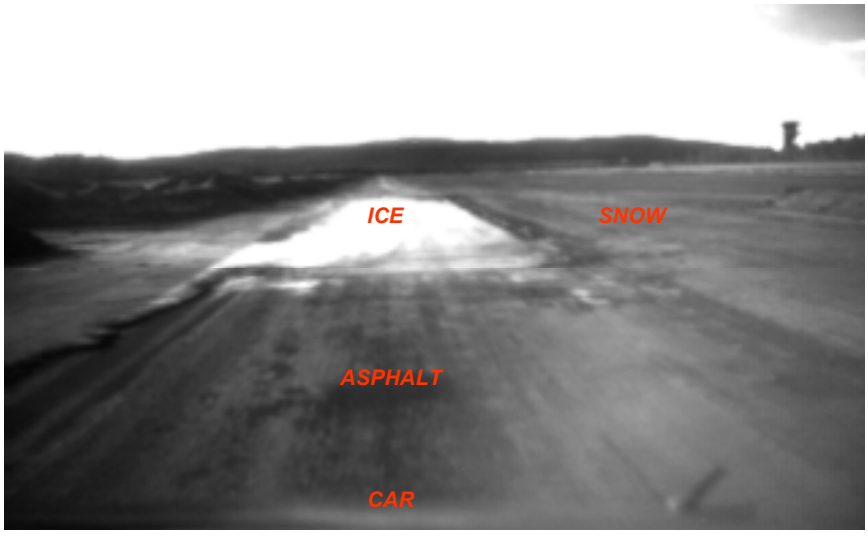

Figure 13. Near infrared camera image from a test track in Ivalo, using a 1600 nm band pass filter. Ice is clearly visible from a distance.

However, the existing cameras, which operate above 900 nm, were considered to be too expensive for ADAS applications. Therefore, an alternative approach was selected: the current prototype is based on a stereo camera body by Videre Design and additional polarization filters. The camera system uses low cost silicon detectors, which limit the bandwidth to below 950 nm. The camera system uses mainly the visible spectrum instead of near infrared.

The system does not include any dedicated illumination. It relies on ambient illumination from external light sources in order to keep the hardware costs low. The illumination level in the visible band is usually sufficient for the camera when driving. However, when no other light source than the car's own headlights are available, performance drops.

If the sensor was required to work as a stand-alone system, the lighting could be re-considered. However, IcOR, like most environmental sensors, would work best when its output is combined in an application with other information sources. IcOR is also designed with other camera-based ADAS applications in mind, such as lane keeping; several applications should be covered with a single camera.

The IcOR system includes two different analysis methods:

- polarisation difference
- granularity estimation.

The polarization measurement principle is displayed in Figure 14. Light reflection from a mirror-like surface (ice or a wet patch) reduces the amount of vertically polarized light compared to the horizontal plane [44]. When comparing the relative difference between horizontal and vertical polarization planes (I_h-I_v), and ignoring absolute intensity levels, ice or water reflectance causes an "abnormal" change. A detailed description of the measurement principle can be found from [45].

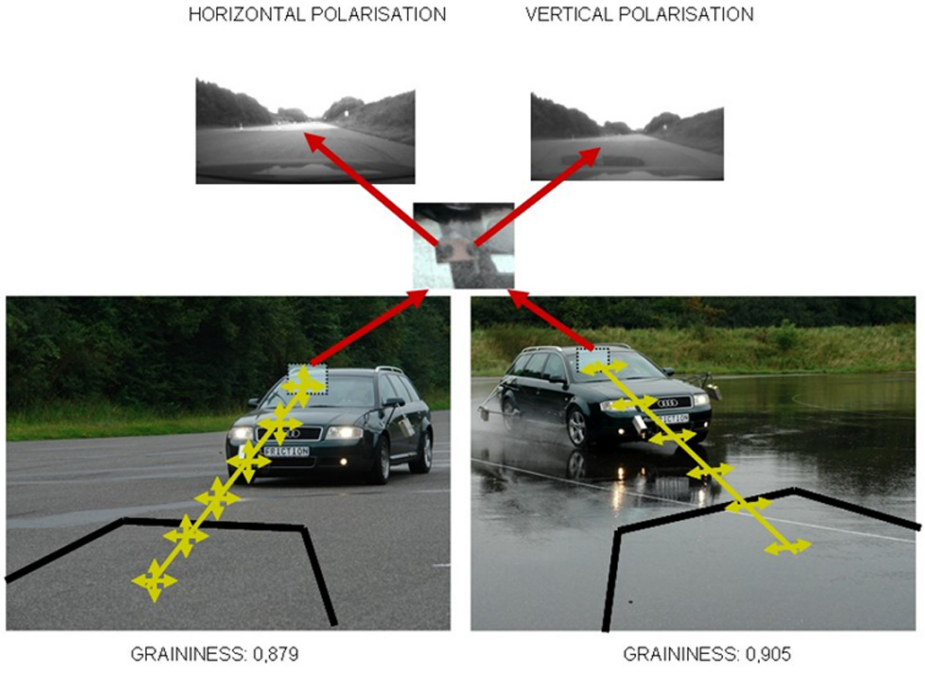

Figure 14. The IcOR uses a measurement principle based on suppression of vertical light polarisation when reflecting from mirror-like road surface. In addition, graininess analysis is used to distinguish icy and wet roads. [40]

Graininess analysis supports the detection of road conditions since hypothetically an icy road is smoother than snow or asphalt, which typically forms a granular surface. The key idea is to perform low-pass filtering for an image and calculate the contrast difference of the original and filtered images. This provides information on the graininess of the picture.

The polarisation analysis enables the detection of wet and icy road surfaces. Graininess calculation is needed to recognise snowy roads. According to first tests, the IcOR system is able to classify icy, snowy and wet roads with 70–90% accuracy [45, 40, 2]. However, the system performance degrades when visibility

is poor due to low light, dirt, strong reflections, heavy rain or snowfall, with camera measurements becoming difficult in general.

The success of the classification depends on manually tuning camera parameters to match background lighting. Future development is aimed at addressing automatic calibration. Alternatively, the performance could be improved with active lighting.

In this study the IcOR camera and Road Eye were used for different purposes, compensating for the weaknesses of each other: the Road Eye has a faster response time and higher reliability, but it measures only a single point just in front of the vehicle. The IcOR system has the advantages of

- being able to detect patches of ice 10–30 meters beforehand
- theoretically measuring over the whole lane and even for different vehicle trajectories (only partial implementation was tested during this study)
- to make granularity-based road-type classifications.

A software tool running in a Windows laptop exists for setting up the camera, saving data and running the analysis. For data fusion purposes it was designed to broadcast the confidence values of ice, dry, water and snow classifications to a vehicle CAN (Controller Area Network) and capture the time stamp from the network in order to synchronise the sensing.

3.2.4 APOLLO/FRICTI@N project tyre sensor

Of the sensors originally developed and tested during the APOLLO project [3], Helsinki University of Technology chose an optical displacement sensor for FRICTI@N project purposes. The optical tyre sensor has been a tool to study dynamic tyre behaviour. It is mainly intended for research purposes and studying the information available from deformations of the tyre carcass. The basic idea is to find a correlation between carcass deformations and forces applied to the tyre.

In addition to vehicle and tyre state estimation, the optical sensor can be used in validating tyre models.

The sensor uses a PSD (Position Sensitive Detector) chip mounted on the rim together with a convex lens to measure the movement of a Light Emitting Diode (LED), which is glued to the inner liner. This is illustrated in Figure 15. The figure also shows an example of measuring lateral displacement. Output from

the optical sensor is the measured displacement of the diode on the inner liner, relative to the rim.

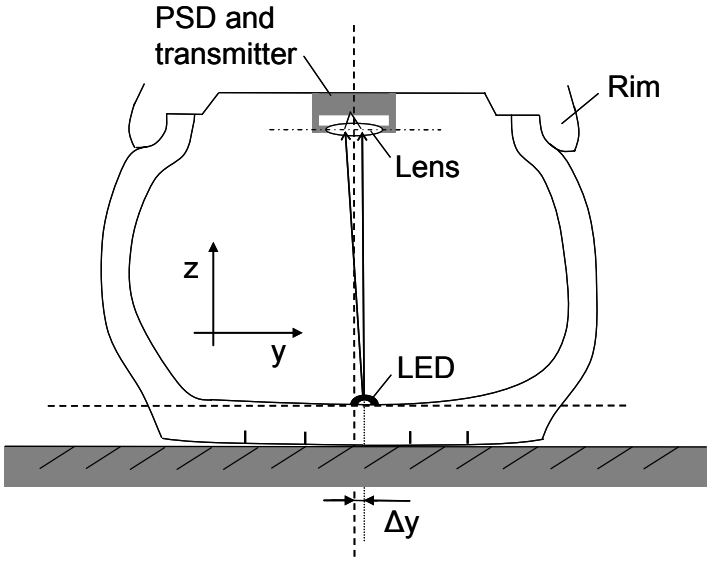

Figure 15. Optical tyre sensor set-up and illustration of measuring tyre carcass lateral deflection from inner liner.

Horizontal movement changes the current at the four borders of the PSD. With decreasing distance between the PSD and the light emitter, the light intensity will increase, increasing the overall current. Lateral displacement is a result of lateral forces, longitudinal displacement indicates longitudinal forces and vertical displacement is a result of wheel load change.

A digital radio system is used to transmit the measured data. The data is transmitted using the 433 MHz ISM (industrial, scientific and medical) radio band. The receiver translates the data protocol to signals which are made available at a CAN bus. The receiver box and the measurement tyre are shown in Figure 16. [3, 2]

Figure 16. Measurement tyre in Aachen tests, August 2008

During the FRICTI@N project, a new sensor housing was developed, data communication was enhanced and force calculations were advanced to be done in real-time, which was a requirement for online friction estimation [46]. Most of the development work was done by the Helsinki University of Technology.

The longitudinal movement signal (Figure 17) carries most of the information. It reveals the contact length – the amplitude is proportional to the contact length – and the longitudinal forces. The update rate is, however, limited to one sample per rotation, so the forces cannot be accurately measured e.g. during ABS braking.

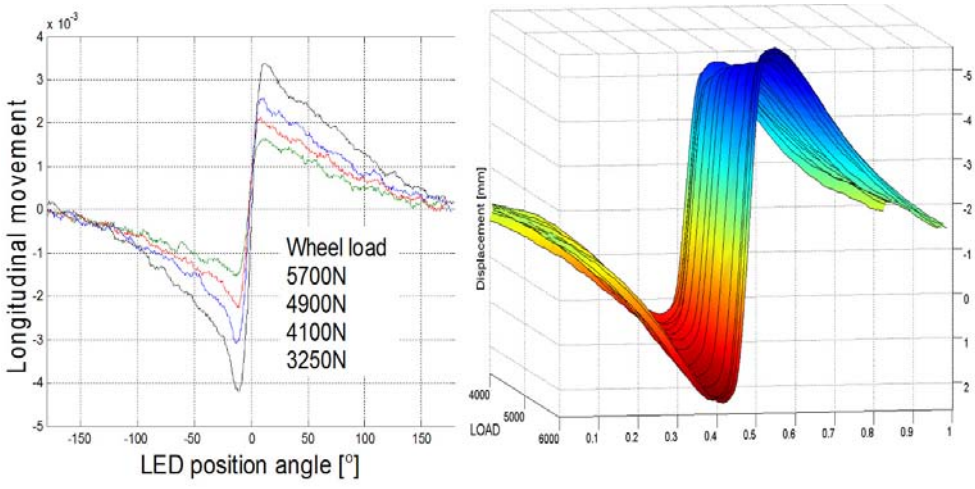

Figure 17. Tyre sensor longitudinal movement with different wheel loads. Measurement on left by Helsinki University of Technology and FEM by Nokian Tyres [2].

The longitudinal movement signal can further be used to also estimate vertical force and wheel load. Even if the vertical movement correlates better with the vertical force, the LED intensity signal used to measure the vertical movement depends on temperature, supply voltage and orientation angle. The longitudinal movement signal is almost independent of these factors.

The lateral tyre force enables an estimation of the vehicle slip angle quickly: the tyre force starts acting before velocities can be measured from the chassis.

Changes in tyre inflation pressure introduce a bias to the force estimates. Therefore the tyre pressure must be measured or estimated.

The optical sensor has also been demonstrated as able to detect different stages of aquaplaning based on tyre deformations. A detailed analysis of an optical tyre sensor in aquaplaning can be found from [47].

The general possibilities for detecting the friction potential with tyre sensors were studied with FEA simulations during the FRICTI@N project by Nokian Tyres. The tread pattern is "testing" the friction potential all the time in the contact patch through contact deformations (e.g. tread lug compression and release), but the deformation differences between different friction potential levels are small. In the inner liner, these differences are even smaller and cannot be measured with conventional sensors.

In the friction estimation system of this study, the main outputs used from the tyre sensors were friction used values for each tyre. The tyre sensors can provide

useful information in situations where one tyre is using more friction than the vehicle on average. Moreover, the effect of wind speed, which causes uncertainty and error for vehicle sensors, does not disturb the tyre force calculations.

As the sensors were available for only a few select tests rather than throughout the study, the tyre outputs were given a complementary role in data fusion, providing detailed information on friction used and aquaplaning.

3.3 Summary and sensor development

Simulations have shown that a tyre sensor could theoretically be the one sensor capable of continuous friction potential estimation. Accuracy, durability, power generation and communication problems, however, delay their introduction. Besides, even tyre sensors cannot measure the friction in front of the vehicle. A data fusion approach is generally required to support a broad range of applications.

Environmental sensors have large potential in detecting the road conditions for future automotive applications. The sensor readings can give a good idea of friction levels that can be used as an initial estimate for applications, much in the way that the driver perceives his environment. In particular, broad attention has been given by Nordic R&D projects to the new spectroscopy based sensors (e.g. from Optical Sensors and Sensice) targeting automotive applications and the detection of ice, snow and water on the road.

The need to utilize current environmental sensors to their fullest is evident in laser scanner and radar development. Enhancing current sensors with abilities to estimate friction potential would be a cost-efficient approach. VTT has demonstrated ice, snow and water detection with radar frequencies and Ibeo has added rain and snowfall detection to their laser scanner.

Figure 18 shows the coverage of environmental sensors available in the FRICTI@N project, where several approaches show promise. The yellow colour marks the areas where future work is perceived.

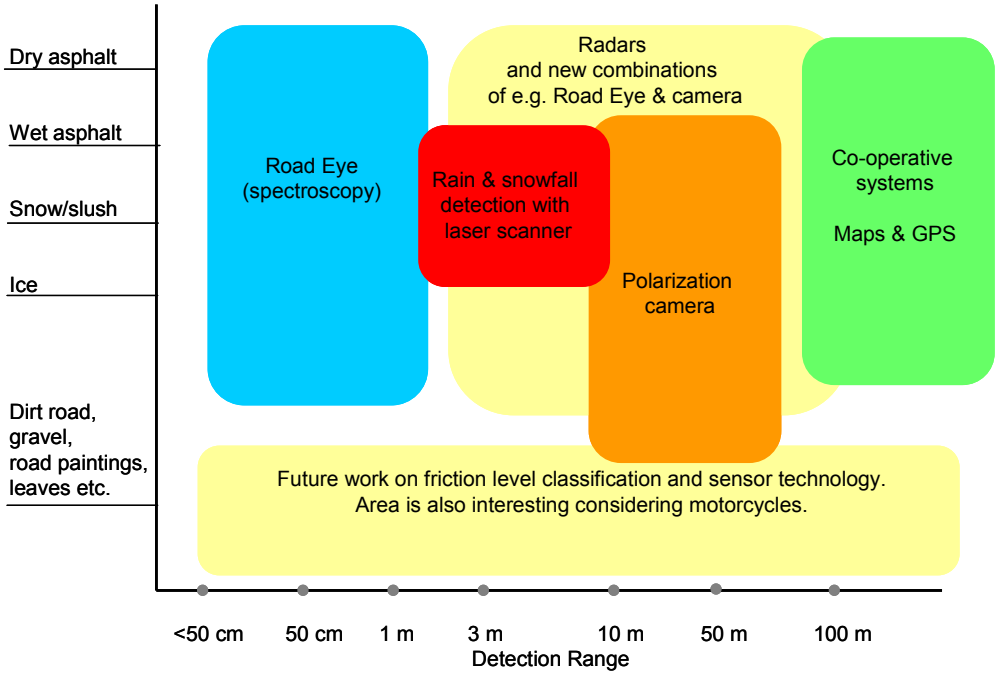

Figure 18. Environmental sensor coverage in the FRICTI@N project.

Future environmental sensor development could be perceived e.g. with camera-like sensors measuring wide areas using spectroscopy principles, as point measurements do not reliably cover the vehicle path.

During this study a need was seen for an improved classification and mapping of measured road and weather conditions to friction levels. Many factors affect e.g. friction potential on ice, such as sunshine and previous braking polishing the ice. These factors are mostly known but their exact relationships and prioritization of key variables for measuring friction is complicated. This could be addressed in further environmental sensor research.

The classification requirements could also be viewed from the point of view of motorcyclists: Detecting small slippery areas such as pit cover plates, road paintings and leaves would then become more important than with cars.

High-grade roadside sensors such as the Vaisala Remote Road Surface State Sensor DSC111 are able to measure ice, snow and water layer thicknesses, but the sensors of this study rather indicate certain minimum layer thicknesses that they are able to detect. The layer thickness affects the measurement readings of

both Road Eye and IcOR camera, but an accurate classification in a moving vehicle remains a topic for development.

With vehicle dynamics sensors, cost has been a limiting factor for using high-performance IMUs and also when considering additional sensors for e.g. steering torque. For accurate friction detection, at least a high-grade IMU would be beneficial for estimating the true ground speed and vehicle rotations during braking. The true ground speed compared with wheel speed gives the wheel slip, an indicator essential to friction potential estimation. The IMU used in this study was a common automotive grade test sample from VDO Automotive AG. It is necessary to take roaming (growing integration error over time) into account when designing true ground speed estimation with automotive IMUs.

The following chapter presents how the selected sensors were used in the data fusion and introduces methods for environmental sensor data fusion, combining vehicle dynamics measurements.

4. Friction Processing and Data Fusion

The friction estimation system of this study was designed to support different sensor configurations, where the performance of the available sensors can vary in different weather and driving conditions. To achieve this, a modular architecture was used.

4.1 Friction processing architecture

The friction processing model (Figure 19) is based on sensor data fusion from various sources:

- environmental sensors (e.g. camera)
- vehicle sensors (e.g. accelerometer, wheel speeds)
- tyre sensors (APOLLO project prototype).

The sensor signals are gathered within the input **data gateway**, which filters the data and passes them to three friction feature fusion modules: environmental (EFF), vehicle (VFF) and tyre (TFF). Features, according to [48], are "an abstraction of the raw data intended to provide a reduced data set that accurately and concisely represents the original information".

The data gateway is intended to be the only interface which has to be updated for different cars, sensors and applications. The system parameters and the final and intermediate outputs can all be accessed via the data gateway. This also enables the feature fusion modules to utilize the results (detected features) of other modules. In the main, it is the VFF module, which is always required, that produces calculations for friction used and slip to support the other modules.

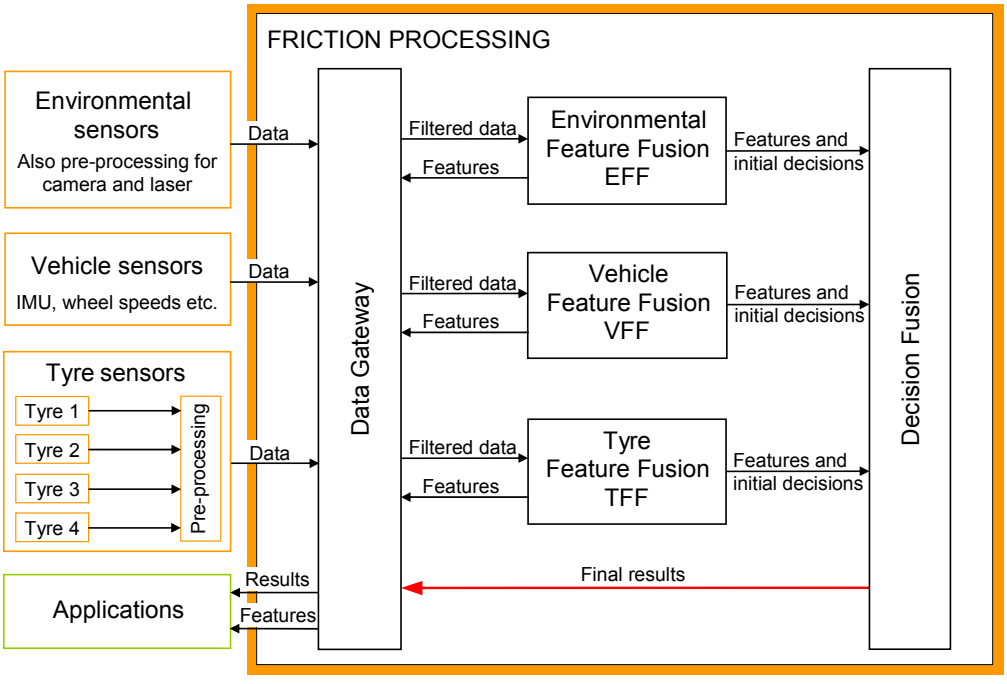

Figure 19. Friction Processing Architecture.

The gateway takes care of two main data conversions:

- Receiving specific messages from the vehicle bus and converting them to specified input signals for the friction estimation system. The input signals and their ranges are listed in Table 5, Chapter 4.2.
- Receiving outputs from friction processing and converting them into vehicle-specific messages (Table 7). If the friction estimation system does not include all three modules, all outputs cannot be provided.

The purpose of the three **feature fusion modules** is to analyze and combine data coming from sensors in their category. For example the environmental feature fusion module (EFF) calculates an initial probability for ice on the road based on camera and temperature readings. The VFF provides processed information based on sensors measuring the vehicle state. It produces for example friction used readings based on acceleration measurements. The TFF module processes information from tyre sensors, yielding e.g. the risk of aquaplaning.

The main outputs of each friction estimation module are

- friction used (not valid for EFF as non-contact sensors)
- friction potential
- upcoming friction (valid only for EFF and its forward-looking sensors)
- validity of the information
- additional information on road conditions and vehicle & tyre status.

The output is dependent on the modules' capability and the available sensors. All friction values produced by the feature fusion modules are tagged with validity information (the exact use will be presented later). In addition the type of error distribution should be available for fusion, when applicable.

The friction information and additional outputs of the feature fusion modules are combined in the **Decision Fusion** module, which provides the final system outputs. Decision-level fusion, according to a general description [48], "seeks to process identity declarations from multiple sensors to achieve a joint declaration of identity".

In all, the selected architecture is based on traditional *feature extraction* and *decision fusion* models, with an emphasis on modularity.

The realization of the architecture with MATLAB Simulink for the demonstration vehicle, as presented in Figure 20 and Figure 21, consisted of:

1. Data acquisition and data gateway running at 100/200 Hz. The camera, laser and tyre sensor data have already been pre-processed before entering the main processing. This is due to the amount of raw data handled by these sensors.

2. Friction processing running at 100 Hz. The detailed architecture is displayed in Figure 21.

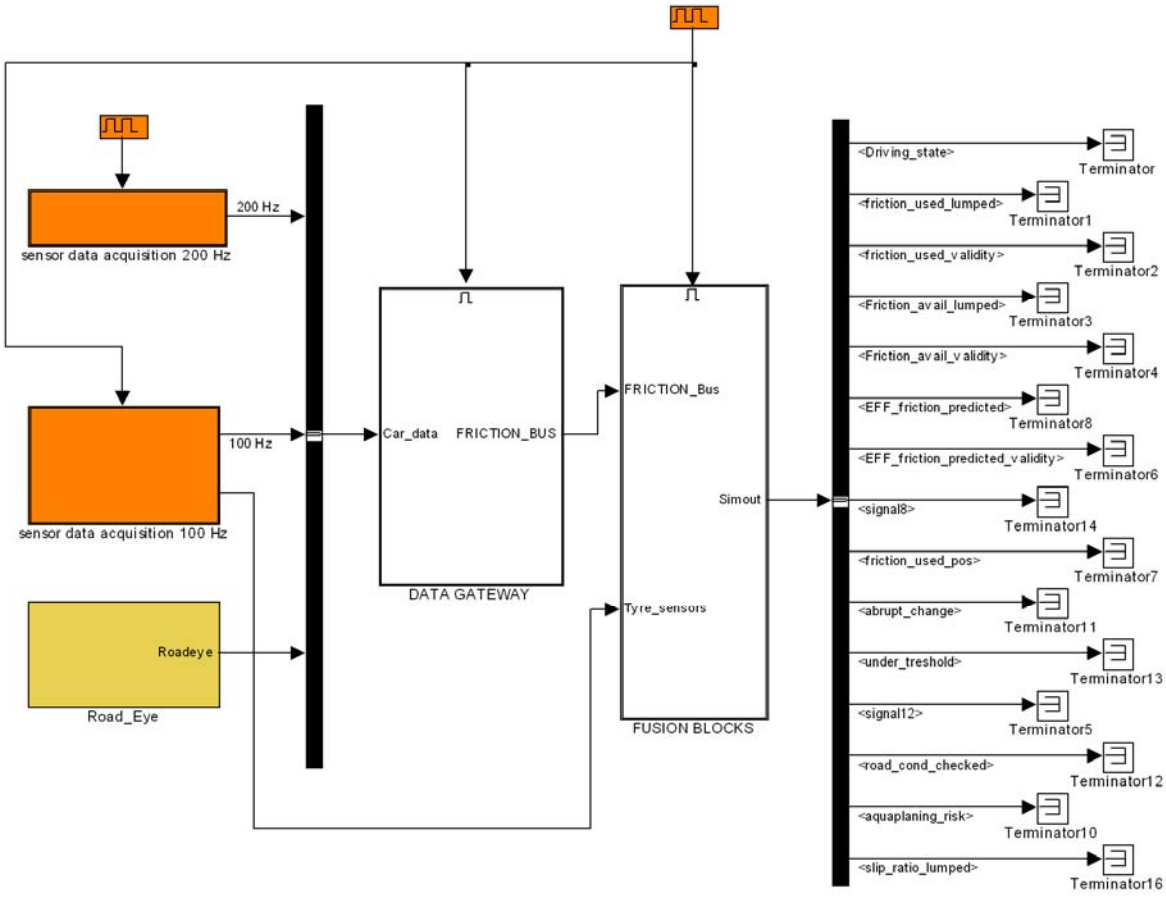

Figure 20. MATLAB Simulink top level view of implemented software. The data acquisition and gateway on the left and friction processing in the middle, running 100 Hz.

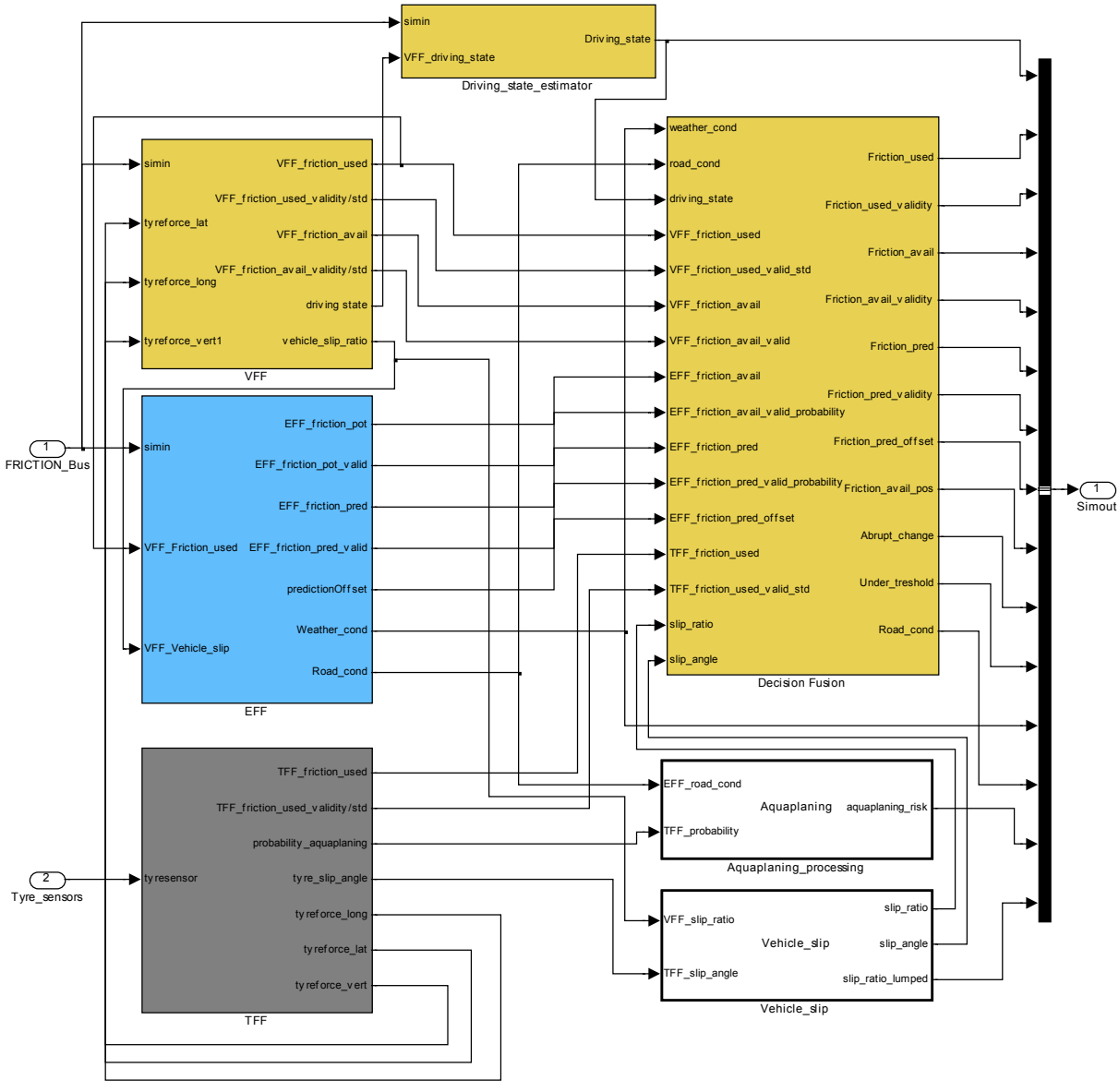

Figure 21. Simulink realization of the friction processing block of Figure 20.

The VFF, EFF and TFF blocks, on the left side of the Figure 21, provide friction used and friction potential estimates to be combined by the Decision Fusion. Additionally the figure shows blocks for driving state analysis, aquaplaning in-

formation processing (final decision at Decision Fusion level) and combining vehicle slip calculations based on VFF and TFF data (also Decision Fusion level). The architecture design did not require modifications when implemented, although the modularity aspects are not as evident in a single Simulink model. The EFF and TFF blocks can be fully disabled in the system, representing cases where these modules are not available. In most vehicles at least the road temperature is available for EFF processing.

The 100 Hz processing was found to be sufficient for the friction fusion with the sensors used. The camera, laser and tyre sensors use different internal sampling in their processing; the 100 Hz refers to the vehicle sensor, e.g. IMU acquisition.

As an example of the effect of different sampling frequencies, Figure 22 presents a maximum braking test captured with the development vehicle accelerometer. The measurements are for longitudinal direction only. The top-left graph is the velocity and the others show the longitudinal acceleration captured with different frequencies (MATLAB resample from 100 Hz data). For simple requirements, a sampling rate of 5 Hz is sufficient to capture the moment of maximum braking, but more advanced calculations seem to require at least 10 Hz.

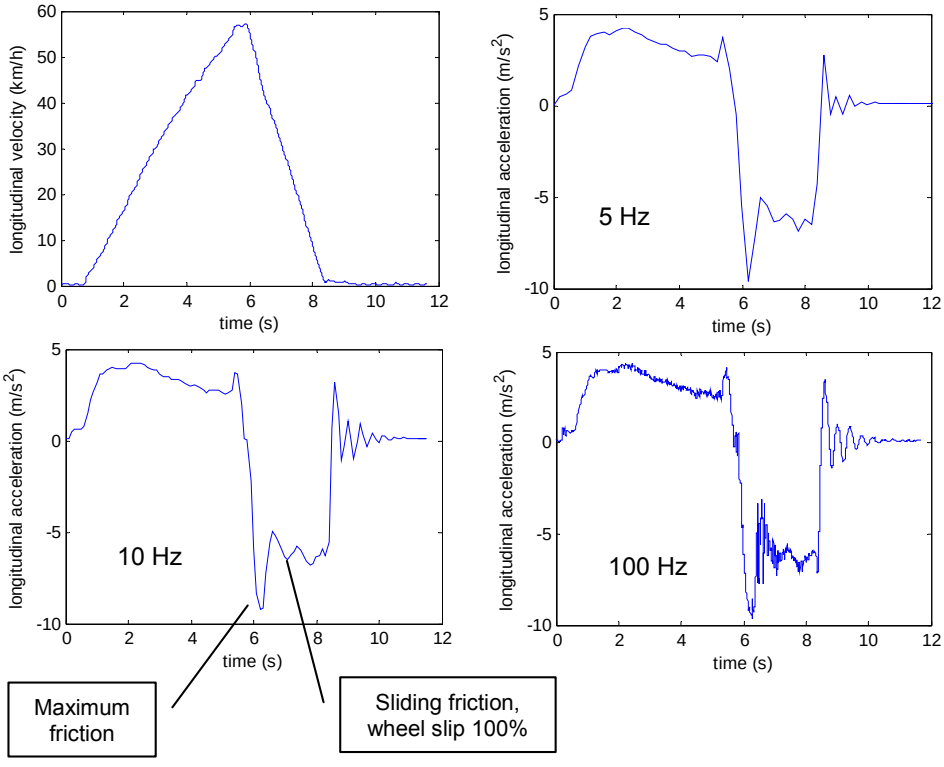

Figure 22. Maximum deceleration captured with different sampling rates.

4.2 System inputs and outputs

The system inputs are raw sensor data except from tyre, camera and laser sensors. These sensors used separate pre-processing in this study.

Most input signals are or were made available on the development vehicle buses (internal communications networks). The friction processing Rapid Prototyping Unit (RPU) provided input connections for signals that were not available on the vehicle bus. Chapter 5 further discusses the implementation in the development vehicle.

Different sampling rates are accepted, but due to the processing, a frequency of 100 Hz was preferred. The sensors that have a notable latency in their processing (due to e.g. data transmission) need particular handling to properly synchronize their data with other sensors.

For each sensor a definition for the Region Of Interest (ROI, where the measurements originate) and installation co-ordinates in the vehicle frame are required. The provisional sensor inputs are listed in the following table.

Table 5. Inputs to the friction estimation system as defined in the FRICTI@N project [2].

Input sensor signals	Corresponding signal name	Unit	Used by			Remarks
			VFF	EFF	TFF	
Steering wheel angle	delta	rad	x	x		
Longitudinal acceleration	ax	m/s^2	x		x	
Lateral acceleration	ay	m/s^2	x		x	
Vertical acceleration	az	m/s^2	x			
Pitch rate	pitchRate	rad/s	x			
Roll rate	rollRate	rad/s	x			
Yaw rate	yawRate	rad/s	x		x	
Wheel rotational velocity	vWheelij	m/s	x		x	one for each wheel
Brake pressure	pBrakeij	Pa	x		x	one for each wheel
Brake signal	brakeSignal	Boolean	x			1 bit
Engine torque	MEngine	N·m	x		x	
Steering torque	MSteering	N·m	x			
Vertical force	Fz_ij	N			x	ij *
Lateral force	Fy_ij	N			x	ij *
Rotational velocity	vel_tyre_sensor_ij	1/s			x	ij *
Risk of aquaplaning	aquaplaning_ij	%			x	0% none; 100% full
Tyre estim. Frict. Potential	myy_tyre_sensor_ij	-			x	ij *
Air temperature	airTemperature	°C		x		
Road temperature	roadTemperature	°C		x		
Precipitation density (Laser)	precDensityAl	-		x		
Ground Truth vehicle Velocity_x (Laser)	vehicleVelocity-GroundTruthX	m/s		x		Optional sensor. IMU or a separate ground speed camera can be used
Ground Truth vehicle Velocity_y (Laser)	vehicleVelocity-GroundTruthY	m/s		x		
Ground Truth vehicle Velocity_x, confidence (Laser)	vehicleVelocity-GroundTruthXConf	%		x		
Ground Truth vehicle Velocity_y, confidence (Laser)	vehicleVelocity-GroundTruthYConf	%		x		
Road Eye sensor based on spectroscopy	Wave-length1_Intensity	-		x		Data to be processed in EFF

	Wave-length2_Intensity	-		x		
Camera system based on light polarization plane differences	icePolarization	%		x		0: Dry; 1: Icy 4: Wet; 7: N/A
	icfePolariza-tion_conf			x		Confidence level ** 0: 100–80% 1: 80–60% 2: 60–40% 3: 40–20% 4: 20–0% 5: not updated *** 6: not valid
Camera system based on light intensity in 1200–1600 nm wave-lengths, result and confidence	roadCondNIR	-		x		Optional sensor. 0:Dry; 1:Icy 2:Snowy; 3:Slushy; 4:Wet; 7: N/A
	roadCondNIR_conf	%		x		confidence
Vehicle velocity	vVehicle	m/s		x		
Tyre pressure	pTyre	Pa	x		x	

* ij ∈ {00=FL, 01=FR, 10=RL, 11=RR}

** Definition used in the prototype system

*** The value could not be reliably estimated. The output will be the last valid value.

The friction estimation system also requires a number of input parameters to be defined on the data gateway. These are values describing the car geometry, mechanics, wheels etc. Especially the VFF contains vehicle-model-based approaches requiring detailed information. Also the EFF algorithms have parameters such as thresholds. The following table gives an example of the required parameters.

Table 6. Some required system parameters.

Required system parameters	**Unit**
Sampling time	s
Static wheel radius at front axle	m
Static wheel radius at rear axle	m
Moment of inertia of the wheels of the front axle	$kg \cdot m^2$
Moment of inertia of the wheels of the rear axle	$kg \cdot m^2$
Distance from centre of gravity to front axle	m
Distance from centre of gravity to rear axle	m
Wheel track of the front axle	m
Wheel track of the rear axle	m
Total mass of the vehicle	kg
Weight on the front/rear axle	kg
Height of the centre of gravity (from axle level)	m
Moment of inertia of the car around its z-axis	$kg \cdot m^2$
Understeer coefficient	deg/*g*

The system must deliver the friction estimated by the algorithms and additional information concerning weather, road and tyre condition. The system outputs are listed in Table 7.

Table 7. Current outputs of the friction processing.

Output type	Signal	Unit	Range		Remarks
			min	max	
Estimated friction used	Friction_used	–	0	1.6	if TFF active, separately for all tyres
Estimated friction potential	Friction_pot	–	0	1.6	
Predicted upcoming friction potential	Friction_pred	–	0	1.6	
Estimated friction used validity	Friction_used_valid	–	0	6	Alternatively a decimal value between 0.00–1.00 or mapped to confidence levels: 0: 100–80% 1: 80–60% 2: 60–40% 3: 40–20% 4: 20–0% 5: not updated ** 6: not valid
Estimated friction potential validity	Friction_pot_valid	–	0	6	
Estimated upcoming friction validity	Friction_pred_valid	–	0	6	
Time to reach friction predicted	Friction_pred_offset	ms	0	60000	
Estimated friction potential position	Friction_pot_pos	–	0	3	0: left side; 1: right side 3: overall vehicle
Vehicle slip ratio	Vehicle_slip	%	0	100	lumped value for the whole vehicle
Weather condition	Weather_cond	–	0	7	0: Rain; 1: Snow 2: Fog; 7: N/A
Road condition	Road_cond	–	0	7	0: Dry; 1: Icy 2: Snowy; 3: Slushy 4: Wet; 7: N/A
Tyre force – vertical	Tyreforce_vert_ij *	N	0	8 000	ij *
Tyre force – lateral	Tyreforce_lat_ij *	N	–8 000	8 000	ij *
Risk of aquaplaning	Aquaplaning	–	0	7	Devel. stage of aquaplaning 0: 100–80% 1: 80–60% 2: 60–40% 3: 40–20% 4: 20–0% 7: N/A
Possibility of aquaplaning position	Aquaplaning_pos	–	0	3	0: left side; 1: right side 3: overall vehicle
Abrupt change	Abrupt_change	–	false	true	post-processed according to thresholds
Under threshold	Under_threshold	–	false	true	post-processed according to thresholds

* ij ∈ {00=FL, 01=FR, 10=RL, 11=RR}

** The friction value could not be reliably estimated. The output will be the last valid friction value.

4.3 Sensor data fusion principles

The following describes the details of the architecture implementation: the algorithms and outputs from the VFF (vehicle) and EFF (environmental) feature fusion modules, and the Decision Fusion approaches used. The use of TFF (tyre) algorithms is discussed from a fusion standpoint.

The general data fusion approach of this study is based on the *construction of expert systems*. First the sensor data is analysed for the identification of friction related features. An example of this would be ice detection with a camera. The features are then used in determining road conditions.

When possible, each detected feature is also assigned a probability or "validity" to enable fusion with other similar measurements. The validity was, depending on the case, based on

- the likelihood of detection
- algorithm internal validity checks
- time after the previous update of the measurement.

Statistical distribution for the measurements could also be used to combine features, but this information was not available during development. For some EFF and VFF algorithms, tests were made in different conditions to estimate the reliability and come up with e.g. weight factors for fusion.

In studies such as the ProFusion2 project [49], the "completeness of the detected feature" has also been used for fusion validity checking.

Plausibility checking of detections and road conditions is done in many phases in the algorithms. For example the plausibility of ice detection from a camera is low if the road temperature is measured to be +20 °C. However, even if the surface would not be icy, it may have a similar level of friction potential and some matching features. Both assumptions of slippery surface are clearly false if the vehicle is at the same time using a friction coefficient of 0.3 or higher.

Force, acceleration and slip measurements are also used directly in various VFF and TFF algorithms to estimate friction used and friction potential. In addition to analysing features, the feature fusion modules provide these *initial estimates* for friction used and friction potential. Even the EFF module provides an estimate for friction potential, although it does not directly measure forces. EFF learns from recorded historic friction levels on different surface types. If no re-

corded match exists, a rough classification in ice, snow, wet and dry asphalt classes is used to provide a literature-based average value for friction potential.

The used fusion approach is a hybrid. It contains several modules and cannot be simply described as using e.g. fuzzy logic or neural networks to estimate friction. The tools most similar to the used methods are Bayesian network and decision trees.

The Bayesian networks can be used to describe e.g. the relationship between rain and a wet road, where there could be a 90% chance that the road is wet, given it is raining. This study first used this simplified link between rain and a wet road, but later the laser scanner's precipitation value (when classified as rain) was chosen to increase the probability of a wet road detected by IcOR and Road Eye together. This second simplification creates a link between the amount of rain and the amount of water on the road, but also lacks detailed modelling. For example, it would be important in further studies to model the time aspect: a road does not instantly become wet when it starts raining. During the winter time, however, if rain drops are super cooled, ice could form in an instant.

Decision trees use a tree-like model of decisions and their possible consequences. They can also be used to classify road conditions by performing consecutive checks [50]. For example the road temperature could be either below or above zero. As a next step of classification, there could be rain or not.

Weighted averaging is a simple fusion method, useful when combining results from similar sensors. This approach was used especially in EFF, after the weights were identified based on experiments. Moreover, driving state detection was used in VFF to select and give momentary weights for different algorithm outputs.

In the early phases of the FRICTI@N project, a neural network approach was unsuccessfully tested for the VFF full raw data set. This does not mean there is no room for such methods (see e.g. [51]), especially when data has been post-processed and the relationships and latencies are already analysed.

Considering the complex phenomenon and the required driving conditions to detect friction potential, the problem is maybe best addressed in defined pieces instead of using large "black box" models. The suggested friction processing architecture was created to match the user needs listed [11] in the FRICTI@N project and especially to fulfil the requirements of modularity.

The EFF architecture has particular similarities to the fusion framework introduced by ProFusion2 [49], a subproject of PReVENT IP, in 2007. The framework suggested by ProFusion2 for object detection has three main data abstraction levels for processing data:

(I) sensor refinement

(II) object refinement

(III) situation refinement.

The Figure 23 gives an overview of the EFF data processing mapped to ProFusion2 levels. The actual EFF implementation is later explained in Chapter 4.3.2. The term 'object refinement' is renamed as 'feature refinement' for the figure, as a generalization of the architecture. The original work discusses detecting objects on a road.

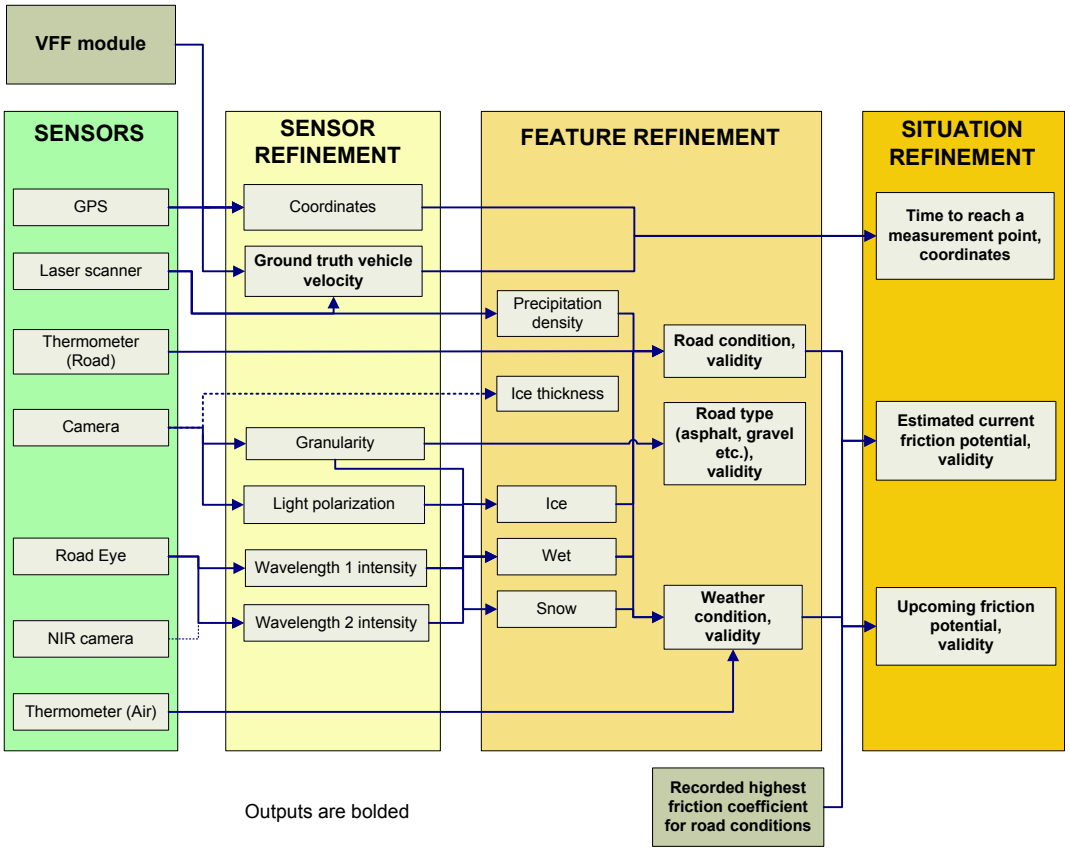

Figure 23. EFF data processing described using ProFusion2 architecture.

4.3.1 VFF – Vehicle Feature Fusion

The vehicle dynamics sensors capture the vehicle motion and states, such as acceleration in different directions and steering angle. These measurements as well as the vehicle dynamic response to different driving manoeuvres can be used to estimate friction.

Generally the effects caused by friction are small, with low values of acceleration and slip. In [31] a lateral acceleration of 0.3 *g* was required as an input to an algorithm to estimate friction potential on different surfaces. When analyzed, this lateral acceleration requirement actually means three things:

1. friction potential on ice (< 0.25) would not be detected using the algorithm before high slip occurs
2. on snow and asphalt, the algorithm would be able to detect the friction potential before uncontrolled sliding
3. the estimate is not available continuously, for example, not during straight driving.

The general difficulty in distinguishing a difference between friction levels can be explained with Figure 24. With the small values of friction used, the curves and their slope are close to each other. There are differences, but common measurement noise makes it difficult to detect them until either (or both) a slip of about 5% or a friction used value of about 0.3 is reached. This is a problem especially in systems aiming at fast tracking friction [52].

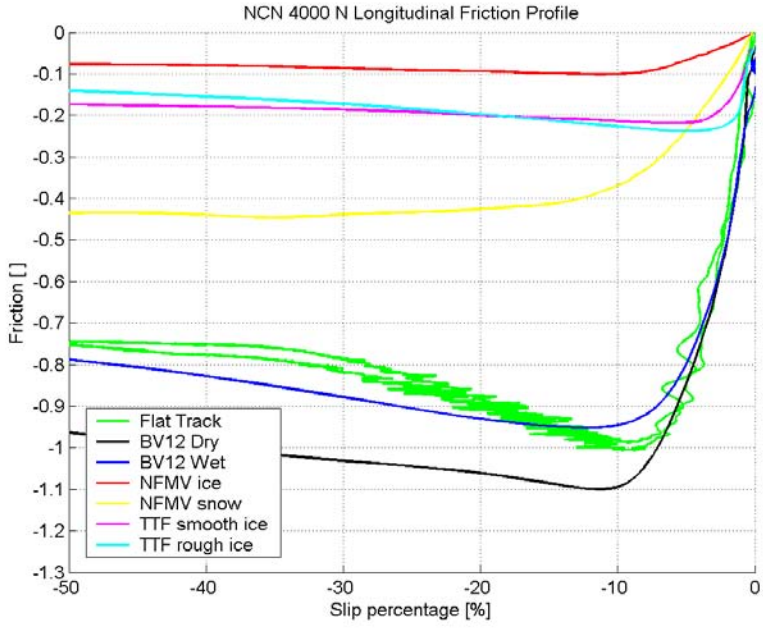

Figure 24. The friction profile of Nokian Tyres' WR 205/60R15 (NCN). Tests for dry and wet asphalt performed with Pirelli Flat Track and VTI BV12; Nokian Friction Measurement Vehicle for ice and snow; VTI Stationary Tyre Test Facility for smooth and rough ice. Load 4 kN. VERTEC project material. [12]

Similar conditions for clear differences can be derived from the following figure that plots the relationship between lateral forces and slip angle. Lateral forces are equally used to detect friction potential, although the algorithms do require cornering at a certain minimum speed.

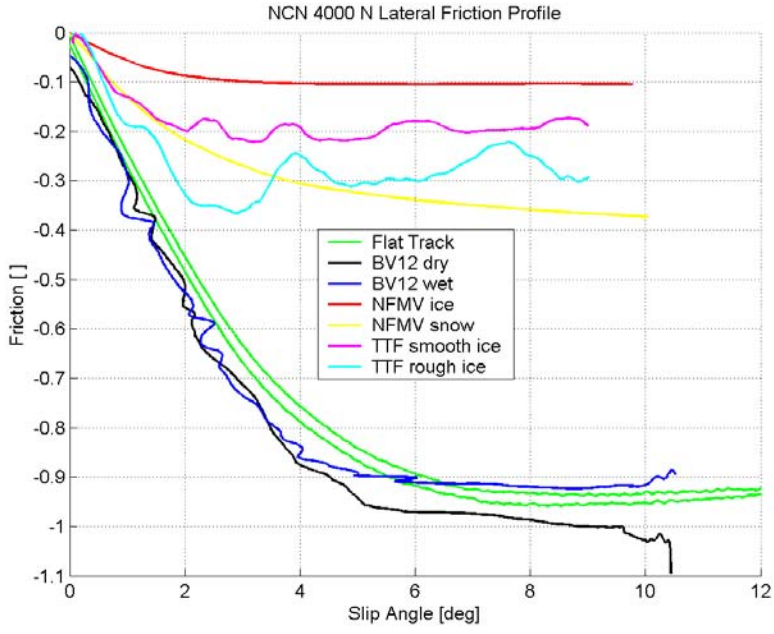

Figure 25. Same as Figure 26, except for lateral forces. [12]

The following algorithms were implemented in the VFF block:

- friction used calculation based on IMU acceleration measurements
- two wheel slip ratio estimation algorithms: one compares wheel speeds with integrated velocity from IMU during braking, the other uses a Correvit ground speed camera for reference during the study
- two separate approaches for friction potential estimation based on lateral forces. These algorithms were provided by VDO Automotive AG (Continental corporation) and CRF (Centro Ricerche FIAT S.C.p.A.).

VFF output respectively consists of

- friction potential estimated value
- friction potential validity
- friction used measurement with an estimated error range
- slip information to be used in decision fusion.

4.3.1.1 Friction used calculations

The definition for friction used was given in the Introduction while Equation 2 described it simply as the ratio of horizontal acceleration and gravitational acceleration when the vehicle was on an even surface. This simplification assumed perfect contact to the road and all four tyres active. Also air resistance slows down the vehicle even without friction forces at the tyre–road contact. The following figure shows the acting forces in more detail:

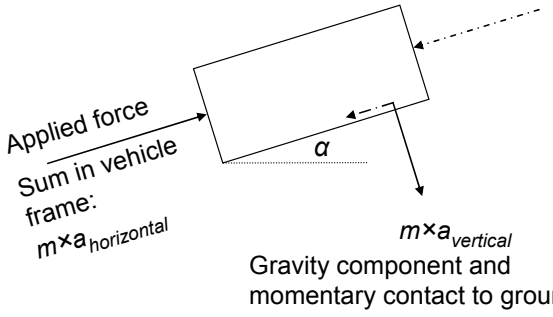

Frictional resistance, air resistance (~0.014 *g* deceleration when 100 km/h and 2000 kg car) and gravity component

(also rolling resistance, e.g. 0.01 *g*, and other dissipation, but in this work they are defined to be part of friction used by the whole vehicle)

Figure 26. Forces acting in the friction used calculation.

The friction used for the whole vehicle is calculated in this work using the following equation:

$$\mu_{used} = \frac{\sqrt{\left(a_x \cdot m + \left|F_d\right|\right)^2 + \left(a_y \cdot m\right)^2}}{\left|a_z\right| \cdot m}, a_z < 0 \quad (3)$$

First, the air resistance (F_d for "drag") is added to longitudinal acceleration (a_x) measured in the vehicle frame (co-ordinate system). This is a simplification due to not knowing the actual wind speed and approximating air resistance only in the direction of longitudinal movement. As a second step, the horizontal forces are divided with vertical forces. All accelerations are measured with an IMU fixed such that the x-axis gives vehicle longitudinal movement and the z-axis vertical acceleration in the vehicle frame.

Air resistance as calculated for the development vehicle of this study – an Audi A6 with a mass of 2188 kg, area (A) of 2.2 m^2 and a drag coefficient (C_d) of approximately 0.3, using the commonly known Equation 4 – causes a deceleration of 0.014 *g* at a speed of 100 km/h (assuming zero wind speed). The value

1.2 in the equation is an approximation for air density, affected by temperature and pressure.

$$F_d = 0.5 \cdot 1.2 \cdot v^2 \cdot A \cdot C_d \tag{4}$$

The air resistance is relatively small compared to friction levels used in maximal braking and therefore the simplification of Equation 2 is useful for a quick estimation.

If the vehicle is parked on an incline, it is using friction without any acceleration. When the vehicle is braking on an inclined road, a gravity component affects the deceleration. However due to the friction used definition, when both the vertical and horizontal acceleration are *measured in the vehicle frame*, the inclined road does not affect the calculation!

Usually the climbing angle on roads is small enough to be ignored, but even on a theoretic 30° incline and measuring a 1 *g* deceleration, the definition would correctly give |–0.5/0.866| for friction used (not including air resistance). Only half of the deceleration would result from use of friction and the other half is gravitational acceleration.

The rolling resistance of tyres and e.g. transmission resistance are often considered separate in detailed force and brake performance calculations, but this work includes these in the definition of friction used. This is because especially the VFF module studies accelerations for the vehicle as a whole and because generally friction between two objects includes both sliding friction and rolling friction. The rolling friction is, however, an interesting case: a free rolling tyre can be defined to have zero slip, even though the rolling resistance causes torque and a (small) pulling force or driving torque would actually be required to maintain speed [53]. Often the value is simply left out from calculations due to the small magnitude (around 0.01–0.02 *g*) compared to braking and due to being e.g. dependent on velocity, tyre model and surface. Some 1.5–3.5% of rolling resistance is even due to air resistance [13].

The presented definition for the vehicle as a whole makes friction used in certain cases a more useful indicator of a driving situation or driving style than plain acceleration:

- On inclined roads, acceleration measured with an accelerometer is partially due to gravity, but this does not mean the driver is accelerating. The acceleration readings may become misleading for analysts, while friction used still describes the situation.

- On snowy roads, vehicles might never reach acceleration-based definitions of “critical braking”, e.g. >0.7 *g*. However, the vehicle may be using all available friction.

Lumped friction used measurements do not capture differences between the wheels. The development vehicle was four-wheel drive, making some simplifications possible, but with 2-wheel drive cars and especially during acceleration, the friction used must be analysed for each wheel separately. The maximum acceleration for a 2-wheel drive vehicle is limited by friction more often than braking or cornering, where all wheels participate. Naturally the engine also sets limits for acceleration, around 0.4 *g* for the development vehicle but varying with velocity.

The vehicle pitch and roll angles are error sources for the lumped friction used calculations due to its definition. With the development vehicle, the pitch was measured at under 2° under hard braking and roll at under 5° during maximum cornering. As the IMU drift was considered too large to constantly detect the angles and the resulting errors were small except during maximum cornering (sin(5) = 0.087), these variables were left out of the final calculation. Further, pitch and roll angles as well as load transfer between tyres during hard manoeuvres affect more the accurate detection of dry asphalt friction potential than the detection of slippery surfaces, where the accelerations and load transfer are smaller. Sensors and algorithms approximating the vehicle pitch and roll angles could nonetheless improve the friction used estimations.

Figure 27 shows that larger changes in gravitational acceleration measurements can actually be induced by the pitch rate rather than the pitch angle itself. This sensor inaccuracy should be removed by filtering. Using the simple averaging of Equation 5 addresses both unwanted gravity measurement changes due to pitch rate and general acceleration sensor noise. In the equation, g_{t-1} refers to the previous averaged result of acceleration due to gravity.

$$g_{filtered} = \left(g_{t-1} \cdot 30 + g_t\right)/31 \tag{5}$$

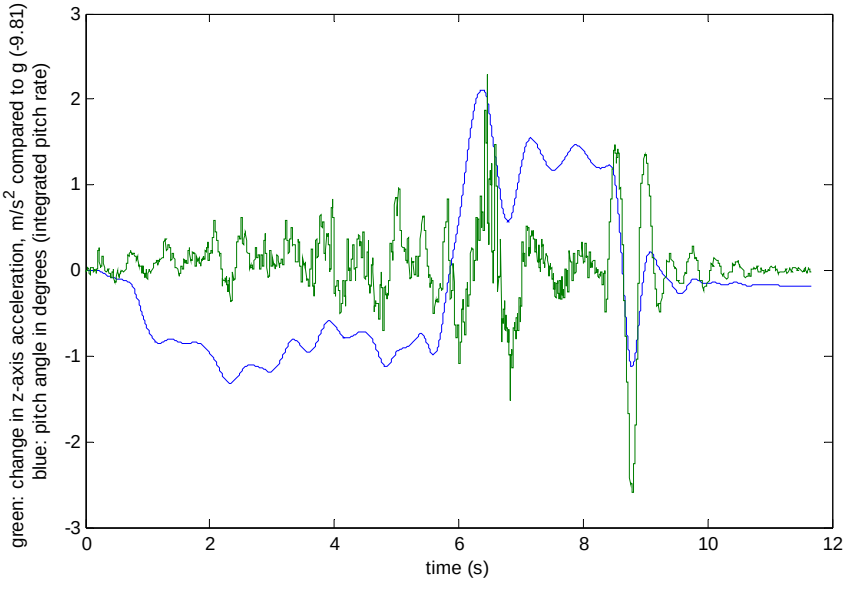

Figure 27. Integrated pitch angle (blue) from pitch rate and measured changes/errors in z-axis acceleration (green). The pitch angle itself causes a small error but the rate of change can have a larger effect.

Speed bumps and rough road surfaces also affect acceleration sensor measurements and momentary friction used calculations. The author conducted an indicative test (during the TeleFOT project in 2009) using BroadBit's GPS and acceleration logger prototype to assess the magnitude of these effects. The logger was fixed with tape near a passenger car parking brake.

A few measurement runs over speed bumps, attempting to keep a steady speed, showed that the bumps induced acceleration sensor measurement noise, and, when the readings were low-pass filtered using an adapted version of Equation 5, there were approximately changes of 0.1 *g* in car longitudinal acceleration. In vertical acceleration the speed bumps caused changes up to 0.5 *g* at legal speeds. The bumps were so long that the whole car was momentarily on the bump. As the car was driven manually in only four experimental runs and the accelerator pedal was not fully steady, these results are only indicative. No special bump compensation has been implemented into the friction calculations – it seems the errors would be rather small (0.1) compared to friction levels used while braking, as well as being momentary.

Similar tests on cobblestone and gravel showed that these surfaces cause higher than usual acceleration sensor measurement noise: logger's horizontal and vertical noise amplitude was around 2 m/s^2 vs. 0.7 m/s^2 on dry asphalt, without any filtering. However, no special filtering or surface classification based on acceleration was implemented in this study.

As a summary, friction used was calculated by a simple algorithm using filtered IMU-based acceleration measurements and an estimate for air resistance. The result was a lumped value for the whole vehicle. Tyre sensor measurements were optionally used to provide calculations at tyre level to detect possibly higher friction used values due to uneven force distribution.

4.3.1.2 Wheel slip estimation

Wheel slip is commonly divided into longitudinal slip ratio and side slip angle. Equation 6 shows a way to calculate slip ratio, comparing tyre spin velocity (r is the wheel radius, ω the angular velocity) with the linear speed of the tyre centre (v). Minor variations exist in the literature for a different handling of the cases when either speed is zero: in Equation 6 the slip varies from −100% to infinite, but depending on the exact definition, it can also be the other way around or limited to ±100% in both directions. [13 (pp. 18–19)]

$$slipRatio = \left(\frac{r\omega}{v} - 1 \right) \times 100\% \tag{6}$$

The tyre slip angle is defined as the angle between a wheel's actual direction of travel and the direction towards which it is pointing (Figure 28). The slip angle creates a lateral force (and vice versa).

The side slip angle is mainly due to the lateral elasticity of the tyre. For the passenger car tyre tested in Figure 25, the maximum cornering force was reached at about a slip angle of 8°. This varies with tyre type.

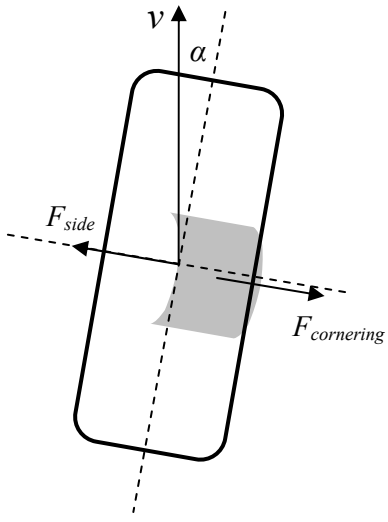

Figure 28. Slip angle (α) and cornering force visualized according to [13], when the direction of the wheel is different to ground velocity (v). The contact patch is shown with gray colour.

The offset between the cornering force vector and the side force applied at the wheel centre (also called the pneumatic trail) creates a torque commonly known as the self-aligning torque [13].

Measuring wheel slip gives very important factual data on the road surface, especially when combined with friction used. Tyre friction profiles (e.g. Figure 24) can even be used to classify road conditions based on just these two values. As an example, a friction used of 0.3 together with a longitudinal slip ratio of under 5% (and no slip angle) already gives a strong hint of the surface being either wet or dry asphalt.

This study concentrated on measuring longitudinal slip ratio, as two separate VFF algorithms were available for estimating friction potential based on slip angle and self-aligning torque. The slip angle was not otherwise used in the data fusion, but the longitudinal slip was used e.g. for plausibility checks: by selecting limit values for slip and friction used (as in the previous paragraph), certain surfaces were ruled out. Also, an assumption of reaching the friction potential at around 10% pure longitudinal slip was used to check that the friction potential output should still be slightly higher at e.g. 7% slip than the friction used. Only a conservative check was implemented and not an actual tyre friction profile.

Without knowing or updating the exact tyre slip and force characteristics during driving, matching the slip to the friction potential can however result in sur-

face classification errors. In future work, the plausibility checks based on slip and friction used should also include learning and recording the actual tyre performance. This would also enable an improved analysis of tyre longitudinal and lateral friction profiles.

Without accurate ground true speed measurements, both slip values are just estimates based on vehicle sensor readings. In the study, using IMU and wheel speed measurements, the longitudinal slip could only be estimated for around two seconds of braking, until the integrated values from the IMU acceleration and rotation were badly affected by drift (error growing over time). Even using the Correvit, the reference ground speed camera in this study, the slip values under 5% were often noisy. The wheel speed measurements were available at 50 Hz but during slow rotation, under 12 km/h, the information was considered to be unavailable due to measurement inaccuracy.

Even filters used for pre-processing the data can cause time shift between speed measurements and therefore error in slip ratio. A filtering approach based on maximum acceleration – assuming the vehicle cannot reach a higher acceleration than 2 *g* in a no-crash situation – was used in this study to remove spikes from speed measurements. This approach caused practically no latency.

In the main, a slip ratio between 5–15% seemed usable in the friction estimation to make comparisons with tyre friction profiles and also to estimate how close the forces are to the friction potential. The methods used for slip estimation should be improved in further work, as an accurate slip ratio and angle are essential for this type of study.

4.3.1.3 Friction potential estimation based on vehicle lateral dynamics

Two separate approaches for friction potential estimation, developed independently by VDO Automotive AG and CRF, were integrated in the VFF block. A detailed description by the companies can be found in [2].

The approach by VDO uses cornering to estimate friction. It compares yaw rate sensor measurements with estimates from a reference vehicle model. The reference model is a common two track model with a specifically parameterized tyre model, where the car body and chassis are treated as a rigid body. The inputs to the model included lateral and longitudinal accelerations, braking flag, individual wheel braking pressure, engine torque, wheel speeds, yaw rate, steering wheel angle and steering torque.

The approach by CRF is based on steering torque and relies on the tyre self-aligning torque saturating at lower values of side slip angle than the lateral force (Figure 5). This algorithm allows estimation of the friction potential at comparatively small values of side slip angle. The requirement was measured by IKA and CRF to match lateral acceleration of 0.3–0.4 *g* for high grip surfaces (an example can be seen later in Figure 33). However, the algorithm requires sensors to measure the overall steering torque. This is a limitation for traditional Hydraulic Power Assisted Steering (HPAS) systems, but cars with Electric Power Assisted Steering (EPAS) would be able to provide the required inputs. [2]

The inputs for the CRF model were steering torque (driver + assistance), steering wheel angle, yaw rate, lateral acceleration and vehicle speed. They were used to estimate tyre forces and torque using a reference model. Similarly with VDO's approach, the model outputs are finally compared with sensor measurements to estimate friction potential.

4.3.1.4 Driving-situation based preliminary fusion for friction potential

As both the CRF and VDO algorithms detecting friction potential require lateral acceleration and their results were found to complement each other in the first FRICTI@N project validation tests by IKA, these partners implemented a preliminary fusion block to merge the outputs.

It was decided to use driving situation detection (providing states such as braking, cornering and straight driving) as an input for selecting the better output. The performance of the algorithms was tested in various manoeuvres when building this fusion. This fusion strategy allows for more reliable information to be obtained from the similar approaches.

The two algorithms for friction potential generally provided an estimate within ±0.15 when compared to the friction coefficient measured with braking tests for the surface. The combined performance is further discussed in the chapter on validation, that is Chapter 6.4.3.

For the data fusion, the friction potential estimate from the two algorithms was considered to be true at least in 80% of cases. As a next phase of the fusion, the output was also compared to friction used, while it was possible to further filter out some clear error cases, especially where the estimate was under the friction used. The estimation success is also higher for dry than wet asphalt for example, but the EFF classification was not yet used to check validity.

4.3.2 EFF – Environmental Feature Fusion

The estimation of friction potential with environmental sensors is based on collected experience and literature studies on how different road conditions affect tyre–road friction. The expected friction levels on e.g. icy and snowy road were discussed in Chapter 1.2. The ranges for these values in the literature are quite large (e.g. 0.5–0.9 for wet asphalt, excluding aquaplaning) due to the wide selection of tyres, the exact properties of the road surface, and the challenge of distinctly classifying road conditions. As stated in the conclusions of Chapter 3, a more accurate mapping of variables that affect friction potential is one goal in future environmental sensor studies. This chapter suggests a simple mapping tool and discusses its benefits in friction estimation.

The EFF concentrated mainly on *estimating probabilities for water, ice and snow on the road with different sensors*. The laser scanner also provides precipitation densities that are further used to classify rain and snowfall. Any number of road condition sensors can be used in the friction estimation system.

In the next phase of EFF module processing, temperature measurements and friction used values (from VFF/TFF) are also used in classifying and plausibility checking the initial findings (e.g. "ice detected by Road Eye"). Each finding, or rather feature, must also come with a validity estimate (defined previously in 4.3) for the fusion.

The block diagram in Figure 29 shows how the environmental sensors of the study (Chapter 4) provide probabilities for environmental feature fusion.

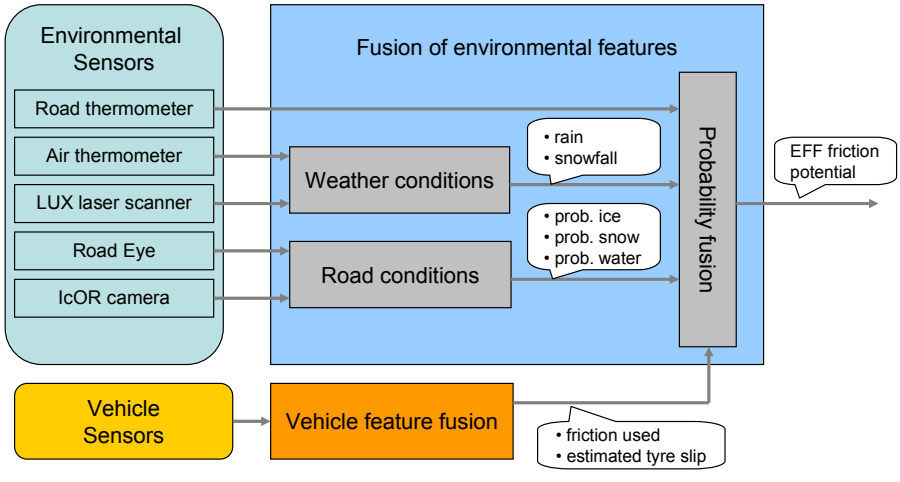

Figure 29. Block diagram of environmental friction estimation. The internal structure of the Probability Fusion block is later presented in Figure 30.

The fusion of detected environmental features so as to estimate the current friction potential is performed in 3 main processing phases:

1. Feature extraction

First, a feature extraction is performed for all sensor devices separately. The features feed blocks providing initial estimates of road and weather conditions. Road Eye, IcOR and a road thermometer provide information on road conditions, while a laser scanner and air thermometer are used to classify rain and snowfall.

2. Probability fusion

In a probability fusion block the initial probability values for water, ice and snow are combined to classify the road conditions.

Precipitation measurements were used to increase the probabilities of water and snow on the road. First, the precipitation was both classified and scaled to rain and snowfall factors based on its amount and air temperature: If air temperature is colder than −5 °C, only snowfall is expected. If the temperature is higher than +5 °C, rain is expected. Between the two temperatures, both detections gained a larger factor with a ramp function. Different amounts of precipitation were handled with thresholds. The factors were added to the water and snow probabilities. Due to the low amount of rain and snowfall data for data fusion verification, this is only a preliminary concept.

The road conditions for the classification were

- dry asphalt / high friction potential
- wet asphalt / medium to high friction potential
- snow / low to medium friction potential
- ice / low friction potential.

In addition to the validity flags provided by or pre-calculated/estimated for the sensors in general, the plausibility of the detected road conditions can be checked using 1) the VFF friction used, 2) vehicle slip and 3) air and road temperatures.

Temperature plausibility checks are performed on the sensor-given probabilities of ice, snow and water by multiplying them with temperature-based factors.

For example, ice detection was not considered plausible when the road temperature was above +10 °C. In lower temperatures, it gains plausibility with a ramp function.

If the sensors detect ice, but a high coefficient for friction used proves this impossible, basically the EFF could not give an estimate. However, a learning functionality changes this (presented below), and the EFF can theoretically match any sensor input to a friction level. This also means that the EFF can output "low friction", even without the presence of ice.

As the EFF provides outputs for both the road conditions (e.g. ice) and friction level, these can be handled separately in the decision fusion when needed.

3. Learning over time

The EFF holds a mapping function, the EFF Friction Database, that records measured (high slip) friction potential values from VFF/TFF together with the corresponding EFF environmental conditions. This database is updated while driving and it gradually learns the best matches between sensor readings and friction potential. The limited scope of environmental sensing naturally limits the classification accuracy – the system currently learns around 100 different cases – but the system is still able to narrow down e.g. the range of friction levels for what can be generally expected on snow *with the vehicle and its tyres*. This functionality also enables quick learning, when for example the vehicle is set up with summer tyres in winter conditions and therefore the expected friction potential is unusually low.

The database is updated when a reasonably high slip (configuration parameter depending on tyres, e.g. 8% longitudinal slip) is detected and the friction potential estimate is valid. Several measurements are required to gradually change the expected friction potential for the road conditions (or rather: for such sensor detections).

The learning feature enables

- starting work on more accurate road weather vs. friction potential classification, using data from several sensors
- developing friction information exchange for co-operative applications by providing a possibility to normalize the effect of tyres
- measuring the effects of worn tyres and the experienced friction after changing tyres.

As these topics are difficult to approach otherwise, the mapping/learning functionality is an essential part of the EFF.

Figure 30 presents the idea of using either static friction level classifications from the literature (friction potential for ice, etc.) or the EFF Friction Database as the final output from the EFF. If the map does not yet contain a recorded value for the exact sensor readings, an average friction potential value is given based on the road weather classification (e.g. snow, assuming packed snow). Figure 30 presents probabilities as inputs for the DB (Database) but also the raw output of Road Eye has been tested and it seems to work even better.

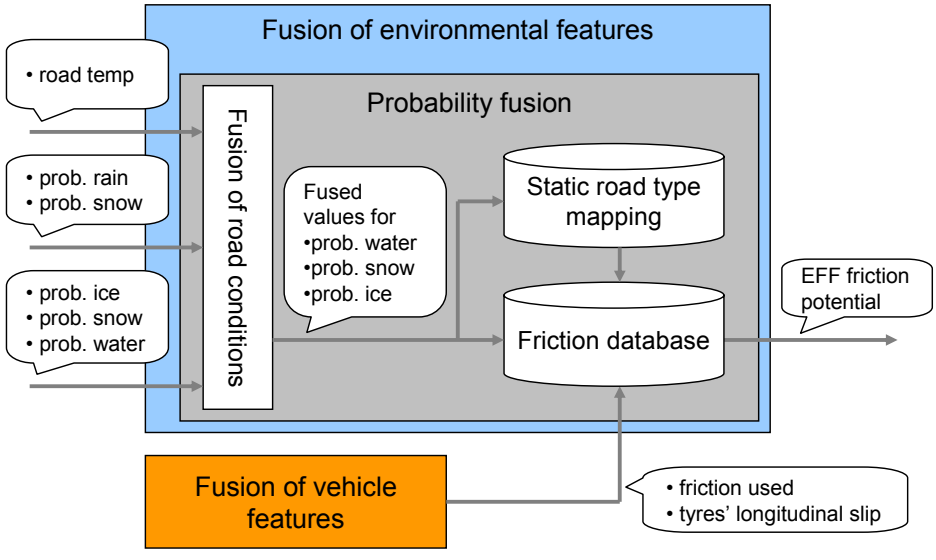

Figure 30. Simplified model of probability fusion and learning functionality (database) within the EFF.

So far only limited tests have been performed with the mapping functionality enabled in the model. These are reported in Chapter 6.4. When a recorded friction potential for environmental-sensor raw data readings exists, the estimate was accurate in these tests. When the mapping was done using the probabilities of water, snow and ice only, the limited number of mapped cases caused re-learning e.g. on different types of "wet asphalt", and therefore errors.

The sensors of this study are not likely to handle many separate cases, even when raw data (from Road Eye) is used, and this places requirements for future environmental sensing if more accurate mapping is to be attempted.

In addition to the expected friction potential, the EFF module outputs the classification for the road condition. It also provides information on how far in front the friction estimate is taken from.

It should be possible to match the area from where the environmental measurements are taken with the vehicle trajectory (or several potential trajectories) in applications. A selection of Region of Interest definitions are visualized in Figure 31. The yellow colour marks a chessboard type of definition, which would likely suit the largest range of applications. This level of spatial accuracy is, however, not truly possible with the sensors used in this study: currently only point-sized measurements can be performed with Road Eye and the IcOR camera also has a limited resolution. This study only matched the EFF measurements approximately with current vehicle trajectory, but e.g. the several optional trajectories calculated in collision avoidance places higher requirements on future environmental sensing.

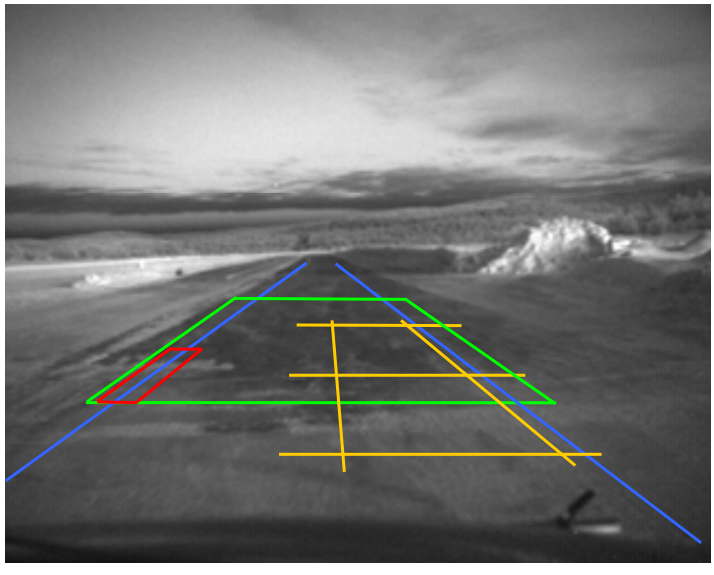

Figure 31. Visualization of different Region of Interest (ROI) definitions on a near infrared image based on vehicle and tyre trajectories. The blue lines represent (approximately) tyre tracks based on current steering. The green area was used in this study. The red area gives an example of trajectory based selection of ROI, for a single tyre. The yellow area shows an example of tiles, which is the suggested method to support a wide range of applications and steering options.

4.3.3 TFF – Tyre Feature Fusion

The TFF module has mainly been discussed in this work as a tyre sensor and its outputs (see previous chapter 3.2.4). It was designed to be an optional module in friction estimation and it has separate pre-processing.

The TFF module provides tyre forces and friction used for each measurement tyre. It also detects phases of the developing aquaplaning [47]. During the development, outputs for slip angle and wheel load have also been designed, but these were not used in the friction estimation. All the outputs except the measurements for friction used are also available directly as final outputs of the friction estimation system.

The tyre forces were tested as an input for the VFF, since they can potentially be used to improve VFF accuracy. For the VFF however the main development goals have been on current production vehicles, not having a tyre sensor yet, and only a few comparisons were made.

The main interest from the fusion perspective was the TFF output for friction used. The information of even a single tyre using high or low friction levels during a manoeuvre is valuable:

- the highest value gives the friction potential more accurately than the averages calculated by the VFF
- the forces indicate tyre–road contact.

In the current prototype, the TFF gives an output vector for friction used in the format $[f_{fl}, f_{fr}, f_{rl}, f_{rr}]$, where for example f_{rr} is the friction used for right rear tyre.

TFF measurements also comprise the effects of wind speed on friction used, while the VFF has only an estimate for air resistance during calm.

The VFF's value for friction used was used as a plausibility check for the friction used measurements from the TFF, when all forces were combined as a lumped value. The VFF was used to detect and compensate for potential TFF offset in the measurements.

As was presented in Figure 31, the measurements for each tyre separately can be better synchronized with camera and Road Eye detections (their ROI) than what can be done with a lumped value.

4.3.4 Decision fusion

The decision fusion block combines the friction used and friction potential values from the three feature fusion blocks. It also introduces a rough classification for estimated friction potential levels based on μ–slip curves. This classification utilizes the measured friction used and longitudinal slip ratio to determine which road conditions and friction potentials are plausible. For example, ice (or low friction potential) is not plausible when friction used is already very high, e.g. 0.6. On the other hand, dry asphalt is likely when friction used is over 0.6 and slip is under 5%.

The logic would benefit from accurate slip angle measurements, but the VFF or TFF estimation algorithms for slip angle were not used due to their early development phase. A kinematic model of the vehicle was used to support longitudinal slip ratio estimates during IMU measured yaw rate (turning).

The main inputs for the decision fusion (Figure 32) were

1. EFF estimate on friction potential and road conditions
2. friction used and potential from VFF
3. TFF friction used for each tyre
4. slip ratio, calculated in VFF (optionally also slip angle).

The EFF's road condition classification (e.g. ice) is compared with μ–slip measurements as a final check for road condition output. A slip-ratio-based road classification is also an input for friction potential fusion.

The VFF friction potential is used as a final output from the system when the estimate is valid and passes plausibility checks. Otherwise EFF estimates and previous valid estimates are combined as a best guess for current friction potential. This means for example that if we used a lot of friction in a curve, this estimate is considered valid for a while longer, *if the EFF road condition classification remains in the same category*. However, the validities of old estimates drop with distance travelled and the EFF estimates are considered less reliable than valid estimates from the VFF. Only the EFF learning features, when performing well, can provide more accurate information on friction than the VFF algorithms.

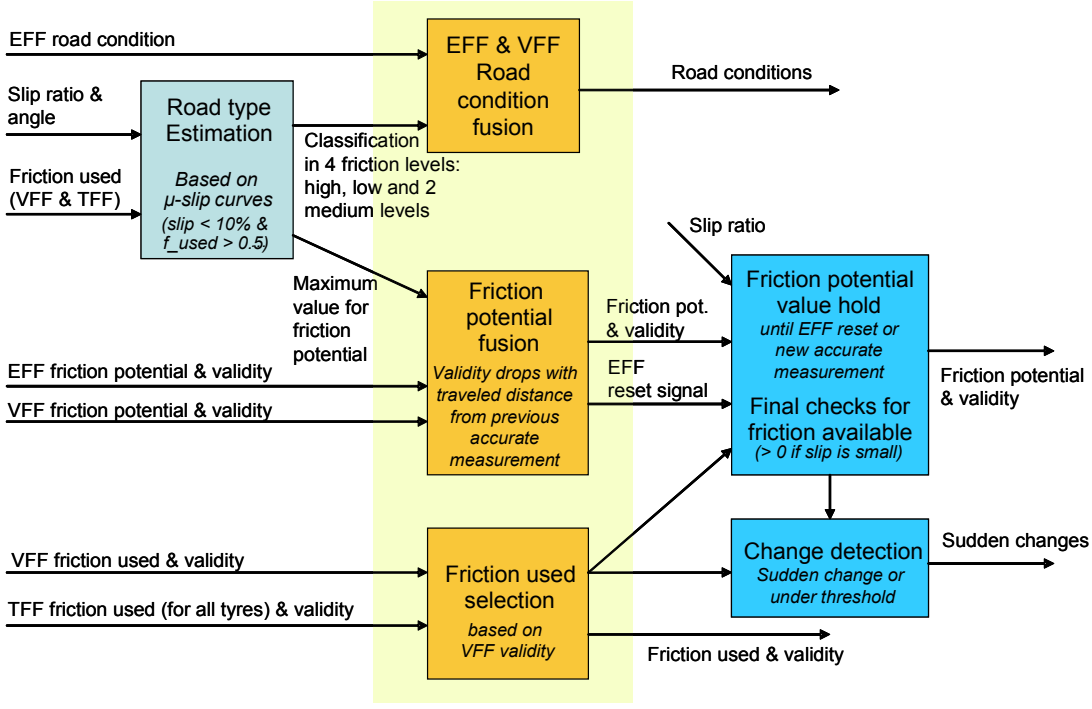

Figure 32. Decision fusion block.

Environmental sensors can provide estimates nearly continuously and can therefore easily end up dominating the friction potential fusion (e.g. if we detect ice, then we expect low friction potential). An error in EFF measurements could badly affect the system. Therefore searching for a fitting balance between continuous and discontinuous estimates/measurements is important for the fusion and for giving safe estimates.

Friction used (measured with acceleration sensors in the VFF and tyre sensors) is a continuous measurement and a fact for the system. As was discussed in Chapter 4.3.1, the measurement has error sources, but these were considered to be small compared to the general accuracy of the friction potential estimation. The friction used measurements were the backbone of the fusion logic and plausibility checks.

Finally, abrupt changes are sought from the friction values to detect dangerous locations and trigger warnings. This was due to the output specifications, where these outputs are included as having potential value for applications.

Figure 33 and Figure 34 present examples of friction estimation, especially of EFF and VFF fusion. The first data shows that when the friction used first ex-

ceeds 0.3, the VFF based friction potential calculation produces an estimate of a friction potential of 1.0. When the VFF measurement is valid, the output for friction potential is 1.0, otherwise the output is the EFF classification default 0.85 (can be set in configuration parameters) for dry asphalt. No learning feature has been used. The VFF overcomes the EFF estimate, being generally more accurate. The EFF default value for the surface is in this case off by 0.2, when compared to the highest friction used value that was measured for the surface in a separate braking test: 1.05. However, having only a few road condition classes inevitably leads to this level of errors with any default values for dry, snow etc.

The validity calculations can be best seen from the lowest part of the figure, where the validity drops when no recent measurement is available from the VFF and the calculation has to rely on EFF values only.

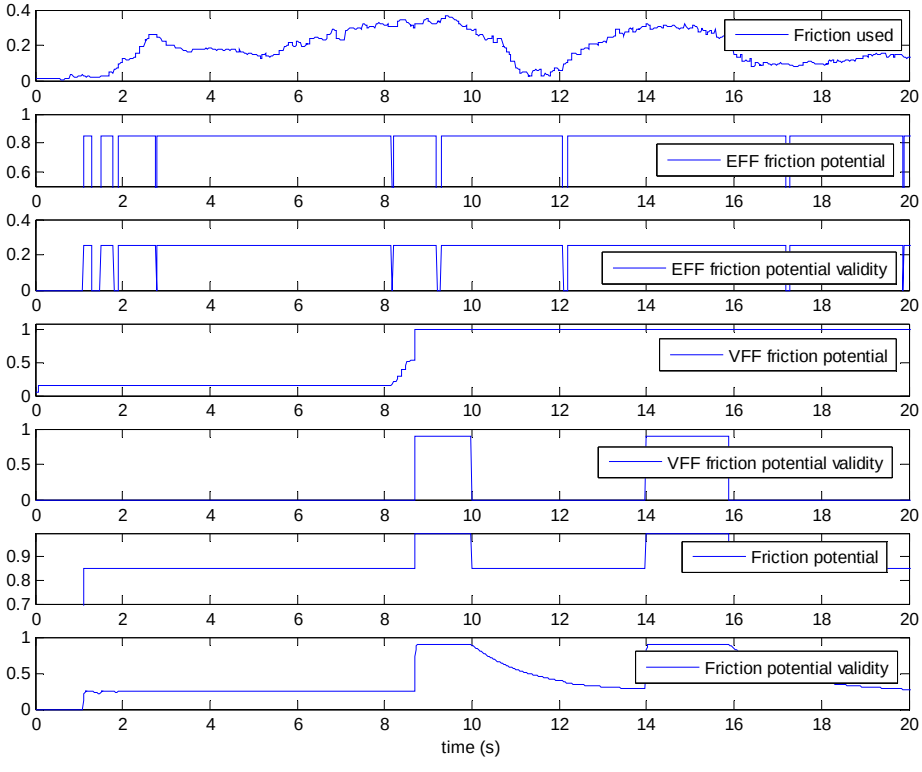

Figure 33. Normal driving on asphalt. System reset has been made and no previous information is available. When the VFF provides a high validity estimate, the final output also receives high validity. At 10 seconds, the validity starts to return to the EFF set value. In the case of the learning features being active, the final estimate would remain high, but in this case, without learning, the potential is also decided by the EFF.

The following data is captured while accelerating and cornering on partially wet asphalt. Also the EFF learning functionality has been in use during earlier driving, including hard manoeuvres, and this improves the estimation.

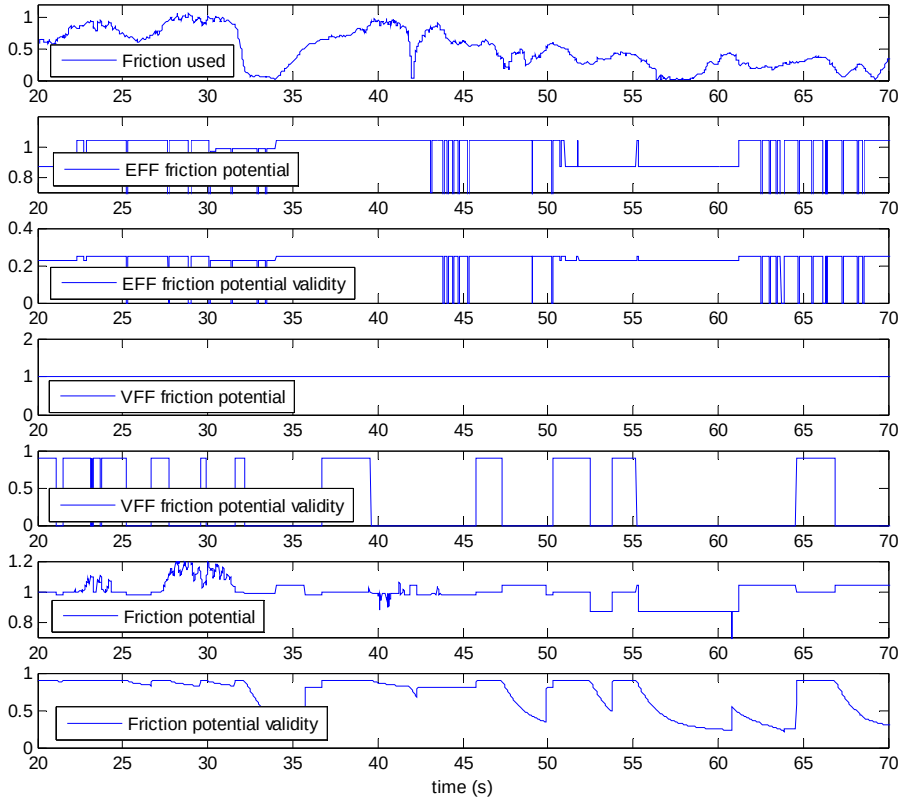

Figure 34. Example of EFF and VFF fusion. Acceleration and cornering on partially wet (51–61 s as recorded by Road Eye) asphalt. EFF learning had recorded highest friction used 1.05 for dry, 0.85 for wet.

The EFF classification for the surface (several types are learned even for dry) now even includes values around 1.05. A clear drop in the potential is visible near 55 seconds, when the vehicle is moving on wetted asphalt. The high friction potential near 30 seconds comes from friction used (highest peak 1.08) and this is where the EFF could update its values for the classification. Due to the lack of proper slip angle estimation and the decision fusion coming to the conclusion that some friction potential would still be unused, the final output for friction potential became momentarily (near 30 s) too high during cornering.

The VFF friction potential estimate is available often in this example due to heavy acceleration. However, the acceleration on the wet segment was not high enough for the VFF to update its estimate. More tests of the system's performance are presented in Chapter 6.

5. System Integration

The friction estimation algorithms developed in the FRICTI@N project were demonstrated in three different vehicles, each focusing on slightly different applications:

- Studies with a passenger vehicle demonstrator, Fiat Stilo, focused on a minimum sensor configuration using vehicle sensors and the VFF module only. The friction information was used to improve the operation of the APALACI collision mitigation system (presented later in chapter 5.3 as relevant to this study).
- The commercial vehicle demonstrator, Volvo FH 12 truck, was the main test bed for environmental sensor studies. Also a partial VFF module was implemented. The main focus was in co-operative applications in collaboration with the EU projects SAFESPOT and CVIS.
- The full friction model and the sensor data fusion approach of this study were developed on IKA's development vehicle the Audi A6. The vehicle was instrumented with vehicle dynamics, environmental and also tyre sensors. Only the instrumentation of this vehicle is presented in this work, as the main development vehicle.

An experimental Human–Machine Interface (HMI) approach was designed for all three test vehicles. Chapter 5.2 sums up these experiences.

5.1 Development vehicle

The FRICTI@N project development vehicle, owned by Institut für Kraftfahrzeuge Aachen, has been an important research tool also in several earlier studies. It contains extensive instrumentation, most of which is hidden under the furnishings.

A full validated vehicle simulation model exists for MATLAB Simulink. Using this tool, driving manoeuvres can be simulated before real tests are done to assess their potential value. Measured data can be re-run and used in simulations offline.

The vehicle features are summarised below:

- Audi A6 4.2 l, 220 kW, passive 4WD
- air springs at the rear axle to reduce driving behaviour changes caused by load variations
- ABS/ESC brake system
- hydraulic power steering with variable hydraulic steering torque support (open interface)
- active steering with variable steering ratio (not utilised in this study)
- dedicated CAN bus interface (not vehicle CAN) available on dSPACE Autobox
- sensors for individual brake pressure at each wheel
- prepared for easy installation of new sensors.

The car is not authorised to be driven on public roads. Consequently the development has to take place on closed proving grounds.

In Figure 35 you can see the Audi in winter tests at Ivalo airport.

Figure 35. The development vehicle of the study, Audi A6, equipped with extra sensors and running a test program in Ivalo, Finland, 2007.

New sensors and algorithms were tested and accumulated for the vehicle during the FRICTI@N project.

5.1.1 Network architecture

The development and demonstration vehicles used a network architecture (Figure 36) designed for experimental purposes. Dedicated buses for additional sensors were used in order to avoid interference with normal vehicle functions. A Rapid Prototyping Unit (RPU) collects information from sensors and performs the calculations.

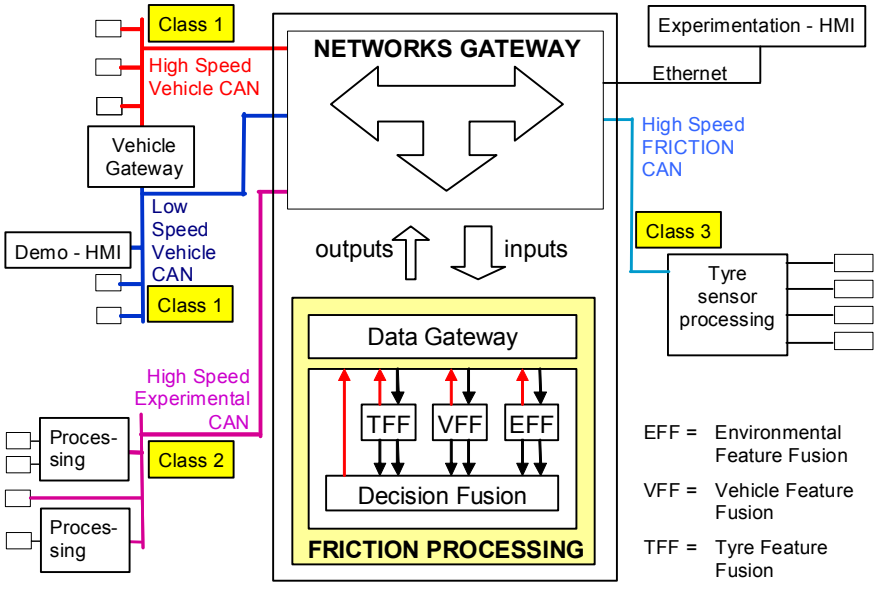

Figure 36. Experimental vehicle network architecture by Magneti Marelli and IKA [2].

The following table (Table 8) explains the network classes of Figure 36.

Table 8. Network Classes [2].

Network class	Description	Specifications
Class 1	Vehicle normal production buses (high and low speed CAN)	Only normal production signals utilised by friction estimation system are specified.
Class 2	New buses for experimental activities other than FRICTI@N	Only experimental signals utilised by friction estimation system are specified.
Class 3	A dedicated FRICTI@N bus (high speed)	All signals are specified.

The development vehicle had 2 dSPACE AutoBoxes as the RPUs, the other being reserved for tyre analysis for the sake of development simplicity.

The tyre sensor system needs particular care due to the nature of the data coming from it: The system is made up of a receiver unit for each wheel. The outputs are available on dedicated point-to-point high speed (1 Mbps) CAN buses. Such buses are completely saturated and cannot be directly connected to the "FRICTI@N Bus". For that reason a secondary Rapid Prototyping Unit was used in order to pre-process the signals.

5.2 HMI concepts

There are a few issues which affect the Human–Machine Interface (HMI) design of friction estimation systems that provide driver information. Firstly, the friction potential is difficult to estimate as a continuous value. With the comprehensive set of sensors used in this study, an attempt could be made. However, the periods when there is no valid estimate for friction potential make it generally difficult to present the value to the driver.

Secondly, the friction potential can vary a lot in the vicinity of the vehicle. This is the case for example on winter roads, where snow and asphalt alternate. The areas of high or low friction and the changing risks need to be somehow included in the application. Also, with today's environmental sensing technology, the friction estimation is limited to some tens of meters in front of the vehicle. The quality of information often drops with distance.

Averaging friction potential estimates over road segments to provide rough classifications is an option. An interesting case for future research would be e.g.

matching this type of averaged information with drivers' subjective estimates of the road slipperiness, as was suggested by the Finnish RASTU project [27]. This might enable a warning to be given to the drivers of slippery road segments according to their own understanding of dangerous conditions.

The FRICTI@N project experimented with two HMI approaches in its attempt to visualize the friction information: one for warning about low friction in front of the vehicle, estimated with environmental sensors only, and one for displaying the current friction used relative to the friction potential.

To collect background information for the work, Volvo Technology (VTEC) interviewed professional truck drivers in Sweden [2]:

- A common view amongst the drivers was that black ice is the most aggravating condition. If there is no ice or snow elsewhere on the road, the driver may not drive carefully enough.
- The most common way for the drivers to receive information about the road conditions was by calling colleagues. They say that a driver never trusts systems.
- A warning was seen as a possible complement, when it does not smother senses with excessive information. A large, simple symbol was preferred and also an additional voice message might be something to consider.
- Many drivers viewed the road temperature measurements as a good help, especially when the weather is changing fast. They rely on their experience on these occasions.

The warning of low friction potential was demonstrated by VTEC with their R&D truck, which has an advanced dashboard (Figure 37) where different HMI approaches can easily be tested.

Figure 37. The configurable instrument cluster in the truck demonstrator

The HMI approach included two icons (Figure 38): an informative (orange-yellow) and a warning (red with triangle). Further tests are needed to verify their appearance. Since the small icons are shown on the display behind the steering wheel, they may also go unnoticed in the absence of an additional sound.

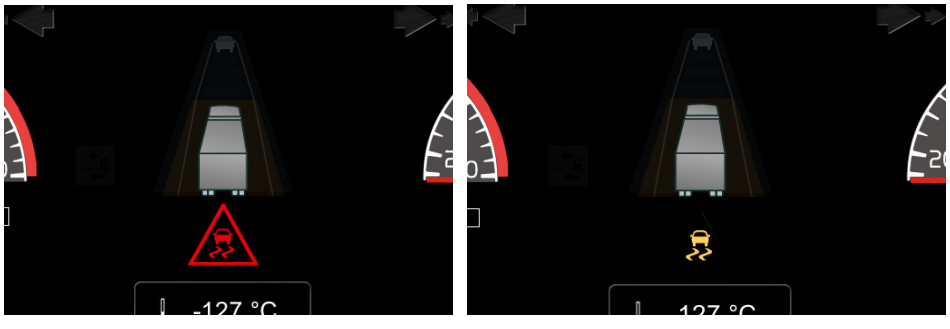

Figure 38. VTEC HMI design for demonstrations. Images courtesy of VTEC.

The test subjects commented that the information icon may be unnecessary during daylight when the driver's sight exceeds the capabilities of the Road Eye sensor. At night and when using the IcOR camera or other environmental sensor

with a longer range (than Road Eye's 1 meter), the icon could be a more useful addition. For details about these tests, see VTEC's report included in [2].

It is understandable that environmental sensing, particularly its range and certainty, can seem limited when compared with human vision and intellect. However, as pointed out by a recent study comparing drivers' estimates of road slipperiness with road weather station values, the drivers do have difficulties trying to estimate the maximum tyre–road friction coefficient [5]. This suggests more detailed work is needed on identifying driver weaknesses and on finding ways to support them with friction estimation. An example of a new type of function for the driver information system could be giving out black ice warnings when the vehicle's current trajectory both requires high friction and is projected to travel over ice. The driver might have made a miscalculation in that situation.

When driving on a snowy road where the friction potential is low all the time, an information icon easily loses its significance as a warning. Therefore the friction estimation output of a sudden change in friction potential could be more useful in winter conditions. Also if the slipperiness can be expressed in meaningful categories for the driver, a category change could be given as well.

The second approach visualised the friction used and friction potential estimates using a bar graph. Variations of this approach were developed by CRF and Magneti Marelli for the Fiat, and by VTT and IKA for the Audi demonstrator. The design for the development vehicle is shown in Figure 39.

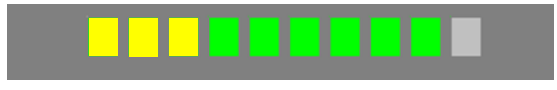

Figure 39. A bar graph concept showing friction levels. Yellow represents friction used, green is friction available (up to friction potential) and gray is used to fill the bar to a maximum value 1.0.

When the friction used is very low and friction potential high, the bar graph of the figure is almost completely green. When friction used gets higher, the graph becomes more and more yellow. If the friction used is near to friction potential, both the friction used and friction available turn red – this was to alert the driver. In the right end of the bar the number of gray boxes depends on the estimated friction potential compared to the maximum value 1.0. In this test the estimate for friction potential was continuously shown regardless of its validity.

A value 1.0 was used as the maximum for the HMI, even though the vehicles can occasionally reach higher values. When the vehicle is using more friction than 1.0, the bar graph simply shows that all friction is used. Respectively, potentials higher than 1.0 are all presented as the best possible grip.

The bar graph provides the driver with a straightforward graphical representation about of much friction the car is using and how much is available. The information can be understood with a quick glance.

The first experiences from using the two presented methods were promising, but as they both

1. increased the driver information load
2. mostly showed something that the driver already knows

it is as yet difficult to suggest a HMI approach for product implementation. It was presupposed in this study that the main use for friction information is through other ADAS, by enhancing their performance. However, as the estimations become more and more accurate, continuous and even occasionally surpass the driver's observations (based on e.g. [5]), there is also room for new HMI concepts.

5.3 FRICTI@N-APALACI demonstrator

The collision mitigation system developed in the PReVENT's subproject APALACI [54] was adapted by CRF during the FRICTI@N project to utilize friction estimates coming from the VFF module. The purpose of this was to demonstrate the benefits of friction estimation in an ADAS.

CRF decided that only existing vehicle sensors would be used in estimating friction potential, so as to study a concept that would be as close to the market as possible.

VFF alone does not provide a continuous estimate of the friction potential or any future estimates, but rather a history value to be conservatively used in assessing possible manoeuvres. However, the VFF estimate can be better utilized in timing the collision mitigation warning signals given to the driver.

In a dangerous situation the FRICTI@N-APALACI demonstrator first gives a warning, and if a collision becomes unavoidable, it activates the brake system to reduce impact speed. It is able to start the braking very efficiently as it e.g. preconditions the brakes by sending a low deceleration request.

The Figure 40 shows a model that has been used in APALACI to predict the distance where collision avoidance is no longer possible. This is the distance where the collision mitigation systems usually start full braking. A low energy impact is, however, expected. There exist also collision mitigation variations in which collisions would not be expected at all, such as the Volvo City Safety system at speeds under 15 km/h (measured against a static obstacle) [55]. Collision mitigation timing is further discussed in Chapter 7.

Prediction of distance for steering manoeuvre (simple model)

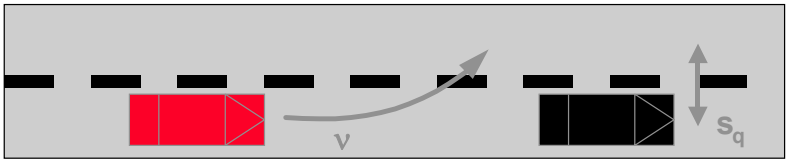

Distance for steering manoeuvre: $s_A = v\sqrt{\frac{2 \cdot s_q}{\mu_y \cdot g}}$

Influence of maximum friction available: $1/\sqrt{\mu}$

Figure 40. Collision avoidance by steering actuation as calculated in the APALACI project [11]. The symbols used in the figure correspond to the list of symbols of this work.

The APALACI application provided a clear case to demonstrate the benefits of friction estimation: on low friction surfaces, the original system, in keeping with all current collision mitigation systems, starts braking too late.

The following table shows an example reduction of impact speed and larger warning distances, when the VFF friction estimates were provided for the APALACI application.

Table 9. CRF's tests with FRICTI@N-APALACI demonstrator in a forward collision scenario with a stationary car-like object. Initial host vehicle speed 40 km/h, nominal friction coefficient 0.5. The Crash Energy Index describes the improvement in reduction of kinematic energy. [2]

Initial host vehicle speed : 40 km/h Initial obstacle speed: 0 km/h Nominal friction coefficient: 0.5		
	APALACI	**FRICTI@N+APALACI**
Host vehicle Impact Speed (km/h)	28.13	25.31
Distance at warning activation (m)	10.35	15.12
Distance at Brake activation (m)	7.46	11.87
Crash Energy Index: 19%		

As a conclusion from the experimental tests conducted by CRF, the system performance "was improved in a meaningful range of driving situations and road conditions" [2].

The collision avoidance calculation method and timing of collision mitigation that will be presented in Chapter 7 are different to that used by the FRICTI@N-APALACI demonstrator. The estimated braking distances will be compared.

6. Friction Tests and Algorithm Validation

This chapter gives an overview of the validation steps performed for the algorithms and the main test sessions during this study. The main goal was to verify and further improve the suggested data fusion concepts. Due to the environmental and tyre sensors used being prototypes and the numerous changes in their setup and software during this study, the compiled results can, however, be indicative at best, in regard to any future product implementation.

The FRICTI@N project test procedure comprised the following steps:

1. setting up vehicle simulation models
2. defining relevant driving situations for real world measurements
3. real world driving tests for building a measurement databank
4. offline tests and algorithm development
5. parameter setup and validation of outputs in offline testing
6. real-world driving tests.

The first three steps covered building a comprehensive measurement databank for offline algorithm development, while the final steps concentrated on evaluating and improving the performance in driving tests.

6.1 Choosing driving manoeuvres and collecting a databank

Simulation can help to identify relevant driving manoeuvres for studying friction. Several manoeuvres were simulated in the FRICTI@N project by CRF and IKA to estimate for example the levels of acceleration and tyre forces. These variables are relative to friction used and give a magnitude for the friction effects that could be visible in the measurements.

The simulation results proved to be helpful when planning tests to collect a comprehensive measurement database. Especially for the development of vehi-

cle sensor-based algorithms (VFF module), many different tests with a strict differentiation between longitudinal and lateral acceleration were considered to be useful. These included steady state manoeuvres for lateral acceleration, such as steady state cornering with increased speed or increased steering angle. For longitudinal measurements, acceleration and braking manoeuvres were planned using different levels of brake force. The manoeuvres had to be performed on different surfaces. Hard braking was required in each test session to define the friction potential for the surfaces.

After the development vehicle was instrumented and prepared for data collection, the first main test campaign was held in Ivalo, Finland, during winter-time. Several test sessions followed and the most important are described in the following chapters.

Nearly 200 measurement runs in total were saved and documented in detail including the manoeuvres, weather and vehicle set-up during the test, sensor signal naming and pre-processing algorithms, track dimensions etc. When the data fusion algorithms and especially the EFF self-learning features for building a database reached an operational stage, their run-time values were also saved in the databank for the last ~40 test runs.

The following figure shows an extract of the databank, from summer tests conducted in Aachen by IKA:

executed test procedures in FRICTION tests in Aachen								FRICTI@N
file name	track	manoeuvre	speed [km/h]	cruise control	signals	cog profile	measure-ment inter-rupted	comment
0141	ika test track	Lenkwinkelsprung - left - 4m/s2	60	yes				right curve bevore maneuver
0142	ika test track	Lenkwinkelsprung - left - 4m/s2	60	yes				right curve bevore maneuver
0143	ika test track	Lenkwinkelsprung - left - 4m/s2	60	yes				right curve bevore maneuver
0144	ika test track	open loop - steady state cornering - right		no				
0145	ika test track	open loop - steady state cornering - right		no				
0146	ika test track	open loop - steady state cornering - right		no				
0147	ika test track	open loop - steady state cornering - left		no				
0148	ika test track	open loop - steady state cornering - left		no				dry area at the end and in between
0149	ika test track	open loop - steady state cornering - left		no				
0150	ika test track	closed loop - steady state cornering - right		no				
0151	ika test track	closed loop - steady state cornering - right		no				
0152	ika test track	closed loop - steady state cornering - right		no				
0153	ika test track	closed loop - steady state cornering - right		no				
0154	ika test track	straight	30					
0155	ika test track	straight	30					
0156	ika test track	straight	30					
0157	ika test track	straight	60					
0158	ika test track	straight	60					
0159	ika test track	straight	60					
0160	ika test track	double lane change	30	yes				
0161	ika test track	double lane change	30	yes				
0162	ika test track	double lane change	30	yes				
0163	ika test track	double lane change	60	yes				acceleration on area dry
0164	ika test track	double lane change	60	yes				acceleration on area dry

Figure 41. Extract of an executed summer test protocol in Aachen, August 2007.

6.2 Winter test sessions

The first winter tests were performed on the Nokian Tyres / Test World track in northern Finland, next to the Ivalo airport, in February 2007. The track offers a long and broad snow covered runway, an ice circle and a specially prepared μ-transition track (Figure 42). The μ-transition track enables testing transitions between snow, asphalt and ice in short distances. It was especially used for studying friction effects during straight driving.

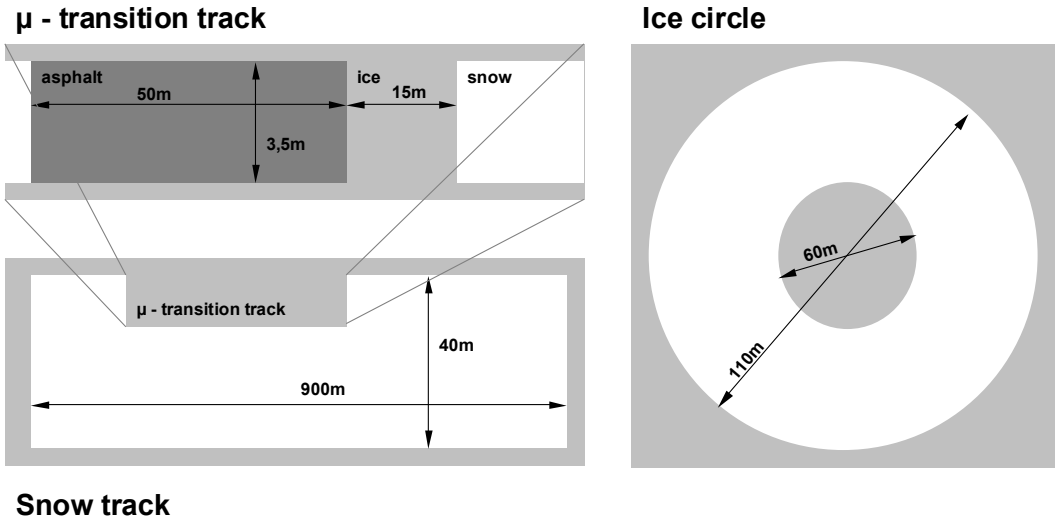

Figure 42. Ivalo test track dimensions [2].

The test was essential also for setting up the development vehicle and integrating several sensors provided by the project partners (Figure 43). The vehicle state sensors for the VFF module remained practically intact throughout the project, while the environmental and tyre sensor set-up varied extensively between tests.

Figure 43. The development vehicle set up for the first measurements.

The collected databank was used for offline algorithm development until additional data sets were collected during the next winter. The costs involved in preparing full test campaigns and the early development phase of the systems made it practical to perform most tests by concentrating only on a selected set of sensors and algorithms.

The main environmental sensor validation tests were carried out in Arjeplog, northern Sweden at the end of March 2008. A VTEC truck was instrumented for the occasion (Figure 44). The truck was driven from Gothenburg to Arjeplog recording 1500 km of data for Road Eye, the IcOR camera and laser scanner algorithm validation. Additionally, experiments were carried out at the Arjeplog site.

Several factors such as the amount of ambient light (IcOR), varying performance on different road conditions (Road Eye and IcOR) and prototype sensor mounting (all used sensors) affect the collected results. The classification success during the FRICTI@N project EFF tests was observed to vary between 70–95%, the highest reliability being achieved on dry asphalt. The IcOR and Road Eye performance in the Arjeplog tests are further analyzed in [40].

Figure 44. VTEC truck in Arjeplog tests. Photo courtesy of VTEC.

During the final tests in late 2008 the project suffered from lack of snow even in the north and therefore the project also used artificial slippery surfaces as discussed in the following chapter.

6.3 Summer time tests

The main summer tests with the development vehicle were performed on IKA's proving ground. The track is located in Aachen, Germany. The Figure 45 gives an aerial view of the track and its dimensions.

Figure 45. Aerial view of the IKA's proving ground, Aachen, Germany. Photo courtesy of IKA.

The track has at least two types of asphalt, but this was not a major factor in tests as the friction estimation had trouble differentiating between asphalt types (e.g. the IcOR camera provided granularity analysis but lacked spatial resolution). The track can be artificially watered and this was often used to test e.g. cornering on wet asphalt and the detection of different levels of wet with environmental sensors. To reduce the friction potential further and to simulate icy conditions, a watered synthetic coverage was used to perform tests on friction potentials around 0.2.

Figure 46 shows a collection of photos of the surfaces used in the tests.

Figure 46. Different conditions of the test track. Photos courtesy of IKA.

Similar tests on slippery surfaces were also performed with the truck demonstrator by VTEC on a different test track. Additionally, the FRICTI@N project had access to separate aquaplaning test tracks for tyre feature fusion algorithm testing.

For optical sensing, night-time testing was also performed on IKA's proving ground. Figure 47 shows an example of "black ice" studies on an early October morning, using a baking tray and frozen water. The Road Eye sensor detected ice reliably, but the fusion algorithm gave a very low plausibility for the detec-

tion due to the ~10 °C road temperature at the time. The IcOR camera system was at the same time tested for night-time detection capabilities.

Figure 47. Night-time test of environmental sensors, especially ice detection. Aachen, October 2008.

6.4 Algorithm testing

The friction estimation algorithms were developed using MATLAB Simulink and the data was collected in driving tests as described earlier. The offline runs with recorded data covered mostly 5–30 seconds. Real driving tests were therefore essential to

- test the output of the algorithms during longer periods of driving (test tracks only)
- to find out algorithm bugs and undesired outputs related to manoeuvres and road conditions not existing in the measurement database (e.g. when reversing or driving on grass)
- develop the learning features
- develop the driver information system and HMI.

The measurement database had been recorded at 3200 Hz, so as to capture full data from sensors that have a high sampling rate. Several signals were filtered to remove noise during database post-processing. For the final demonstrations the sample rate was dropped to 100 Hz to be able to perform all calculations in real time. New filters (similar to Equation 5) were designed for online processing, with the goal to avoid a large input lag (time shift) caused by filtering.

In Decision Fusion testing, first the outputs from single systems were compared to measured references (peak braking tests) from the test area. Then the system outputs were monitored during different driving manoeuvres. The output and reliability of some algorithms depend on the driving manoeuvre. Based on the separate tests, weight factors and other parameters were decided for the fusion.

6.4.1 Continuous friction potential estimation

One of the goals of this study was to achieve continuous friction potential estimation. The accuracy and validity of the estimation form the criteria for this goal.

The following test (Figure 48) shows 90 seconds of normal driving on a dry asphalt road. It was recorded when the development vehicle was returning from IKA's test track to the garage. The EFF learning feature was in operation.

The VFF estimate does not capture a difference between 1.0 and the actual values 1.05–1.1 that the EFF has learned and recorded for the surfaces during the previous hour. The EFF database contained a few separate values for the area, as during past experiments, the raw sensor data was used in the learning phase, instead of only the "dry asphalt" class.

In this 90-second recording, environmental sensors can classify the road surface 94% of the time (the rest of the time a historical classification is maintained in later fusion steps). Their relative reliability is always considered low (set with a configuration parameter). A VFF lateral-acceleration-based estimate was available 5.3% of the time. The VFF calculated friction used is available continuously – and slip values, when wheel speed exceeds 12 km/h. The final output alternates between the EFF and VFF estimates. The system can be configured as to how long (both in meters and seconds) it considers the VFF outputs are still valid for the surface. Also a contradictory new EFF measure makes the previous estimates invalid.

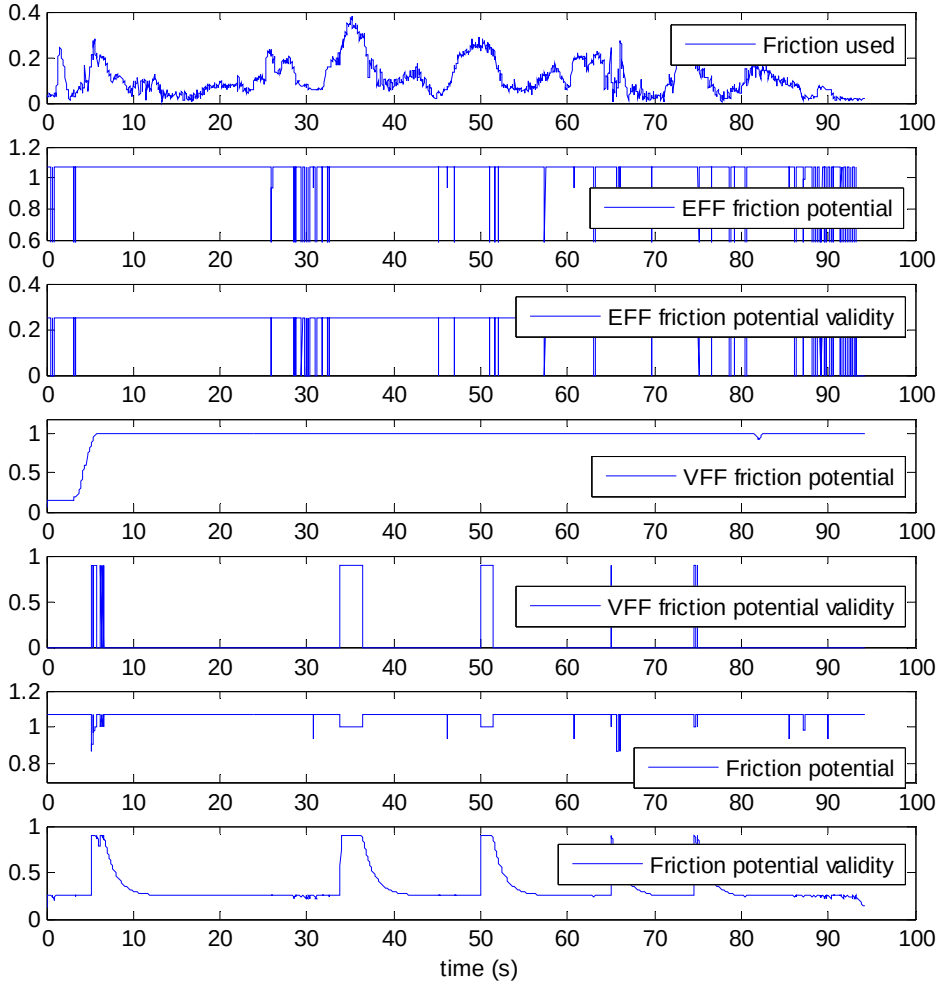

Figure 48. Driving for 90 seconds on dry asphalt. October 2008, Aachen.

This type of test shows a reasonable robustness against false detections. No large estimation errors are visible – the low friction potential should not have been present in the measurement. The validity of the estimate stays near EFF levels much of the time due to the low excitation (under 0.2 *g* horizontal acceleration most of the time) for the VFF module.

On slippery surfaces the same levels of acceleration cause more slip and the VFF is more often able to give a reliable estimate. However, this also depends on the driving style as drivers can reduce their acceleration to avoid slip. On the

other hand, aggressive drivers are known to utilize ABS and TCS frequently on snowy roads.

6.4.2 Transition tests

The moments when the road surface and friction potential changed were frequently studied in the testing. During straight driving at constant speed the detection is based only on environmental sensing, but use of longitudinal or lateral forces, i.e. accelerating, braking or turning, greatly improves the reliability of this detection.

Figure 49 shows an extreme case based on vehicle dynamics measurements, where the surface changes from snow to ice while braking with the wheels locked. The friction used is 0.2–0.4.

The system classified the road surface as icy slightly earlier than the actual change happened, due to deceleration dropping under a threshold value. VFF estimation inaccuracies also caused a momentary false detection of ice in the beginning of the braking.

The friction potential estimate changed only from 0.353 to 0.348 when braking started, showing the potential of the EFF learning feature to record similar conditions. The system would give an estimate of ~0.4 if no history information would be available (including a recent VFF estimate). When moving on the icy patch the estimate for the friction potential is close to 0.2. Due to the high slip the VFF estimate is constantly used instead of EFF classification based values.

Some more friction would be available on ice by using a smaller slip ratio. Full sliding is usually not the most efficient way to brake. On snow, however, the build-up of snow in front of the tyre seems to produce the highest deceleration even in this measurement.

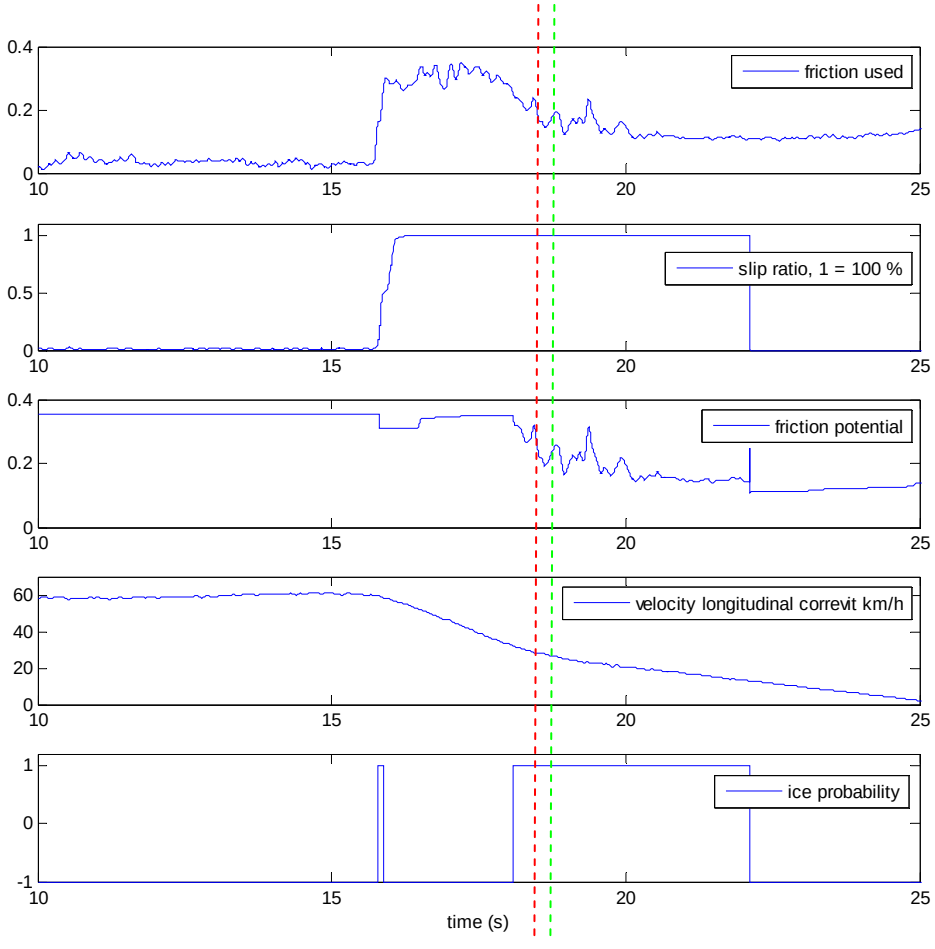

Figure 49. Ivalo tests 2007: transition from snow to ice while braking (high slip, initial speed 60 km/h). The red line represents the moment of change (18.5 s), recorded with a manual trigger during the test run. As there was a small drop between the surfaces, an IMU pitch change indicates the drop for the front tyres happened at 18.8 s (green).

The following figure shows a transition from mostly dry asphalt to wetted asphalt. In previous driving the learning functionality has learned 0.87 for the wet and 1.05 for dry. The output values of the algorithm are therefore as correct as the (lumped) acceleration-based friction used calculation; the main error source is rather the road surface classification. Naturally errors can happen also in the learning phase, e.g. changing the learned value too easily and on an incorrectly classified surface.

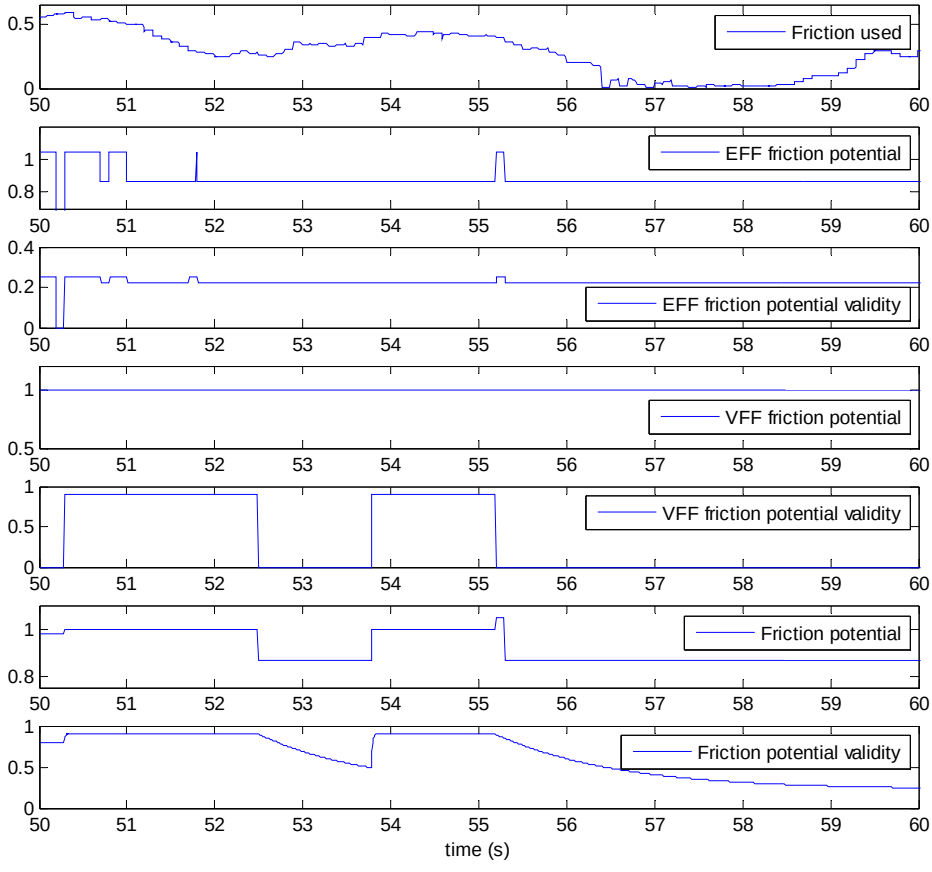

Figure 50. Transition and cornering from dry to wet asphalt. EFF learning has been in use before the test. October 2008 Aachen.

In the figure the EFF turns to wet (0.87) earlier than the final output, which is affected by the VFF. The VFF algorithms are operating near their limits, with friction used 0.4, and constantly produce an estimate 1.0. This causes a momentary classification error especially at 54–55 seconds, where the VFF output for its internal validity is high.

The following figure (Figure 51) shows the same example, but this time without EFF learning. The difference is visible in the EFF friction potential output, which uses configured values 0.65 for wet and 0.85 for dry, based on averages from the literature (see 1.2).

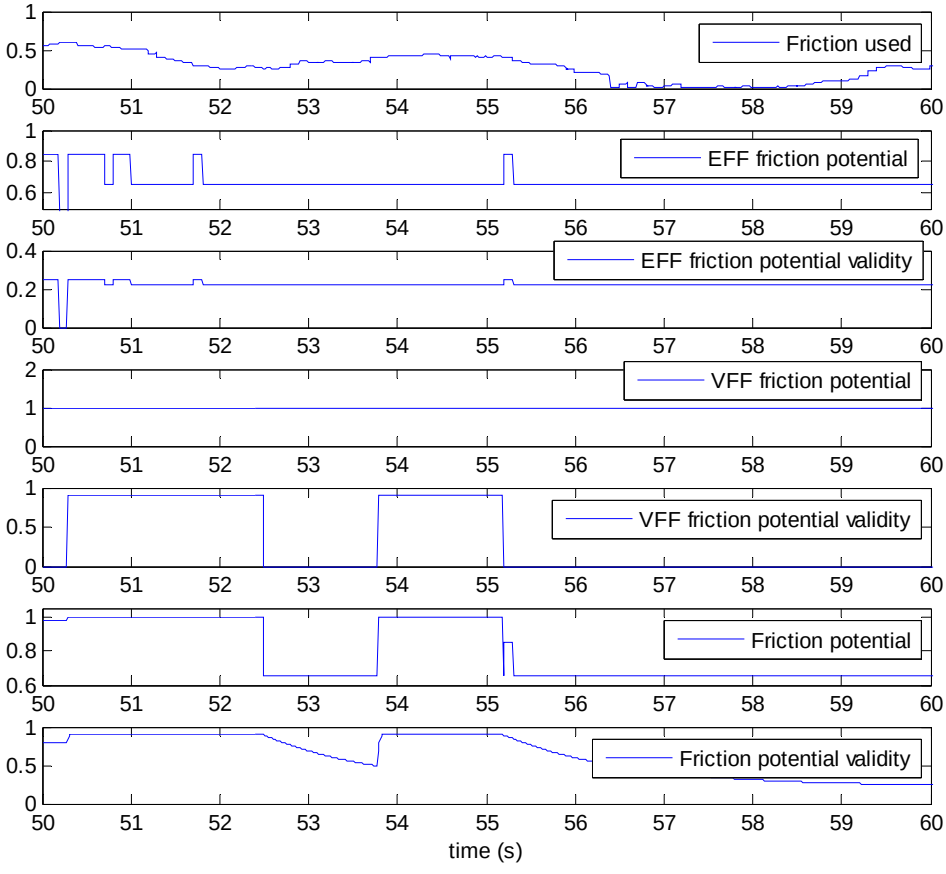

Figure 51. The example of Figure 50 reproduced in a simulation with no learning feature in use.

Generally the system is able to detect large transitions. Rapidly alternating patches of two surfaces can, however, result in momentary errors in classification between the types. The three previous examples also showed that when the friction potentials between the surfaces are rather close, ~0.2 apart, the classification difficulties can cause a delay in detecting the transition. This delay is generally due to VFF classification errors at low excitation, which means that estimates are not updated.

The output without acceleration or cornering is practically plain EFF output, dominated by Road Eye measurements. The change in the EFF estimate is practically instantaneous.

Applications need to decide on how to use the system outputs on surfaces where the friction potential is constantly changing and optimize their operation accordingly, as the environment cannot be accurately mapped (e.g. a grid of the surroundings, showing areas of different friction potential) with the current system.

6.4.3 VFF

The VDO and CRF compared their VFF algorithms based on lateral acceleration so as to later combine the outputs. The tests were made in collaboration with IKA. The results showed that both algorithms required a lateral acceleration of more than 3 m/s^2 to provide a valid estimate for the friction potential. The CRF algorithm was also commented to detect ice (reference value 0.2) at 0.15 of friction used. The tests pointed out driving-situation-specific differences between the algorithms in recognition time and accuracy. A preliminary data fusion block based on detecting these situations was used to output the more reliable estimate. [2]

The estimation accuracy of the two algorithms depends on the vehicle model and its parameters. Changes in parameters and difficulties in accurately modelling the vehicle and its tyres affect the algorithms' performance, especially when driving with low lateral dynamics. This was evident for example with the CRF's algorithm, as it had been originally developed for the APALACI and FRICTI@N projects' Fiat demonstrator, and the different steering system used in the Audi caused difficulties when adapting the algorithm.

Based mainly on the Turin tests by CRF in March 2008, which consisted of 170 test runs on various test track surfaces ranging from friction potential 0.3 (artificial slippery surface) to ~1.0, the CRF estimated the VFF lateral-acceleration-based algorithms to provide friction potential with an accuracy of ±0.15 [2].

This accuracy is a limiting factor also for the fusion system, where the VFF algorithms "decide" the output during high acceleration and these values are maintained as an estimate, while there are no EFF detected changes. In this study, only the learning-based EFF classification and longitudinal high-slip friction used measurements could outperform the accuracy of the VFF lateral acceleration algorithms.

The author tested the VFF performance using databank measurements collected with the development vehicle, and implemented friction used and longitudinal slip algorithms to support the data fusion. Based on the databank offline analysis, for dry asphalt the VFF lateral acceleration algorithms provide an esti-

mate of 1.0 in nine out of ten tests, occasionally outputting water level of friction potential down to 0.7. When moving from a low friction surface to a high friction surface, the acceleration is naturally low after the low friction surface and is usually not enough to update the estimate.

The estimate for wet asphalt varied between 0.5–1 (also in the Turin tests at 0.7 wet asphalt), the variation being larger than for dry asphalt. On snow, ice and artificial slippery surfaces (e.g. 0.3), the estimates stay in the range of 0.1–0.5, during cornering. However, the output can be similar for all these surfaces, making it difficult to reliably differentiate between them, based on lateral algorithms alone. The algorithms also often consider their output as invalid, even when in the correct range.

Especially for the icy and snowy surfaces, additional checks based on friction used and slip provide important support for classification, but only when already using most of the friction potential. For example when moving from asphalt to ice, without accelerating, the VFF cannot update its (invalid) estimate. Already using 0.1–0.15 g longitudinal acceleration does, however, produce enough slip for updating the final estimate from the module. Additionally, recording friction used during (larger than 5%) slip evens out the module output, maintaining the highest value until either the lateral algorithms provide a new valid output or high slip is again detected.

6.4.4 Learning the true friction potential in abnormal cases

On surfaces where the road classification (e.g. in wet and dry asphalt) does not accurately represent the friction potential, such as on the synthetic cover used in the Aachen summer testing, the learning feature of the algorithms provided effective results. The following figure shows a test where the friction potential is learned downwards for the surface. In this test the EFF Database inputs were probabilities of wet, snow and ice instead of raw sensor data.

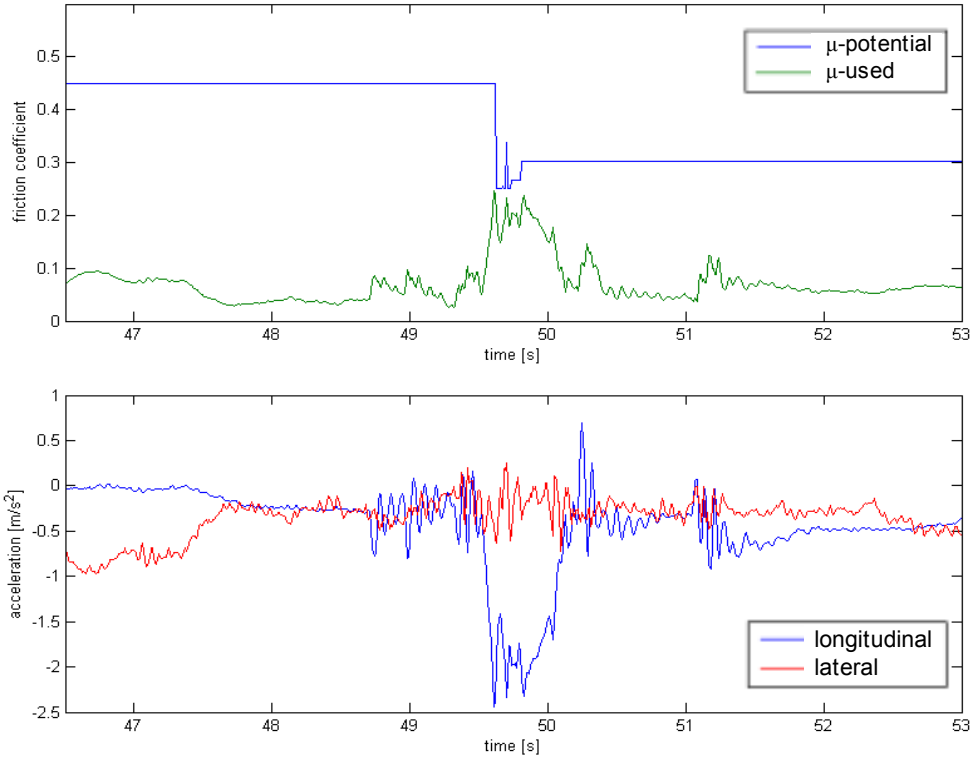

Figure 52. Friction potential detection by learning. Expected friction level 0.3 (watered synthetic cover), vehicle speed 20 km/h. [2]

However, using the probabilities as an input, the limited number of mapped cases causes re-learning on different types of "wet asphalt", as the plastic cover does not differ from normal wet asphalt. This suggests utilizing raw sensor data in the EFF classification to potentially learn the abnormal cases.

6.4.5 Common estimation errors and deciding validity

The estimation errors experienced during the tests have been discussed from EFF and VFF perspectives, but the system's overall performance was also linked to different road conditions. The following table presents the common errors using a road condition classification in dry, wet, snowy or icy and also 'un-known'. This provides a basis for analysing collision avoidance and mitigation performance on these surfaces in the next chapter.

Table 10. Common friction potential estimation errors according to road conditions.

Road condition	**Common estimation errors**
Dry asphalt	Estimation may provide a literature-based conservative value for the surface (in this study the value was set at 0.85) if it has not recently learned a more accurate value. This default value may be slightly too low. Additionally, the classification may momentarily give out low values of around 0.7 due to vehicle algorithm inaccuracies. When the friction potential exceeds 1.0, the algorithms may provide only 1.0.
Wet asphalt	In the worst case, estimates range from 0.5–1, momentarily alternating. During hard braking or cornering (> 0.5 *g*) the estimation is accurate to ±0.15. EFF learning and the data fusion provide estimates within 0.2 most of the time (~90%). The road ahead may not be wet, which would be important for applications to know.
Snowy or icy (asphalt)	Estimates for friction potential generally vary between 0.1–0.5, but due to VFF delays the change is not always instant when driving onto a slippery surface, and a momentary higher value could be given. When ice, snow and asphalt are alternating, only some coordinates are available for the clean icy spots from the IcOR, but not a true model of the road. Due to slip an accurate friction measurement is available more often than on high friction surfaces (when there are no large changes in driving style), but there is no proof that the value accurately represents the road ahead. The system doesn't differentiate snow on ice from snow on asphalt.
Other road conditions not directly supported by the system	The estimation is often unavailable due to the surfaces not matching the programmed models and therefore failing plausibility checks. However, classification-based systems may occasionally come up with a result. In this case the output would contain significant error. The factual data collected on friction used and slip, as well as the EFF learning features matching environmental sensor inputs with experienced friction potential, still provide short-duration estimation.

The validity of the estimates was considered to be high during the VFF cornering or high slip outputs. When only an EFF estimate was available, the validity

of the final friction potential output was set to drop with distance from the previous VFF measurement. This configuration parameter for how the validity drops was not tested from an application perspective. When neither estimate is available, 5–30% of the time (based on separate sensor studies, but generally 10% in the databank collected in daylight conditions), the validity starts dropping further. Even when the validity becomes zero, the previous estimate is maintained as an output.

For learned EFF Friction Database values, the validity could be considered higher than generally for EFF default values for road surfaces. However, this was not implemented and should be tested from an application perspective.

7. Collision Avoidance and Mitigation

This chapter discusses friction as a central starting point for collision avoidance algorithm design. Friction potential affects both the trajectory options available to avoid collisions and the maximum predicted accelerations of other dynamic objects. A new method is introduced for collision avoidance and mitigation calculations, with an emphasis on effective computing.

This chapter also clarifies practical requirements for friction estimation from an application point of view. Finally, simulations are used to show potential improvements in collision mitigation by comparing systems with and without friction estimation.

7.1 Introduction

Collision avoidance algorithms have been extensively studied especially in the field of robotics. Planning a collision-free path from point A to B, being able to recognize obstacles and at least stop before a dangerous collision are common requirements for mobile robots and autonomous vehicles.

Collision avoidance exists at several levels. Although there are no clear classifications, some distinctions between the following categories can be made:

I. Route planning algorithms may utilize a dynamic map, which includes obstacles and blocked directions. A new route can be searched from a large map and a vehicle may completely turn around. Local maps such as occupancy grids[1], where sensor measurements are collected to form a view

[1] A grid format map of the environment, often evenly spaced. The cells contain e.g. the probability value of being occupied.

of the surroundings, are used even for rather detailed planning. Mostly these route planning algorithms consider the obstacles as static and calculate a new plan when required or at certain intervals.

II. When the vehicle kinematics and dynamics are considered, the obstacles move and, e.g. tyre–road friction potential is estimated; this detailed calculation is rather called trajectory planning than route/path planning. Trajectory planning can however reach long distances, especially with fast moving vehicles. The uncertainty in obstacle movement as well as maximum range of environmental sensing usually set limits (time and distance) for this type of accurate collision avoidance. Following a route plan always leads to a level of trajectory planning, when a vehicle attempts to stay on the route and execute turns.

III. Short trajectories and resulting collisions can also be calculated in more reactive control systems, which may not even have a goal direction but are just wondering, searching or mapping the environment. Toy robots for example may turn just before (of after) hitting an obstacle and then continue to a random direction. Collision avoidance does not necessarily mean long distance planning or optimal trajectory! A snapshot of a situation can be used in calculations to effectively prevent collisions. This type of functionality can also be combined with route following/planning: for example to stop, when the route is not free, or to improve the planned route with local collision avoidance.

IV. When autonomous vehicles perform certain manoeuvres such as a lane change, the requirements of this manoeuvre need to be combined with collision avoidance calculations. During a lane change, a safety distance is kept to other vehicles and the maximum lateral acceleration is likely to be limited to ensure a smooth lane change and passenger comfort. The role of collision avoidance algorithms may be just to check if the required space is free during a manoeuvre, or to signal an abort when the manoeuvre cannot be completed safely.

V. Collision warning systems calculate the risk of collision and time or distance before impact. Human operators can use this information to evaluate a situation and decide on actions. As a first action, a vehicle or robot may slow its speed or stop completely. In the event a system detects

a human on the route, it could also sound a warning and wait for the human to move.

Current collision mitigation systems and variations of automatic emergency braking designed to support drivers mostly fall into categories III–V in this classification. In systems such as the APALACI (Chapter 5.3), first a warning is given to the driver and the brakes are prepared. Automatic braking starts only if a collision is unavoidable. During the braking, the vehicle does not change driving direction, but the driver is allowed to do so. Before the collision, seat belts are pre-tensioned.

'Collision mitigation' implies various methods of mitigation and therefore the abbreviations CMbB (Collision Mitigation by Braking) and AEB (Automatic Emergency Braking) are also often used to clarify the exact implementation. CMS is used both to refer to 'Collision Mitigation System' and 'Collision Mitigation Brake System'. The terms do not have an established status and they fall within pre-crash safety systems.

Collision mitigation systems could be considered as different from collision avoidance systems, since they do not necessarily even attempt to avoid collisions but only to mitigate the consequences. For practical reasons, their operation may also be limited to large objects, which can be reliably detected.

It has been a design principle in vehicle safety that the vehicle should not take control while the driver still has a possibility to avoid collisions (e.g. [56]). Light braking could, however, be seen as a way to warn the driver as well as an acceptable early phase of collision avoidance and mitigation.

Potential mistakes in collision avoidance operated through autonomous steering invites discussion about responsibilities and product liability, although braking and other types of mitigation also require high reliability:

- Unnecessary hard braking might cause a rear-end collision if the driver following is unable to stop in time, for example due to interpreting the situation differently or simply being unable to brake as efficiently as a car with the optimized CMS braking.
- Prototype bumper and bonnet designs, which target improved pedestrian protection in collisions, could include irreversible systems such as airbags, if collisions can be reliably detected (Figure 53).

Figure 53. APROSYS project bumper and bonnet concepts for improved pedestrian protection. Project final event, February 2009.

Considering the similar algorithms used in collision avoidance and collision mitigation systems to calculate the time to collisions and the steering angles to potentially escape them, the difference can be very small: collision avoidance starts to apply brakes a split second earlier than collision mitigation. With collision avoidance, however, people usually refer to a *system that evades obstacles also by steering*, while collision mitigation refers to activating countermeasures before impact.

The more autonomous operation (belonging to categories I–II) has been recently demonstrated e.g. in the DARPA Grand Challenges. These competitions for autonomous vehicles, where the United States Department of Defence awards cash prizes for the fastest teams successfully negotiating a substantial off-road course, have been held in 2004, 2005 and 2007. They have been showcases for advanced navigation algorithms and environmental sensing. In the first challenge, which was held in the Mojave Desert, no vehicle successfully completed the route. In the following years the competitors have shown considerable

progress and in 2007 the challenge was last held in an urban environment, where the vehicles also had to be taught some traffic rules. [57]

7.1.1 The uncertainties

When discussing collision avoidance, it is difficult to overlook the uncertainties and approximations usually included in the calculations. This work emphasizes the role of accurate friction estimation, but more generally the topics are:

1. Reliable environmental sensing

Reliable obstacle detection and classification is the basis for the collision avoidance algorithms. A camera sensor system might have difficulties in detecting e.g. a dark-hooded jogger who blends into the background and moves fast. Further, the system should correctly classify small children, pregnant women and even recognize as a human somebody who is carrying e.g. a 40" LCD TV out from a shop and having only his legs visible! Obstacles with practically no weight, such as balloons, cardboard boxes and paper carried in the wind, offer further classification difficulties.

Modelling the road/environment is important for correct trajectory planning; detecting lanes, ditches, kerbs, low bridges and using them in calculations. In normal situations a vehicle should not drive into a ditch, but in critical scenarios this might be acceptable. Similarly, a kerb may be an obstacle or not. Low bridges are obstacles depending on vehicle height and holes in the road are obstacles depending on their depth.

Environmental sensors have a limited field of view and this usually leads to large areas of unknown terrain for collision avoidance calculations. Adverse weather conditions usually affect sensor performance and the performance needs to be validated in the dark, rain, fog, direct sunlight, when covered with dirt etc. Likewise, a bumpy road surface (e.g. cobblestone) and tyre–road friction potential affect vehicle dynamics and are therefore important to detect.

2. Interpreting situations and anticipating movement

When a football bounces in front of the vehicle in a residential area, a computer might not brake for such a small object, but a human often would. The human driver assumes that a child might come running right after the ball! This level of

thinking required would require advanced artificial intelligence or at least a large set of rules for behaviour.

When driving near pedestrians, drivers monitor e.g. if a person appears to want to cross the road. Drivers can usually assume that grown-up pedestrians mostly maintain their direction and speed when walking directly along the road side. Short distances to pedestrians, however, mean a theoretical risk of collision: a pedestrian may for some reason run into the vehicle path. This is examined in the following:

Figure 54 shows optimal braking distances with different levels of friction potential. The calculation is based on Equation 7, where s is the braking distance and v_0 the initial velocity. Figure 55 shows the time to cover these braking distances plus a vehicle of length 5 meters, maintaining speed.

$$s = \frac{v_0^2}{2\mu g} \tag{7}$$

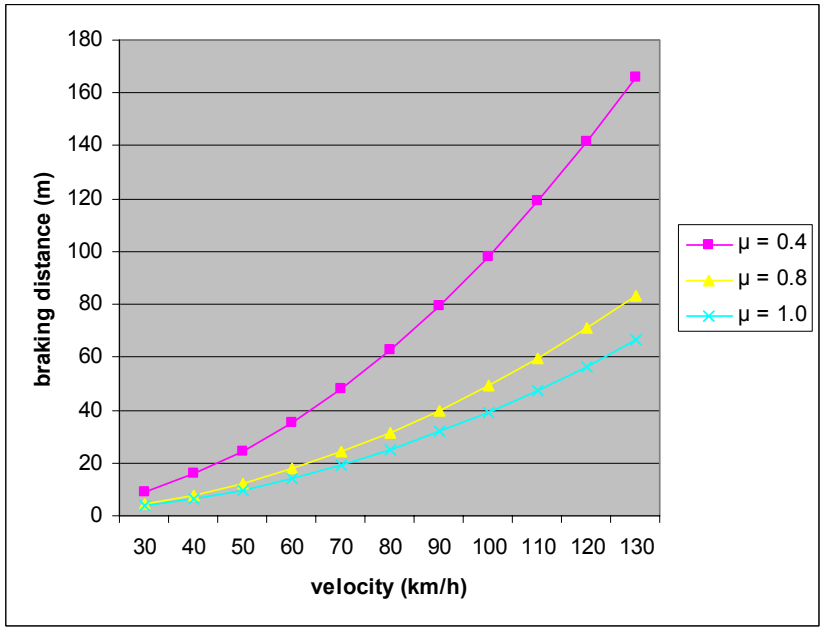

Figure 54. Optimal braking distances with different levels of friction potential.

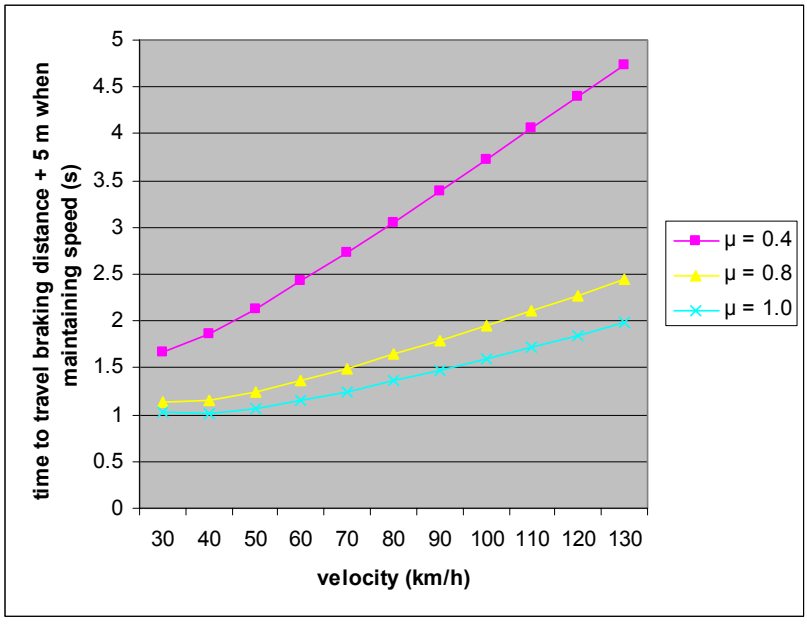

Figure 55. The time it takes for the vehicle to cross the braking distance with current velocity.

When assuming that a pedestrian at braking distance starts moving into the vehicle path, the vehicle can either stop or slightly accelerate; in a case where the pedestrian should not reach the vehicle path in the time it takes for the vehicle to pass the pedestrian, based on current velocity or higher, there would be no collision.

Considering that the author can, from a standing start, sprint 3 meters in 1.2 seconds, 5 meters in 1.5 seconds, and walk 5 meters in 4 seconds, e.g. the following notes can be made about (autonomous) emergency braking and pedestrians:

- On dry asphalt (μ = 1.0), when driving speed is below 70 km/h, collisions with pedestrians standing 3 meters or more away from the vehicle path, could be avoided without first dropping driving speed. Either the vehicle can brake in time or the pedestrian does not have enough time to jump in front of the vehicle.
- On snowy roads (μ = 0.4), the theoretical collision risk with pedestrians walking near the curb is high inside the braking distance (e.g. 35 meters when driving 60 km/h). This could cause an autonomous vehicle to slow down to even below 30 km/h to avoid the risk.

Problems and delays related to detecting the state of a moving object would make the risk of collision higher than in the example, but a collision avoidance system that was also able to steer could perform better.

Whether autonomous vehicles would be allowed to make similar assumptions and take the same risks that drivers do, e.g. when driving near pedestrians, is an interesting topic for legal studies.

3. Accurate trajectory planning

Truly accurate trajectory planning would include the effect of e.g. road bumps and inclined road. Further, large slip, uncontrollable sliding and race car dynamics are difficult to estimate in real time. With motorcycles, the driver's sitting stance affects dynamics and should not be neglected.

Hard manoeuvres at the very last moment before collision may even cause difficulties to keep the vehicle on the road or lane. Therefore the collision avoidance should also prepare for the next turns to make the operation smoother. On the motorway, an early lane change could effectively prevent a collision, if the system would be allowed such early planning.

4. Interaction with users and non-users

Several HMI design issues arise when the vehicle is not going exactly where the driver is steering because the collision avoidance system is changing the course.

Information about the driver's alertness can be used to trigger collision warnings (the driver has not noticed a danger). If the driver is unable to continue driving or likely has a long reaction time, this information could even be used for early triggering of collision mitigation/avoidance to further improve their effectiveness.

A system could possibly prevent a collision with a pedestrian who e.g. seems to be looking in the wrong direction, also by activating the car's horn.

Interesting cases arise if a driver warning system warns at an intersection about a probable collision unless the other driver starts braking, and this happens where the other driver is facing a stop sign. The sign may be missing from digital maps, or be difficult to detect with environmental sensors and therefore not available for the safety system's assessment. The warning would be correctly calculated but possibly unwarranted, as the probability of a driver not even slowing to a stop sign is low.

5. Allow collisions in certain situations

In some designs, the collision avoidance algorithms need to be partially or momentarily overridden to allow for a vehicle to collide with an obstacle: A car should be allowed to pass near bushes and trees, pushing a few branches aside if the driver so wishes. An indoor robot might need to push a door open at low speed. However, it would not be favourable to hit a tree trunk or even a door with high speed. There is a need for advanced obstacle analysis to provide information on which objects can be driven through or moved and under what conditions. In these cases the objects or some parts of them would no longer be considered obstacles in the algorithm.

6. Prioritization and cost estimation

If damage is unavoidable, a driver quickly considers the options and may for example prefer to drive into a ditch than hit a person. This type of prioritization or "cost estimation" is something that an optimal collision avoidance system could include. The calculations could also include which part of the vehicle(s) would be hit.

The traditional potential field method for collision avoidance makes a good example of practical algorithm design and the approximations involved: These algorithms have received wide interest in robotics since the late 1980s e.g. due to their computational effectiveness [58]. In the method, obstacles and the area near them are marked as having high potential and the robot goes towards low potential. A way to visualize the principle is to think of a hilly landscape, where water (robot) flows in the valleys, between the hills (obstacles). The direction of the goal can be for example a vector, which is summed with the direction of the potential field at the origin of the robot. The following figure visualises a variant of a potential field calculation:

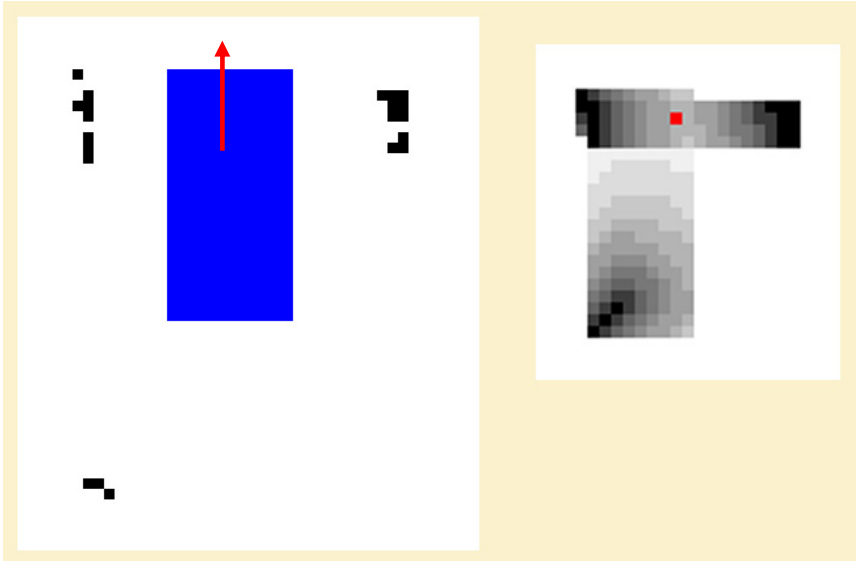

Figure 56. The left side shows detected obstacles around a vehicle/robot. The obstacles are unclassified and only some points have been measured with distance sensors (ultrasound, laser). Red arrow indicates movement direction, which is free of obstacles. The right side illustrates a variant of a potential field calculation where the obstacle distances are calculated from the edges of the robot, making a smaller figure.

In the example, the obstacles on both sides of the vehicle cause the robot to centre its position. This type of behaviour may be effective when driving in tunnels or moving in corridors. In this example, the lowest obstacle is considered to be already too far to affect the calculation. The distances from how far the obstacles affect the robot, can naturally be configured – several variations can be created.

The potential field method forces the robot on a route around obstacles, but the calculation is not accurately planned; rather, it is reactive. The robot also moves further away from obstacles that it passes near, *although it would actually not hit them on its current trajectory*. This behaviour can be interpreted as false avoidance or safety distance, depending on the application. When a robot avoids an obstacle it would not actually hit, and makes a turn towards another obstacle or a danger it does not detect with its environmental sensing, e.g. a ditch, the result can be dangerous. Ditch and hole detection have traditionally been harder than detecting obstacles on the same plane [59, p. 62].

Potential field methods require very reliable environmental sensing and do not cover dynamic obstacles. Some other practical difficulties, such as passing through closely spaced obstacles, are discussed in [58].

7.2 Target Curvature-Velocity Method

In the following, a new calculation method for local collision avoidance named the Target Curvature-Velocity Method (T-CVM) is introduced. It is designed for high-speed collision mitigation and avoidance applications, yet it can perform millions of vehicle trajectory checks and utilize information on dynamic obstacles along with their classification. Tyre–road friction estimates and vehicle dynamics are incorporated in the calculation of pre-simulated trajectories, deciding which trajectories and change of velocity can be executed. The name of the method describes assessing the safety of a list of optional trajectories, each initiating from the vehicle's current velocity and curvature values and reaching certain target values.

The origins of the approach are in the well-known Curvature-Velocity Method (CVM) [60]. The CVM describes movement as arcs and their curvatures (Figure 57). For each obstacle, a minimum and maximum curvature to avoid it, are calculated. The calculation is frequently updated.

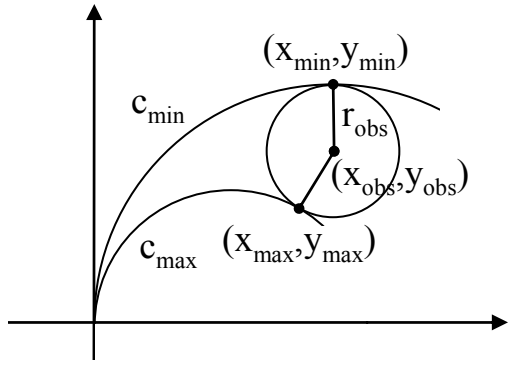

Figure 57. Tangent curvatures for a circular obstacle, according to [60]. The robot/vehicle starts from the origin.

The original work discusses indoor robot applications, where speeds and accelerations are rather limited. Safe operation was reported at up to 60 cm/sec. Partly the speed limitations were due to a lack of computational power in 1996. How-

ever, when moving at higher speeds, a vehicle cannot instantly switch between these steady state curvatures, which causes an approximation error [59]. Delays in steering and overcoming the vehicle inertia need to be considered to cover high-speed applications.

Figure 58 shows example trajectories resulting in the same final curvature, starting from different initial curvatures. The trajectories have been simulated using:

- the demonstrator vehicle, an Audi A6, dimensions 203 × 492 cm and yaw angular inertia 3585 kgm^2
- the common two-wheel (bicycle) kinematics simplification for a car
- no suspension model
- small steering, acceleration and braking delays, where the response time to step steering input was set maximally at 0.1 s.
- friction potential 0.6.

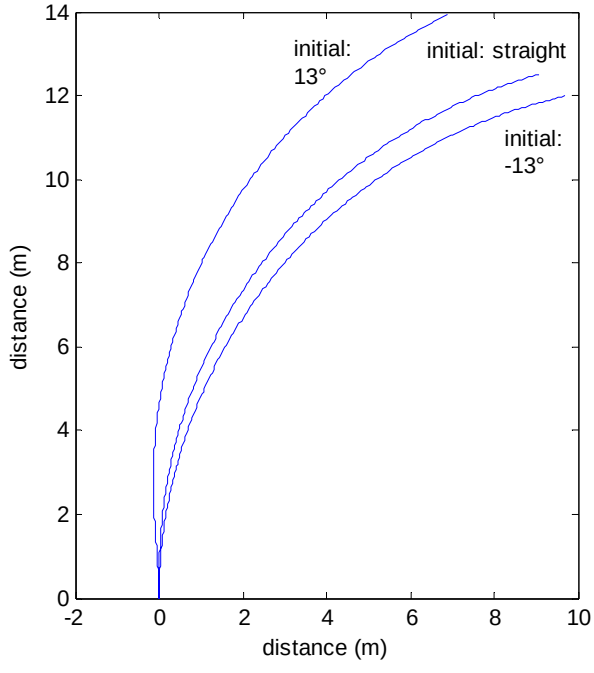

Figure 58. Simulated trajectories when aiming for the same curvature with a constant speed of 30 km/h and different initial curvatures (kinematic model's steering angle ±13°, omitting slip). The plots represent the paths (of the centre point of rear axle) for the next 2 seconds, with friction potential 0.6.

If large steering delays would be included, in addition to inertia and limited friction potential, the time it takes for a vehicle to reach a set curvature could become several seconds, as presented in [59].

With cars, the CVM curvatures can be understood as trajectories characterized by vehicle speed and steering angle. Equation 8 gives the steady state curvature ($1/r$) response with respect to the steering angle of the front wheel (δ_f), wheelbase (L) and vehicle understeer coefficient (K_{us}). For a neutral steer vehicle, the understeer coefficient is zero. [13, p. 379]

$$\frac{1/r}{\delta_f} = \frac{1}{L + K_{us} v^2 / g} \tag{8}$$

Instead of using curvature values in the visualization of the T-CVM calculations, this work uses the "virtual steering angle" of the front wheel (in a two-wheel model) to represent the curvatures and provide an index. This is done for simplified visual analysis of the calculation results, but can also be misleading: It is important to note that the steering angle of the front wheels does not generally correspond to certain fixed curvatures. This is due to a varying tyre slip angle with vehicle speed, oversteer/understeer properties, banked road or e.g. side wind. The steering angle of a kinematic model can describe the curvature only in a geometrical study omitting slip. The virtual steering angle used in this work describes the trajectory tangent rather than the final steering angle of the front wheels.

The final steering angle of the vehicle to negotiate a given curvature for collision avoidance would be decided by separate vehicle control algorithms, covering slip and generally the steering response.

Equation 9 has been used in simulations to match curvatures to virtual steering angles. It shows the calculation for turning a circle radius r with bicycle kinematics in a no-slip situation.

$$r = L \cdot \tan(\frac{\pi}{2} - \delta_f) \tag{9}$$

The CVM method suggests *calculating distances to obstacles for each possible curvature and then selecting one*, which satisfies both the collision avoidance and other objectives [60]. The current operating point and the direction towards the goal are the starting points for selecting a new curvature. The new curvature could be e.g. the closest non-colliding curvature next to the currently used curvature. However, maximum vehicle accelerations set constraints on what velocities and curvatures can be reached in a given time.

The following figure illustrates the idea of calculating distances to the closest obstacle for every virtual steering angle. The example is calculated for the situation in Figure 56, where walls are on both sides of the vehicle. This is a recording from a collision avoidance system designed for VTT's Tracker wheelchair robot in the year 2000 [61, 62]. The robot has car-like properties (4 wheels and dimensions 65 × 145 cm, approximately one third that of the demonstration vehicle), except that the front wheels rotate freely and can reach any steering angle. As the figure shows, the robot sees no obstacles in front (steering angle 0) and could progress freely, but it would hit a wall approximately after 30 cm, if it would start turning either left or right. It can also reverse straight back without collision. This graph can be used as a basis for selecting a new steering angle and velocity to avoid collisions.

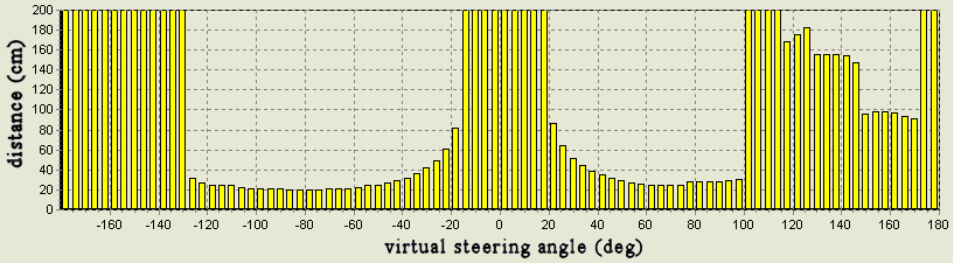

Figure 59. Distance to collision calculated for all virtual steering angles (4° intervals) of a kinematic model for the situation in Figure 56.

From the figure and knowing the current velocity, we can calculate the time to collision (TTC), which is the time available to change steering. The time increases when braking and the extra time gives the robot more possibilities to change curvature.

In cases where a robot has no other objective than to avoid collisions, the curvature with the longest free distance would be selected. In addition, choosing a curvature immediately next to a blocked trajectory might not be preferred to keep larger distances to obstacles when passing them.

The original CVM approximates obstacles as circles and gives them a safety radius. Enlarging either obstacles or the vehicle itself is a traditional approach in collision avoidance algorithms, but calculating collisions exactly and estimating the future movement of dynamic obstacles requires more accurate computation.

This work suggests calculation methods that *avoid making approximations in order to realize the CVM ideas*. Millions of alternative trajectories are pre-simulated to accomplish this, and key parameters are saved to large look-up tables. Additional levels of calculation are added to support dynamic obstacles, the maximum use of friction, and finally obstacle classification.

Besides these additional levels, most of the calculation methods were already developed for the Tracker wheelchair robot, but they have not been previously published in detail. An early CVM variant used with the wheelchair was found to support also joystick driving by correcting driver actions, and autonomous route tracking, where it was the final layer of calculation before actuation [61].

The CVM and its variants can be classified as calculation methods for *local* collision avoidance. As such they are not designed for long-distance path planning that includes several turns and strategies. Path planning also generally requires more information on route objectives, traffic rules and the behaviour of other road users. The number of alternative strategies grows with assessed distance. As with the wheelchair robot, CVM can be combined with path planning by exchanging preferred curvature and velocity values.

The presented T-CVM covers near-miss calculations where a driver has already made or he is about to make an error that leads into collision.

The calculation steps of the method are presented on the following pages, starting from the required pre-calculations. An example T-CVM software implementation for MATLAB is included in Appendix A.

7.2.1 Pre-calculations

The T-CVM is based on simulating up to millions of possible vehicle trajectories beforehand, trying to cover practically all options. The trajectories are similar to the ones previously displayed in Figure 58. Below, Figure 60 shows another example. The trajectories depend on the vehicle kinematics, dynamics, performance and selected road properties, and they should be modelled in high detail to ensure that approximation errors would not be a main cause for the vehicle to collide with detected obstacles. The method can use any set of trajectories as an input, even recordings, as long as they are mapped to initial and target parameters. In this sense the trajectory simulation is a modular part of the pre-calculations that can be easily replaced.

The key variables in the vehicle trajectory simulation are target velocity and curvature. Starting from initial velocity and curvature, first the vehicle is accel-

erated and turned to target values, which are then kept. The transition phase can be long. Only trajectories where the target values can be reached are accepted for further calculations.

Due to using only steady state initial values in trajectory simulation, re-planning actions during e.g. heavy braking includes estimation errors. Further development of the method could look into compensating for these effects either in run-time calculations or in a simulation phase. Other similar error sources include e.g. a change of balance due to heavy load or (undetected) trailer use. However, if the selected trajectory can be executed with acceptable accuracy during driving, the pre-calculations can still be considered valid.

The other parameters describing the trajectories can be selected more freely in an application and would preferably include friction and road inclination, but could also include e.g. angular velocity, allowing a vehicle to rotate on its path.

Although the trajectories do not have to be saved for run-time calculations, their number increases the memory use of the model: the T-CVM relies on very large generated look-up tables to assist in run-time calculations. The size of the look-up tables scales from megabytes to gigabytes, depending on application parameters and accuracy requirements.

The trajectories are simulated for a fixed maximum time forward. In the example given in this work, this time is 2 seconds. The time is generally selected based on a suitable maximum time to collision (TTC) that is interesting for the application and can also be reasonably covered with simulation. For example braking distances, times required for braking (Figure 55) and environmental sensors' field of view are used when deciding a suitable maximum TTC for trajectory simulations. As the simulation does not include executing several turns to avoid an obstacle, this causes a practical limitation for covering the near future with acceptable accuracy.

Due to the transition phase between steady state curvatures the trajectory formulation is not unambiguous. Several strategies exist for reaching the same target values; e.g. first braking and then turning, or braking and turning both at the same time. Especially the case where the vehicle should execute a tighter curve at lower than the initial speed, *attempting the final curvature right away may lead to using all available friction due to centrifugal force*. This leaves no friction for efficient braking. This can be experienced e.g. on snow, where hard turning even at low speeds causes large slip. To be able to make a tight curve, a driver first has to brake.

The simulation aims to calculate a set of suitable trajectories for 1) vehicle control in collision avoidance and 2) to cover possible driver escape routes to detect unavoidable collision. The drivers have numerous options to avoid collisions and it is difficult to cover them all with centimetre accuracy. Simulations can best cover short times and trajectories, where different steering and braking options can be simulated with reasonable resolution.

At high speeds, the braking distances of cars grow to over 100 meters and braking lasts for over 2 seconds (Figure 54 and Figure 55). This leaves the driver time to execute different strategies, e.g. first brake and then turn. The following figure describes this type of difficulty when attempting to simulate long times beforehand with any CVM variant:

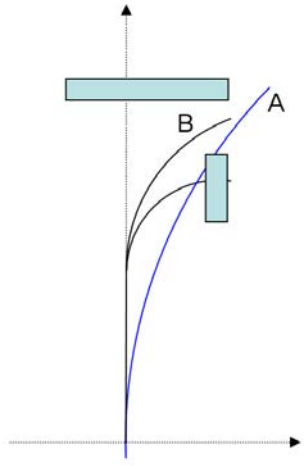

Figure 60. Delayed turning vs. CVM in a special case. CVM trajectories starting to turn right from origin (A) would not find a free path, but trajectories where there is a delay before turning, may still find a collision-free route (B).

Due to time limitations in future trajectory approximation – the number of possible trajectories growing rapidly with time – it can be difficult to accurately cover full braking distances in collision mitigation algorithms. This is the case especially when a vehicle is travelling at high speed and the friction potential is low. If a system attempts to cover the situation of Figure 60, it might suggest braking when the driver actually still has an escape route. The driver can turn right just before the collision. The system possibly notices the opening ("B" in the figure) later than the driver. This special case can be approached with separate path planning and simulating more trajectories (this algorithm extension will

be discussed later), but basically the CVM calculations have a limited time and distance when calculating possible vehicle trajectories beforehand.

The trajectory examples of this work have been simulated mainly by dividing available friction evenly between lateral and longitudinal acceleration. This causes the vehicle to turn quickly. This follows the original CVM, where a robot would almost instantly change curvature. A different approach was, however, taken for the trajectories where hard turning is not possible without first braking, as explained before. An optimal braking/acceleration strategy requires a more advanced controller than has been used in this study.

Naturally banked roads, bumps and friction potential also affect trajectories. The suggested method is unable to directly include road bumps, but banked and inclined roads can be covered by calculating new sets of trajectories for a limited number of planes. This however multiplies memory use with the number of planes and requires reliable real-time estimation of road inclination. Especially being able to detect and include steep (e.g. 10°) uphill and downhill gradients in the application would improve the accuracy of avoidance manoeuvre calculations.

Due to growing memory use and the capabilities of today's friction estimation systems, this method uses *only a single friction potential value at a time for the whole simulation area*. The trajectories are simulated for several different friction levels.

If a future system can provide friction potentials e.g. mapped to a grid around the vehicle (Figure 31), complementing the T-CVM with path/route planning type algorithms, where the grid data could be used, would be an interesting research topic. The current algorithm might also theoretically benefit from this information, if the friction potential would be clearly different for different sectors or curvatures. This would enable combining e.g. two result tables calculated for different friction levels, based on the sector boundaries. Another approach could be generating virtual obstacles where the trajectories can no longer be continued.

The following table sums up the trajectory parameters for the simulation.

Table 11. Inputs for trajectory simulation. The intervals are given using MATLAB notation. Example value ranges are from Appendix A code.

Trajectory parameter	**Range**
Friction used – the highest level of friction used in accelerations and steering when trying to reach the target values.	Constant values for the trajectory Example: [0.1:0.1:1] (size = 10)
Initial velocity	From the lowest velocity to the highest velocity from an application point of view Example: simulation_upper_speed_limit = 130 simulation_lower_speed_limit = –20 [simulation_lower_speed_limit:10: simulation_upper_speed_limit] (size = 16)
Initial curvature	Initial curvatures with required resolution. In high-speed applications, an increased resolution is required close to straightline driving (virtual steering angle near 0). For presentation reasons, this work matches the curvatures to virtual steering angles of a kinematic model. The steering_angle_max is here decided by maximum angle of front wheel(s). Example: steering_angle_max = 0.5645 initial_steering_angles = [0.5645 0.5081 0.4516 0.3952 0.3387 0.2823 0.2258 0.1694 0.1129 0.0988 0.0847 0.0706 0.0565 0.0423 0.0282 0.0141 0 -0.0141 …] (size = 33)
Target velocity	Reachable velocities, calculated from an initial velocity using maximum acceleration (and simulation limits). Example with 5 km/h step size: target_velocities=sort([[initial_velocity: -5/3.6:reachable_velocity_min] [initial_velocity+5/3.6:5/3.6:reachable_velocity_max]]) (size = varies, 10-15 normally)
Target curvature	Relevant virtual steering angles calculated based on the maximum reachable angle with minimum speed.

	Example: target_steering_angles = [steering_angle_max: -steering_angle_max/13:-steering_angle_max] then reshaping steering angles, more angles required near 0; straight driving: target_steering_angles = [target_steering_angles(1,1:8) target_steering_angles(1,9):-steering_angle_max/26: target_steering_angles(1,27-8) target_steering_angles(1,27-7: length(target_steering_angles))] (size = 37)
Road inclination (optional)	Optionally a few inclinations, e.g. 6–10° uphill and downhill (size = 3). Not included in the example but suggested if large variation exists in the application and road inclination can be reliably measured.

Total number of simulated trajectories reaches almost 3 million for the example values (10 × 16 × 33 × 15 × 37 = 2 930 400).

In the next phase of pre-calculations, trajectories are matched with an occupancy grid or several grids of varying size. Figure 61 shows the principle of calculating which trajectories collide with a cell in an occupancy grid.

The main idea is to calculate and *list all different trajectories which can lead to collision with a certain cell in an occupation grid*. Also the time period when the trajectory collides with the cell is calculated.

A detected obstacle can occupy one or several cells. With this pre-calculated information, when an obstacle is detected, the list of trajectories that lead to collision with it will instantly be known.

The occupation grid dimensions and cell size are up to an application. The grid should reach approximately the area the vehicle can travel in the selected maximum TTC.

In the example of Appendix A, several grids were used. The cell size does not have to be fixed but it can e.g. grow with distance. The cells near the vehicle were 30 × 30 cm in size. Obstacles far away may not need accurate calculations. A far-away grid could be added solely for driver warning purposes.

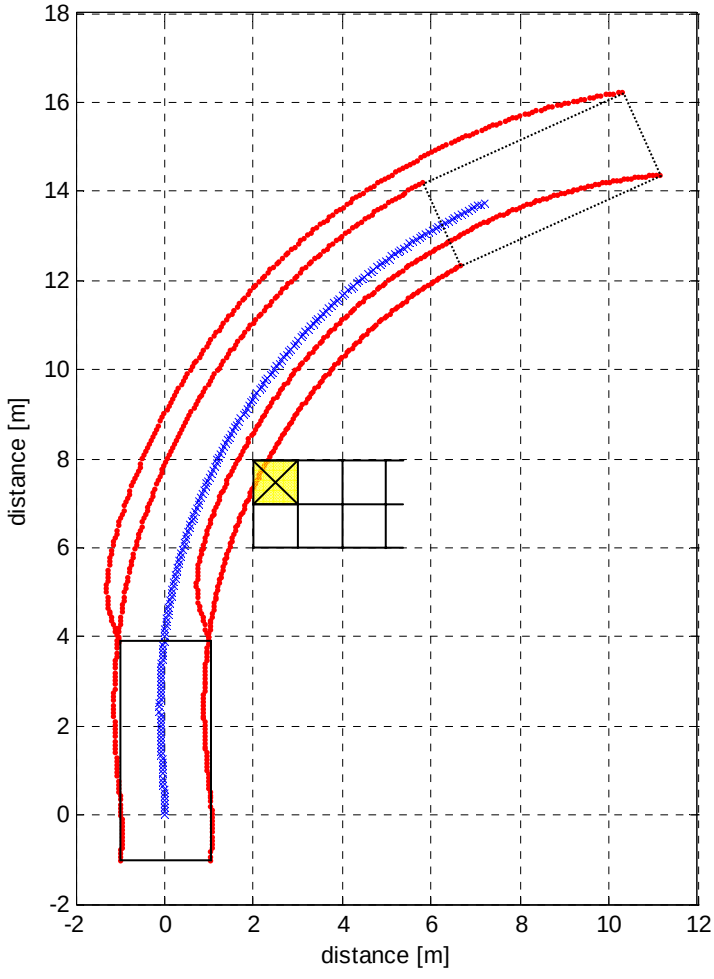

Figure 61. Simulated trajectory collides with a certain cell of an occupation grid in front of the vehicle. Model's virtual steering angle is initially 13° and target is -13°. Constant speed 30 km/h. Friction potential 0.6 and almost no steering delay. The red lines are the vehicle boundary box corners.

The calculation produces a very large amount of information to be saved. Mainly the look-up tables consist of lists of trajectories and their times to collision for each cell in the occupation grids. Saving information about the part of the vehicle that will be hit first in a collision is also an option for improving collision mitigation,

Additionally, the reachable combinations of velocities and curvature are recorded for each initial state. The initial states are defined by a limit for friction

use, initial velocity and initial curvature, as defined in Table 11. They form the main index for the look-up tables.

Figure 62 gives a suggested format for storing the look-up tables. The use of this information will be discussed in the following chapter.

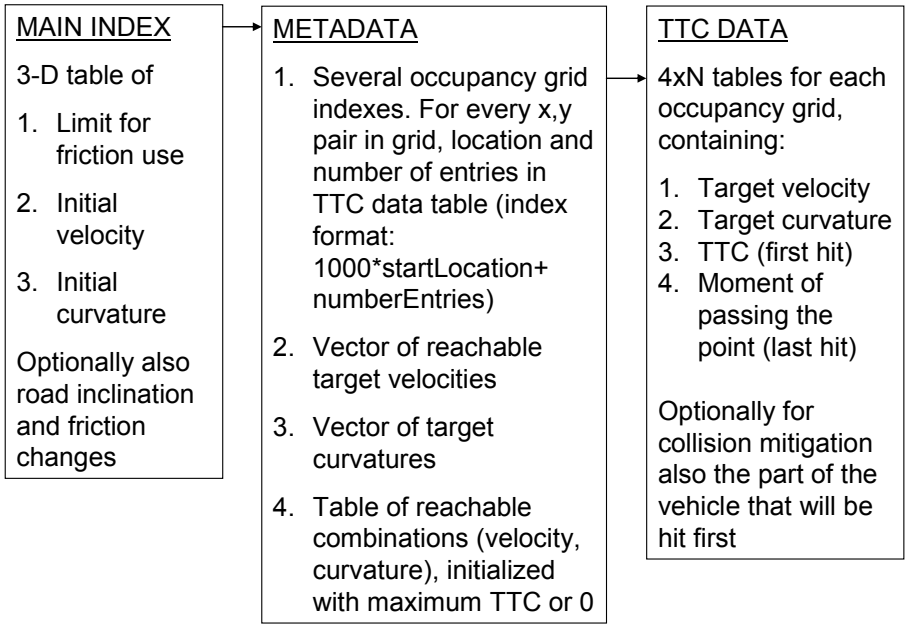

Figure 62. Look-up table levels and indexes.

The pre-calculation phase requires a lot of computations. For each initial state (main index of 3 values), it takes approximately 5 minutes to calculate all potential collisions in the occupancy grid, depending on simulation accuracy. With simulation settings and top initial velocities in Appendix A, the calculation runs even for 60 minutes. This applies to the given example source code for MATLAB and the Intel T2600 processor. Using the number of initial states in the example and 5 minutes for calculation, the total time to compute the look-up tables exceeds 18 days (10 × 16 × 33 × 5 min).

The resulting file sizes produced for different initial states are 100–1000 kB, depending on initial velocity and friction potential. With low initial speed, the vehicle cannot reach as many occupation grid cells as with high initial speed.

The total amount of memory required varies greatly when changing even one simulation parameter, but multiplying the number of initial states in Table 11 with

an average file size of 500 kB we get a total memory use of approximately 2600 MB. The example code, however, does not include mirroring same trajectories for opposite entry angles, which would basically cut the memory use in half.

The look-up table reaches even larger sizes when simulating different levels of friction inside occupation grids or several road inclinations or otherwise higher accuracy. For slow speed indoor robots on the other hand, even a few megabytes can be sufficient as the occupation grid area and accuracy of dynamics can be considerably reduced.

The large look-up tables of the T-CVM are justified with fast run-time calculations, as will be discussed in the following chapter (7.2.2). Alternatively the trajectory alternatives would have to be calculated in real time, which seems difficult to do with the same level of accuracy, and would consume a lot more CPU power and therefore energy in the vehicle, when comparing with almost plain memory operations.

As a post-processing step for the look-up tables, the cells where all combinations hit, should be specially marked to save memory and computation time. The following figure illustrates the number of saved velocity-trajectory combinations for each occupancy grid cell. The highest peak is the area where collision is unavoidable.

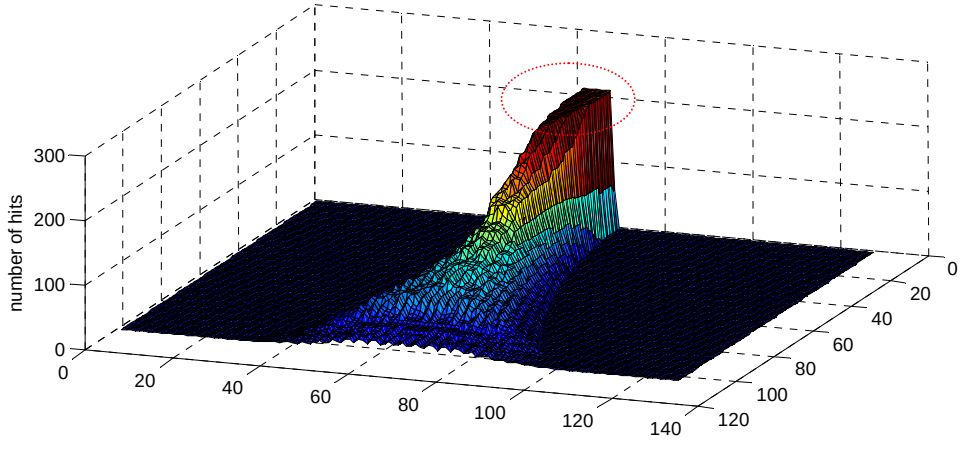

Figure 63. Highest peak (red ellipse) is where all options lead to collision and this should be specially marked in post-processing to save memory. Simulation uses friction potential 0.4 and initial velocity 60 km/h. A single cell in the grid (x and y axis) is 30 × 30 cm and the vehicle is moving downwards in the figure.

When calculating look-up tables for high friction, many target curvature-velocity combinations can be reached and the size of the table grows. Especially a suitable target curvature selection is necessary to cover the occupation grid area effectively. The weakness of T-CVM is black spots for the collision avoidance at large distances. This is a direct result of limited target curvature (virtual steering angle) resolution in look-up tables and the effect is shown in the following figure.

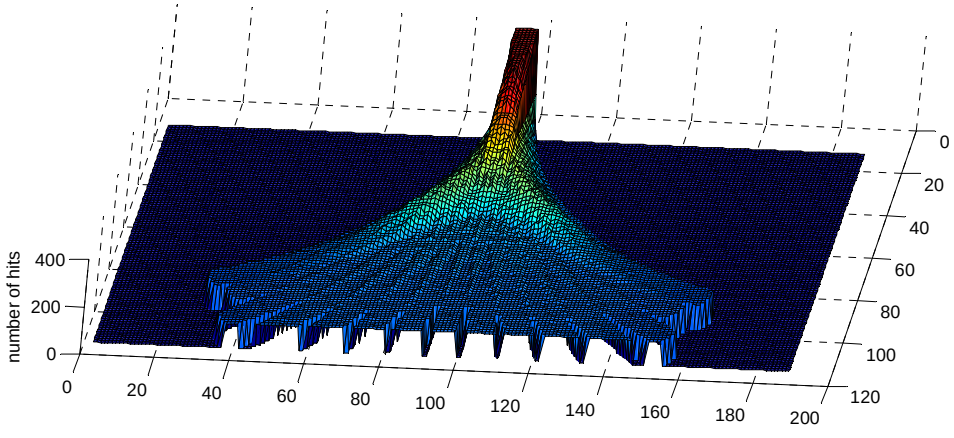

Figure 64. An example of limited target curvature resolution starting to cause black spots with distance, when high friction is available for turning. In the figure some black spots appear at 30 m from the vehicle front (openings at the lowest part of the figure, vehicle is moving downwards). The area of no hits (0) has been dropped for easier visualization. The friction potential has been 1.0 in the simulation and initial velocity 60 km/h.

At lower values of friction use or higher speeds, the gaps do not appear until longer distances; as tight curves are not included, virtual steering angles can be more tightly spaced with the same memory consumption.

With correct settings, the gaps barely appear within e.g. the 2 seconds of simulated movement with the suggested target angle accuracy. In Figure 64, at a steady speed, the vehicle would travel 33 meters and black spots appear at around 30 meters.

For collision mitigation and avoidance, the calculated paths in the area also give good information on how to proceed (e.g. several combinations cause no collision). For collision warning, however, the black spots could cause a slightly delayed warning in some cases.

7.2.2 Run-time calculations

The T-CVM emphasizes the role of look-up tables, which are used to quickly update the driving options after detecting and classifying obstacles. The run-time calculations are mainly for deciding actions based on the situation. The method produces the following type of snapshots of the current situation:

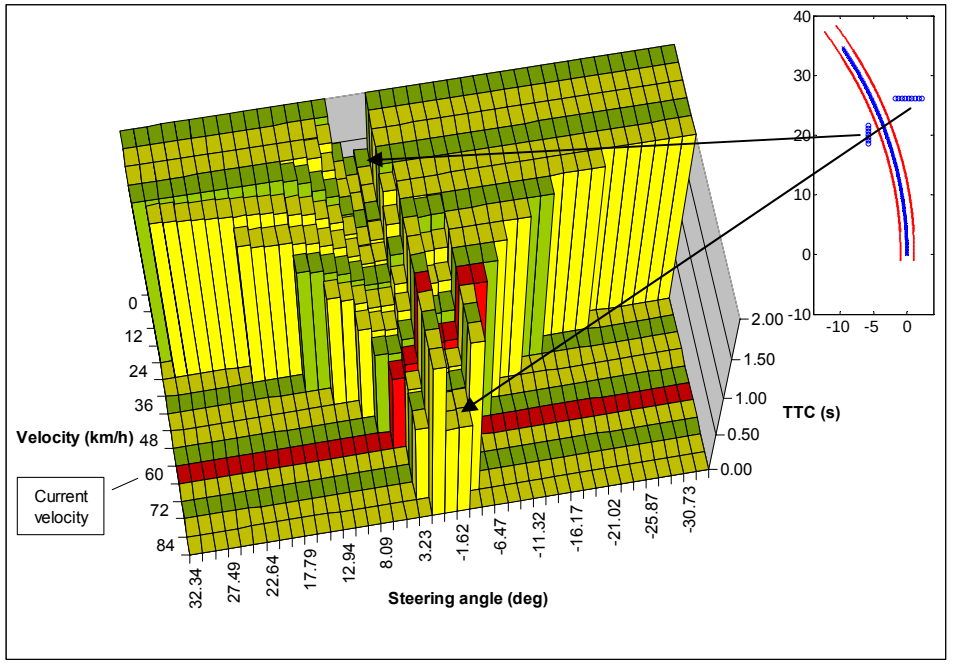

Figure 65. An example T-CVM result plotted as bar graph. The green and yellow colours are only to be able to see the different bars; the red colour represents the steering options at current velocity. The obstacles are shown in the small figure on the right. Simulation parameters: initial speed 60 km/h, driving straight and maximum friction use is 1.0. Curvatures are represented by a linear selection of virtual target steering angles.

In the figure, the bars that reach maximum TTC value of 2 seconds represent combinations of target curvature (virtual steering angle for visualization) and velocity that do not cause collision. The area which has a TTC value 0, represents combinations that cannot be reached during the next 2 seconds with the current friction potential. The other bars that show collision generally become shorter when speed increases; the same obstacle is hit sooner. The red colour indicates current velocity (green and yellow are just for clarity).

When comparing different T-CVM result tables, it is important to note that the method scales the (axes of) reachable curvatures and velocities based on initial conditions: First, the maximum and minimum velocities are calculated that can be reached within 2 seconds. Second, the tightest curvature is calculated that can be executed at the minimum reachable velocity. This type of scaling is done to exclude unnecessary values from the simulations and use memory efficiently to cover as many available trajectories as possible.

The following steps are required to produce the snapshots:

1. Environmental sensing provides obstacle co-ordinates and sizes in the vehicle co-ordinate system (minimum requirement: points, no excessive clutter). Preferably the input consists of boundary boxes of classified obstacles/objects, together with information on their anticipated movement options during the selected maximum time for simulation (e.g. 2 seconds).
2. During each calculation round, the obstacle co-ordinates are matched with the collision avoidance occupancy grids, leading to the occupation of one or several cells, depending on the obstacle shape. In the case of dynamic obstacles, a time period is required for when the cell is occupied. Further, the cells that the dynamic obstacle is considered likely to reach during the simulation period must be estimated for optimal calculation.
3. For each occupied cell, the list of trajectories that lead to collision with that cell is retrieved from look-up tables. For each trajectory, the look-up tables contain the target curvature and velocity together with first and last (when the obstacle has been passed) TTC values. If the cell is occupied during the period that the trajectory collides with it, the information is added to the result table.
4. The result table (Figure 65) contains minimums of all TTC values that have been added to it.

Many strategies exist for deciding a new curvature and velocity when the vehicle is about to collide. The result table only provides information about the available options. Autonomous vehicles select a new trajectory from the non-colliding options based on several goals and selection criteria such as target direction and preferred velocity, keeping distance to obstacles (combinations which are close to a collision are not selected), minimum use of tyre forces etc.

Since collision avoidance designs often involve these various goals that are part of the driving style – the optimization of which is not part of this study – the use of the T-CVM result table in collision avoidance is demonstrated only through near-miss avoidance simulations at the end of this chapter. The near-miss avoidance strategies best show the effects of varying friction potential.

The basic strategy for selecting a new curvature and velocity based on the T-CVM result table is to pick the closest non-colliding bar (parameters) to the currently used parameters where the TTC value has started to indicate an upcoming collision. If the target curvature and velocity are available from e.g. navigation, the selection is made from the closest non-colliding bars leading towards the target.

Naturally, selecting parameters that barely avoid a collision leaves very little room for error. In practise the selection often leaves more free space between objects. In collision avoidance variations that try to avoid collisions early and ensure that there can be no close calls, any colliding trajectories would be avoided as early as the collision can be detected, instead of waiting for the very last moment.

In collision mitigation design, however, braking could start when no options remain, with a clearly longer TTC than with the current velocity and curvature. A suggestion for timing is given at the end of this chapter.

The sensors' limited field of view (Figure 66) usually imposes speed limitations for this type of collision avoidance; the vehicle cannot go fast where it does not see. Otherwise the system has to make assumptions on the road being free of obstacles. Even if the system would not make such assumptions, the driver might.

The figure also shows a detail common to CVM variants: using the longest collision-free trajectory would cause the vehicle, in this case, to leave its lane. Therefore knowing the lane geometry is important for use of CVM variants in autonomous driving. Also, changing the lane generally increases the risk of collision, as environmental sensors may pick up fast moving objects when it is already too late for avoidance.

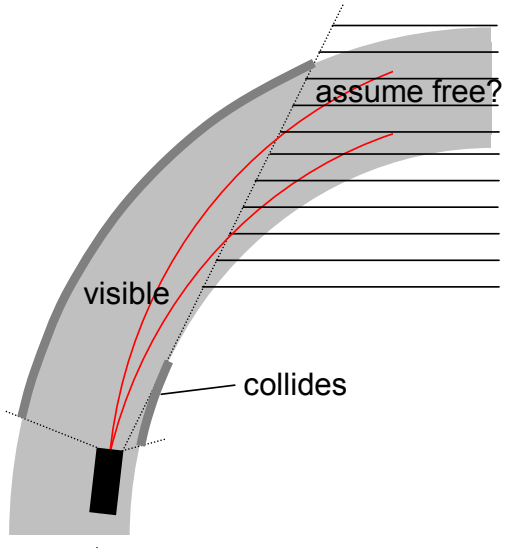

Figure 66. Limited sensor field of view and related assumptions. If the hatched area is considered an obstacle, the vehicle is soon about to collide and should slow down. However, a driver may be using an assumption that the road will be free of obstacles.

The presented T-CVM supports also the following type of calculations:

- Using different levels of maximum acceleration: Path planning software may aim to use a low acceleration level, translating to low friction use in T-CVM calculations. If the table calculated for low friction use does not contain suitable options, the calculation can be repeated for higher friction use, while still below the friction potential.
- Selecting which object type to collide with: In the case of unavoidable collision, certain object types such as ditches can be *removed* from the calculation, opening new trajectory options. These options lead to a collision but with the preferred obstacle type. The look-up tables can also be used to save optional information about the area of the vehicle which would be hit first in the collision.
- Delayed turning for double-checking unavoidable collision calculations: The difficulty to cover all possible trajectories that a driver can use to avoid collisions increases with simulation time and leads to cases previously presented e.g. in Figure 60. *The T-CVM result table can be calculated for situations which first include moving the vehicle to a co-*

ordinate point it will reach on its current trajectory. The delays before starting to brake or turn could be e.g. 0.5, 1 and 1.5 seconds. Repeating the calculations for different delays may help in finding new collision-free trajectories. It is then up to the collision mitigation application to design whether the system would warn the driver in this case. The collision mitigation timing is discussed more in Chapter 7.3.

- Anticipating the moment of unavoidable collision for collision avoidance operating at near-miss ranges: To be able to start evasive action only just before collision becomes unavoidable, the same kind of anticipatory simulation can be used as in the previous case; moving vehicle e.g. 0.1 seconds forward on current (steady state) trajectory. Collision avoidance timing is also discussed in Chapter 7.3.
- Other initial co-ordinate and time shifts: for example a lateral displacement can be used to find out if more free paths become available. This would be required to compensate for CVM methods not covering lane-change type manoeuvres.

The calculation time of T-CVM depends on memory access times, number of cells occupied in the occupation grids and the required number of e.g. different friction levels to simulate.

In basic tests, where 100 cells were occupied (different lines in the grid) and the same result table was calculated 10 000 times, the times to complete this with Appendix A MATLAB code varied between 2–5 seconds. The result table was updated respectively with 2 000–5 000 Hz. However, if the calculation uses 4 000 points that have to be separately mapped on the grid (raw data of Figure), the performance drops to 175 Hz. These values show the speed benefits from using pre-calculated trajectory tables for collision avoidance.

7.2.3 Dynamic obstacles

When an obstacle is moving, separate environmental sensing algorithms need to provide the occupation grid cells that the obstacle is likely to traverse during the maximum simulation time. For each occupied cell, the minimum and maximum times that the obstacle might be present are then compared in the T-CVM with simulated ego vehicle trajectories.

The following figure shows a result plot from a near-miss simulation where 2 vehicles enter an intersection at the same time. The purpose of this example is to

isolate and demonstrate the effect of dynamic objects in the method. As a simplification, the second vehicle is assumed to maintain its course. As can be seen from the figure, such an obstacle can be avoided just by speeding up or braking.

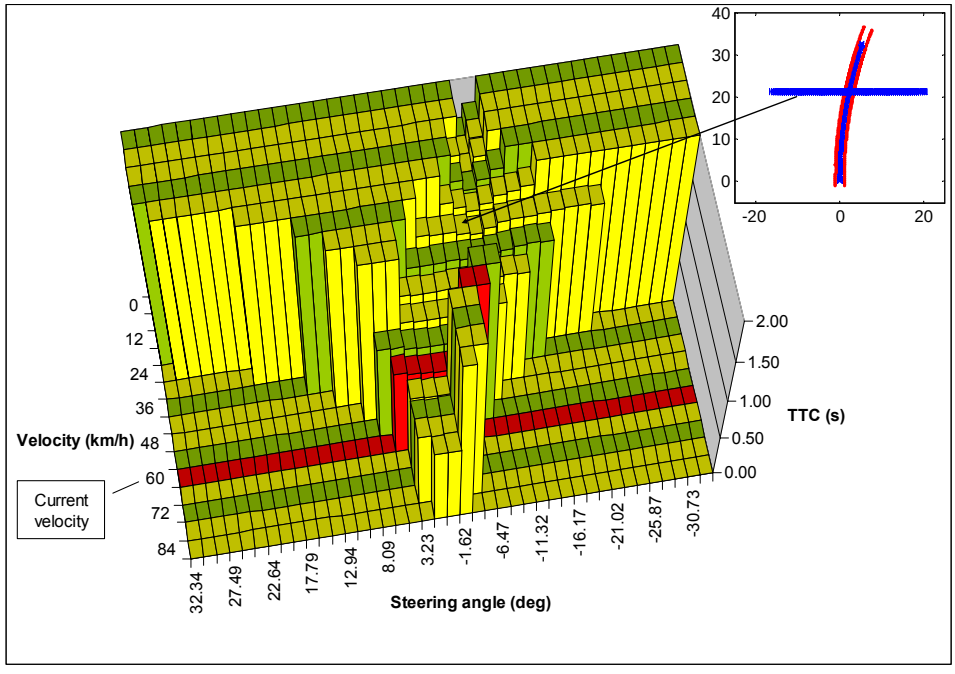

Figure 67. A simulated dangerous situation with 2 cars entering an intersection at the same time, both vehicles travelling at 60 km/h. Friction potential 1.0. Curvatures are represented by virtual steering angles.

The figure does not cover the potential trajectory changes of the second vehicle. Doing so means blocking a larger area in the occupation grid, based on e.g. the anticipated maximum change of velocity and direction for the object class. The T-CVM requires this information from external algorithms.

In the example, had the second vehicle stopped just before the collision – let's assume it is approaching a stop sign – it is likely that the collision calculations would still trigger or at least suggest pre-emptive actions. This is due to the uncertainty of the actions of other drivers. Whether a driver warning would be sounded or other measures taken depends also on whether the applications have information available on traffic signs and road geometry to estimate the likelihoods that the collision would actually happen.

Collision avoidance in intersections has been discussed e.g. in [63], with consideration also for co-operative collision avoidance. Two vehicles can effectively prevent collisions, if the trajectories are communicated and planned co-operatively.

7.3 Friction

The use of friction information in collision avoidance has not previously been a starting point for algorithm development. A common approach is to include friction potential in rule of thumb formulas of distance calculation for initiating collision avoidance or braking (e.g. [64] and Figure 40). In traditional collision avoidance algorithms the manoeuvring speed is low, which helps to simplify the calculation of dynamics even to the point of considering all obstacles to be static and/or assuming instant changes in ego vehicle's steering to be possible. The fastest speeds reported from the DARPA Challenge collision avoidance algorithms, still performing with a reasonable reliability, have been around 55 km/h [65].

The T-CVM uses different levels of friction potential in trajectory generation. In the example of Appendix A, friction usage simply affects maximum accelerations and overcoming the moment of inertia when the vehicle needs to turn. Air resistance also plays a role in calculating accelerations. The accuracy of the trajectory generation could be further improved by utilizing advanced vehicle and tyre models. This precision is, however, not necessary to demonstrate the main effects that different levels of friction potential have on collision mitigation and collision avoidance. Even for a product implementation, it can be questioned as to what constitutes a reasonable accuracy for pre-simulated trajectories, as they can never exactly match a real-life situation due to unexpected road bumps, unbalanced vehicle loading etc.

In curves, the vehicle uses friction to oppose centrifugal force. The remaining potential can be used to turn or accelerate. As the centrifugal force can grow rapidly even with small steering angles at high velocities, and consume all available friction, this causes some difficulty when designing optimal strategies to avoid collision.

Another interesting case for trajectory simulations is attempting to reach target velocities and curvatures when the friction potential suddenly drops and the simulation begins with the vehicle in an uncontrolled slide. Simulating even these situations with reasonable accuracy would benefit the method. Otherwise,

especially in a full slide, the T-CVM calculations have to be inactivated if no trajectories can be assessed to support collision avoidance strategies.

7.3.1 Collision Mitigation

For demonstrating the impacts of friction potential estimation in collision mitigation algorithms, the following simulation was run for snow and dry asphalt: driving forward towards a parked car directly in front and saving the distance when collision becomes unavoidable. The purpose of the simulation was to compare collision mitigation capability to reduce kinetic energy at collision, when

1) the friction potential is assumed to be a fixed value of 1.0 in the collision mitigation algorithm
2) the friction potential is correctly estimated (0.4 for snow in the example) and does not change during braking.

The following table shows the results based on the Appendix A code and also compares them to the APALACI project's distance prediction formula (Figure 40). What can be seen is that the APALACI rule of thumb gives similar estimates, especially since the braking would in practice be suboptimal and would start with a delay. The trajectory simulation also included an approximation for brake pressure build-up during the first tenth of a second.

Table 12. Simulation results of distances and TTC values at the moment when a collision with another car (width 2 m, same as the ego vehicle) directly in front becomes unavoidable. The braking time when continuing to drive straight is calculated as well as the reduction in collision speed and kinetic energy before impact.

	Initial speed 40 km/h	**60 km/h**	**80 km/h**	**100 km/h**
Friction potential 1.0	distance to target = 5.1 m APALACI pred. = 7.1 m simulation TTC = 0.44 s braking time = 0.59 s collision speed = 20.9 km/h kinetic energy vs. original = 27%	distance to target = 8.1 m APALACI pred. = 10.6 m simulation TTC = 0.48 s braking time = 0.57 s collision speed = 41.8 km/h kinetic energy vs. original = 49%	distance to target = 11.4 m APALACI pred. = 14.2 m simulation TTC = 0.50 s braking time = 0.57 s collision speed = 61.5 km/h kinetic energy vs. original = 59%	distance to target = 15.3 m APALACI pred. = 17.7 m simulation TTC = 0.54 s braking time = 0.61 s collision speed = 80.4 km/h kinetic energy vs. original = 65%
Friction potential 0.4	distance to target = 8.4 m APALACI pred. = 11.2 m simulation TTC = 0.71 s braking time = 0.88 s collision speed = 28.3 km/h kinetic energy vs. original = 50% *collision speed if friction incorrectly assumed 1.0 = 33.7 km/h* *incorrect friction assumption kinetic energy vs. original = 71%*	distance to target = 13.8 m APALACI pred. = 16.8 m simulation TTC = 0.79 s braking time = 0.92 s collision speed = 47.7 km/h kinetic energy vs. original = 63% *collision speed if friction incorrectly assumed 1.0 = 53.5 km/h* *incorrect friction assumption kinetic energy vs. original = 79%*	Distance to target = 19.5 m APALACI pred. = 22.4 m simulation TTC = 0.85 s braking time = 0.95 s collision speed = 67.3 km/h kinetic energy vs. original = 71% *collision speed if friction incorrectly assumed 1.0 = 73.2 km/h* *incorrect friction assumption kinetic energy vs. original = 84%*	distance to target = 25.5 m APALACI pred. = 28.0 m simulation TTC = 0.89 s braking time = 0.98 s collision speed = 86.9 km/h kinetic energy vs. original = 75% *collision speed if friction incorrectly assumed 1.0 = 92.6 km/h* *incorrect friction assumption kinetic energy vs. original = 86%*

The braking times (t) in the table were solved from distance values by using the common equation of travelled distance (s) with initial speed (v_0) and acceleration (a):

$$s = v_0 \cdot t + \frac{at^2}{2} \tag{10}$$

Deceleration after detecting an unavoidable calculation was here assumed to be the friction potential multiplied with the local acceleration due to gravity (g), leaving out air resistance. However, during the first tenth of a second the deceleration was considered to be half of the maximum to approximate brake pressure build-up. Adding this period to Equation 10 gives:

$$s = v_0 \cdot 0.1 + \frac{a \cdot 0.1^2}{4} + (v_0 + 0.1 \cdot \frac{a}{2}) \cdot (t - 0.1) + \frac{a \cdot (t - 0.1)^2}{2} \tag{11}$$

The results (and similar T-CVM simulations) show that the TTC values at the start of braking as well as especially the braking times before collision remain in the same range for a single friction potential: braking time ~0.6 s on friction potential 1.0 and ~0.9 s on 0.4. This also means a similar decrease in velocity before the collision. However, the reduction of kinetic energy drops with increased initial speed as the energy is affected by speed squared. Therefore a constant reduction in speed does not suffice for a constant reduction in energy.

Finally, the table lists reduction of kinetic energy, if no friction estimation would be available and it was assumed that friction potential would be 1.0. These numbers apply when there is a possibility for the driver to change lane. If this option can reliably be ruled out, the braking could be started considerably earlier.

The case where an obstacle is not directly in front and only a partial collision can happen would mean even smaller TTC values when the collision becomes unavoidable and therefore less effective collision mitigation. An example of this kind of simulation is presented with collision avoidance simulations on the following pages.

7.3.2 Collision Avoidance

From a number of collision avoidance strategies, three steady speed strategies for late avoidance are simulated for presenting the potential advantages of friction estimation:

Strategy 1. If the TTC for current curvature and velocity drops below the simulation maximum of 2 seconds, initiate action to choose a new curvature with a longer TTC by at least 0.05 seconds.

Strategy 2. Activate avoidance when all optional curvatures lead to a collision in under 2 seconds. This is already risky for collision avoidance and in variable speed simulations the vehicle would start to slow down in search of better options. However, this is still too early for collision mitigation, especially if walls nearby cause TTCs to be continuously under 2 seconds for all other options but driving straight.

Strategy 3. The moment of collision mitigation activation, but calculated by first moving the vehicle position 0.1 s forward on its current trajectory. This is about the last moment for collision avoidance to act, considering the accuracy of the pre-calculated trajectories. The vehicle must also be able to utilize friction to the fullest during the whole manoeuvre, which may be difficult.

A description with code examples is included in the end of Appendix A on the required steps to use the T-CVM result tables in implementing these collision avoidance strategies.

The collision mitigation triggering in strategy 3 is based on the following concept, comparing available maximum TTC with current TTC: when no option provides at least a 0.3 seconds longer TTC than the current steering, collision mitigation is activated. Figure 68 shows the development of maximum and minimum TTCs when driving straight in the situation of Figure 69, “through” a parked vehicle directly in front. At ~2.2 seconds the collision becomes unavoidable and it hits the other vehicle ~2.6 seconds.

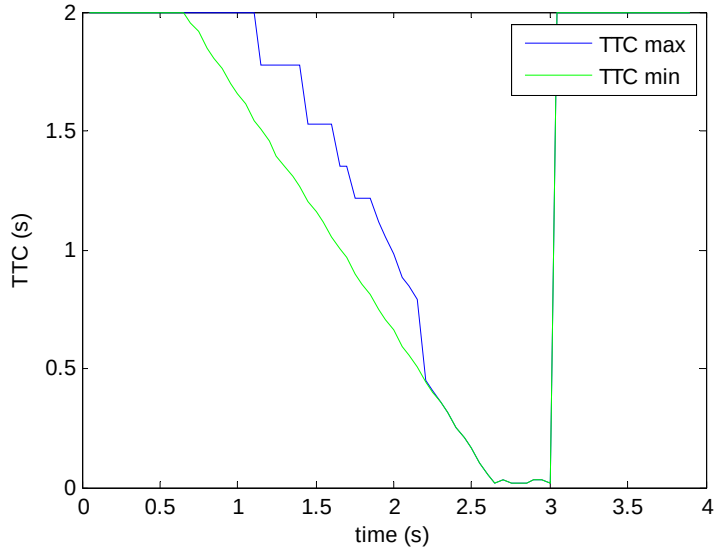

Figure 68. Collision becomes unavoidable in T-CVM when TTC max becomes equal to TTC min. Simulated for Figure 69 situation, straight driving 50 km/h and friction potential 1.0.

In strategy 3 there is no guarantee that collisions can be avoided, but until the maximum TTC equals the minimum, the driver has options to avoid the collision at least for a while longer than on the current path. This triggering means near-miss avoidance.

The simulations for strategy 1 show practically no difference for friction potentials 0.2–1.0, as the avoidance starts rather early. For strategy 2, the differences are also small and can be seen mostly in the end of the avoidance manoeuvre, turning to drive straight as quickly as possible. These simulations are shown in the following:

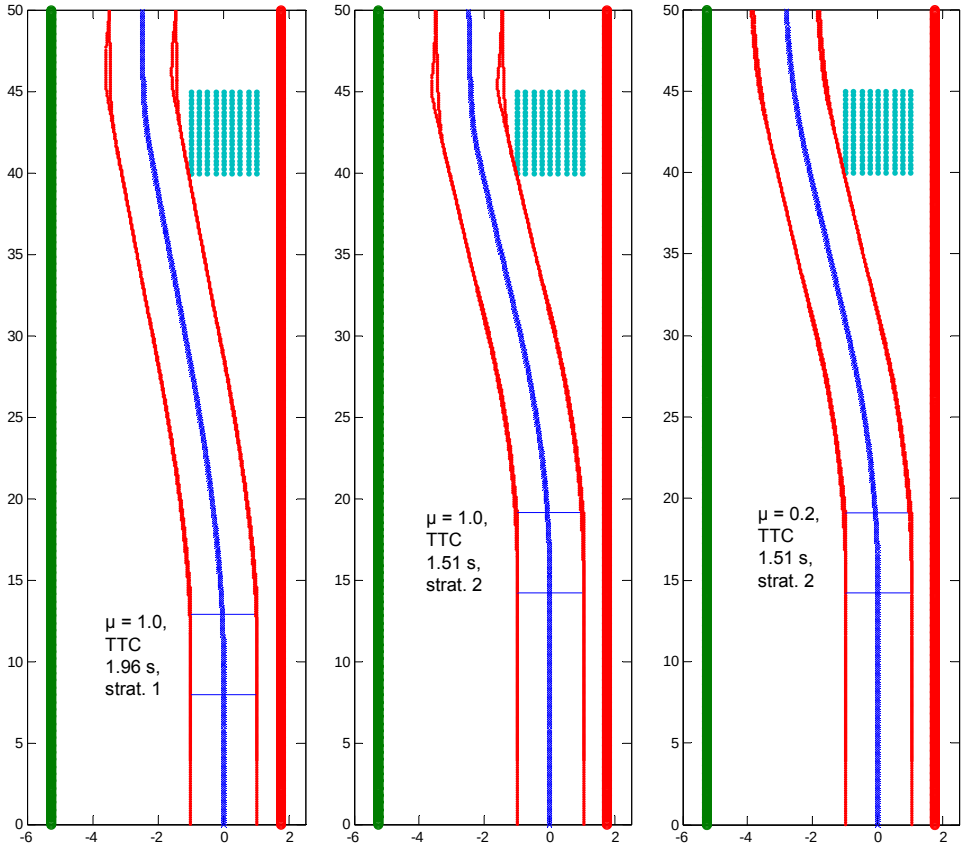

Figure 69. Strategies 1 and 2 are affected only a little by friction potential. The x-axis has been doubled to bring out the differences. The blue line is the centre point of rear axle and the red lines represent vehicle boundary box corners.

These strategies of taking early action to avoid collisions could benefit from friction estimation by being able to estimate the maximum accelerations and therefore the potential movement of dynamic obstacles. In this example simulation, however, the vehicle in front does not move. Other advantages would be selecting/suggesting a safe speed on slippery surfaces or possibly to act even earlier than normally.

Strategy 2 could be a near-miss strategy if there are no other obstacles in the sensor field of view than the car in front. It is also largely affected by the simulated target angle accuracy for trajectories: the more accurate the trajectories are, the later the calculation is able to still find a free path. Therefore the Appendix A

example suggests an increased curvature resolution near straight driving. In this simulation the effect of halving the resolution caused a 0.15 second difference in initiating avoidance.

Strategy 3 for near-miss avoidance shows, on the other hand, clear differences for different friction potentials:

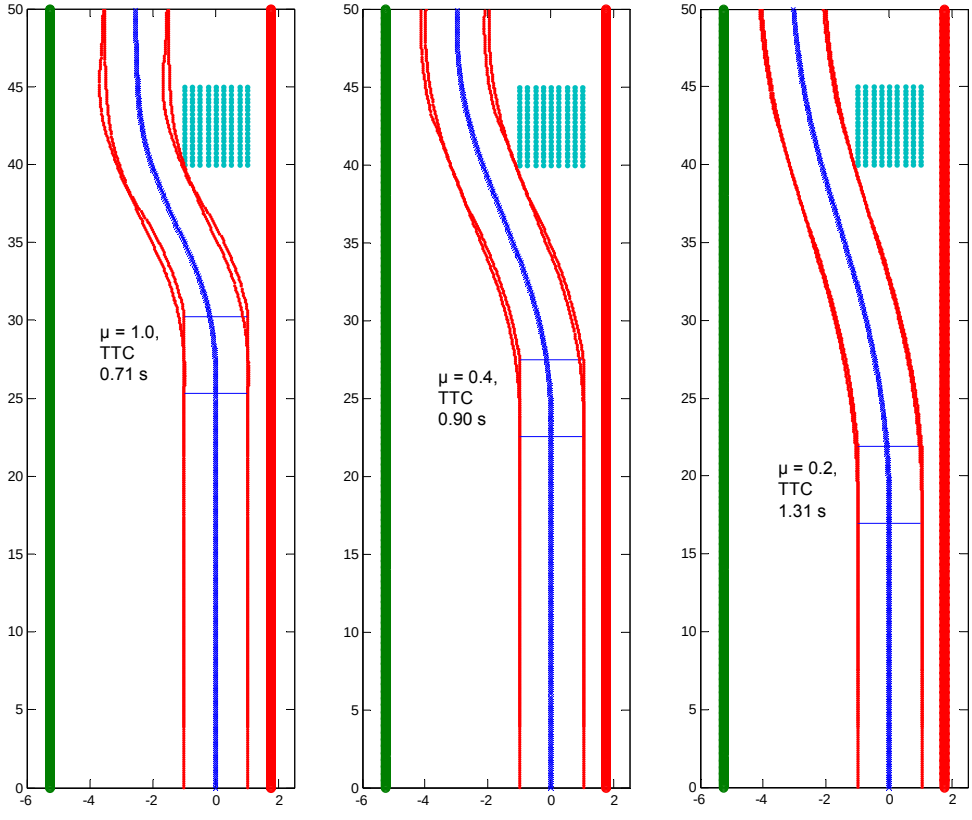

Figure 70. Near-miss collision avoidance (strategy 3) for three friction potentials. The x-axis has been made wider to bring out the differences.

In close-range collision avoidance the impact of friction estimation is similar to the simulated impacts in collision mitigation.

The following simulation, which is run for a parked car on the side of the street, shows that collision avoidance has large safety potential in collisions that involve only a small part of the vehicle's front. Collision mitigation applies brakes very late in these partial collisions, as theoretically the collision can be avoided until the very last moment:

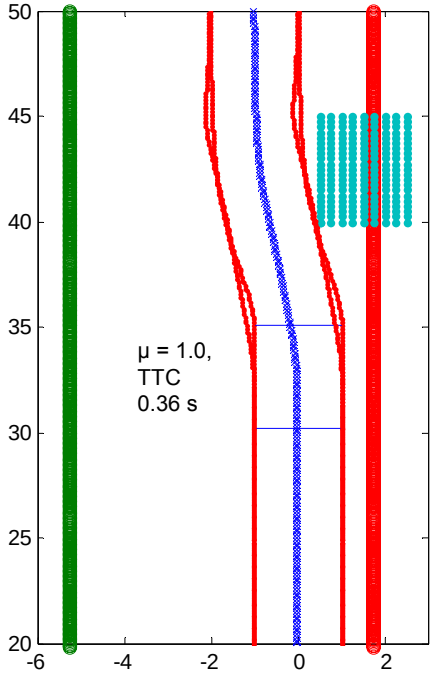

Figure 71. Collision avoidance works efficiently but collision mitigation would apply the brakes very late, losing its safety potential.

Avoiding partial collisions would be an interesting use scenario for further studies. The avoidance manoeuvre could be limited to the vehicle's own lane to minimize the risks of not noticing on-coming vehicles.

Another example where collision avoidance could prove useful is aborting an overtaking manoeuvre: when the vehicle detects a risky situation and has to quickly return to its own lane, an instant T-CVM calculation of three million trajectory options for a safe return might outperform especially inexperienced drivers.

7.3.3 Friction information quality affecting collision calculations

The simulations of Table 12 show that on snow (friction potential 0.4 in calculations) collision mitigation without friction estimation loses an average of 43% of its capability to reduce collision energy with different speeds. Near-miss collision avoidance simulated for the same case starts turning 0.19 seconds too late without friction estimation, which can lead to dangerous collisions. These results

outline the maximum benefits of friction estimation when friction potential is constant during braking and correctly estimated.

When considering the friction information provided by the estimation system of this study, *the main question is the reliability of the friction potential estimate for the area ahead of the vehicle*. The IcOR polarization camera was the only sensor capable of classifying the road surface ahead of the vehicle. It was installed to cover an area between 10 and 30 meters in front. The other sensors and algorithms estimate the current friction potential, looking under the vehicle so to speak. This study proposes using the current friction potential or even historical estimates as an initial value for applications such as collision mitigation, as long as the forward-looking environmental sensors detect no large upcoming changes.

If the classification for the area in front differs from the one for the surface under the vehicle, the estimate given for upcoming friction relies on forward-looking sensors only. The requirement for environmental sensors to provide information on upcoming changes by comparing to measurement history has not been fully addressed in current sensor system development. The IcOR for example can at best provide a rough classification. It can currently provide a single result for the whole area ahead. New collision avoidance algorithms might place a need for separate estimates e.g. in a grid format around the vehicle (Figure 31).

When the friction potential on the vehicle's path is constantly alternating (and while the environment cannot be modelled in detail), the application must decide if a short-term minimum, maximum or an averaged value produces the best results. As an example, even a correct estimate for friction potential on a wet patch of asphalt does not provide the best guess for friction ahead of the vehicle if the road is mainly dry. In cases where road slipperiness varies, the estimation accuracy of the friction potential under the vehicle loses some of its importance; an averaged value for a long braking distance can in the end be estimated only roughly by combining information from forward-looking environmental sensors with current friction. In unvarying conditions, however, the current value of friction potential can provide a meaningful increase in real-world performance, which was evident especially from the CRF's APALACI tests (Chapter 5.3) and the previous collision mitigation simulations.

This chapter discusses the general effects friction estimation has on CMS/CA performance. It would be too simple to state that the real world performance can be modelled using an estimation error of 0.2 to alter the correct friction potential. In learning- and classification-based systems the accuracy depends on the exact

case, while the output varies from not available to as accurate as recently learned friction potential values for the surface.

The largest errors happen with wrong classification and there is a risk of learning also wrong friction potentials for a surface, if the environmental sensors cannot reliably differentiate surfaces. In cases like on a wet road, friction potential also depends on the vehicle speed, tyres, and water depth – this was not modelled in the presented system, although tyre sensors were an available option to produce information about aquaplaning. Learning features were used to record tyre performance for example on snow and ice, and to provide more accurate estimates. However, the system did not yet include a check for having changed tyres.

When the friction estimate is completely unavailable, collision mitigation and avoidance must likely use their default parameters for braking: Collision mitigation would use a high friction coefficient, around 1.0, to avoid taking control of the vehicle too early. Collision avoidance strategies vary, but it does not seem reasonable to require optimal braking conditions to be able to avoid a collision. This suggests a default value under 1.0. However, a low default value could initiate unwanted early action also in collision avoidance, if the application is targeting driver assistance.

The exact design of collision avoidance for driver assistance is still a rather unexplored topic. The main concerns have historically been in reliable environmental sensing to enable safe operation. A collision avoidance operation could be anything from momentary autonomous driving to correcting a trajectory by a few centimetres to avoid scratching the vehicle. The minor corrections might not even need friction estimation, while there could be collision avoidance or ISA approaches that even force a lower speed on icy roads! More autonomous operation brings up several questions such as what are the acceptable risks taken by a system vs. a driver, and can the system truly outperform drivers' estimates. Braking always starts from an estimate of the situation, either by the driver or the vehicle. As long as the vehicle does not outperform the driver's estimates, it cannot take control.

Future co-operative systems could provide more information on upcoming road conditions. However, the spatial accuracy of this information, a requirement for recent information and the dependence on tyre performance present problems. Long-distance warning systems can require a different logic than the presented collision avoidance algorithms and friction estimation, which are very limited in reach.

The following four tables aim to summarize the effects that common friction estimation errors have on collision mitigation and avoidance. They are separated according to road conditions.

Table 13. Friction estimation errors affecting collision calculations on dry asphalt.

Common estimation errors	Estimation may provide a literature-based conservative value for the surface (in this study the value was set at 0.85) if it has not recently learned a more accurate value. This default value may be too low. Additionally, the classification may momentarily give out lower values around 0.7 due to vehicle algorithm inaccuracies. When the friction potential exceeds 1.0, the algorithms are often capped to 1.0.
Effects on collision mitigation by braking	Low estimates suggest initiating early braking and actually a driver might be able to still avoid the collision, although it would be a close call.
Effects on collision avoidance	Near-miss collision avoidance would also start slightly earlier on a low friction estimate, but to avoid collisions despite various calculation inaccuracies (including e.g. potential movement of other road users), an avoidance manoeuvre might not require optimal grip in any case. When the driver is supported earlier than the very last moment, the maximum accelerations would possibly be limited also for comfort. The friction estimation algorithms could probably learn the correct friction potential during hard avoidance manoeuvres and update the trajectory assessment.

Table 14. Friction estimation errors affecting collision calculations on wet asphalt.

Common estimation errors	In the worst case, estimates range from 0.5–1, momentarily alternating. The road may not be wet for the full braking distance ahead. The estimation is more reliable during cornering and if the EFF database contains an estimate matching the exact environmental measurements.
Effects on collision mitigation by braking	Even in the case of momentary errors, driver warning systems can perform averaging on the estimates to better time their warnings. When forward-looking sensors detect no upcoming changes to the friction potential, the estimate can be used to the fullest. However, from varying estimates a system might use the highest value, to avoid acting while the driver still has a chance to avoid the collision.
Effects on collision avoidance	If wet asphalt goes undetected, this error might be large enough to cause a collision in near-miss collision avoidance approaches. When the friction potential estimates are alternating rapidly, it would be sensible to use an averaged value or the lowest recent estimate in collision calculations. If forward-looking sensors detect e.g. an icy spot and currently the vehicle is on wet asphalt, this information on local friction changes might be on the other hand something that the current collision avoidance algorithms could not use in full.

Table 15. Friction estimation errors affecting collision calculations on snowy and icy surfaces.

Common estimation errors	Estimates for friction potential vary between 0.1–0.5. When ice, snow and asphalt are alternating, only some co-ordinates are available for the clean icy spots from the IcOR, but not a true model of the road. Due to large slip, an accurate friction measurement may be available more often than on a high friction surface, but there is no proof that the value represents the road ahead.
Effects on collision mitigation by braking	Despite errors, driver warnings can be timed earlier. Due to possible delays in receiving new estimates, the braking could be started using an old (usually higher) value. Considering it is unlikely that friction potential on a road on average would be ~0.2, it is also unlikely that the very lowest values would be used in collision mitigation strategies to initiate hard braking. Environmental sensing as well as collision mitigation algorithms have difficulties in reliably covering full braking distances (e.g. 200 meters) on icy surfaces. Therefore a likely value to be used on snow and ice both could be around 0.4 or even higher, depending on past averages, distance to the vehicle in front and information from forward-looking sensors. Collision mitigation would still be considerably improved by the estimation.
Effects on collision avoidance	Drivers could be warned about icy spots on the road and also prompted to use slower speed. Very low friction potentials, even if momentary, would suggest early avoidance manoeuvres. This could result in several situations where mathematical calculations conflict with the driver's actions. A driver assistance approach could in this case use collision mitigation strategies instead of collision avoidance, and give out only selected warnings. Fully autonomous collision avoidance would act early and possibly drop speed.

Table 16. Friction estimation errors affecting collision calculations on other road surfaces, not covered by the friction estimation system.

Common estimation errors	The estimation is often unavailable due to surfaces not matching the programmed models and therefore failing plausibility checks. However, classification-based systems may occasionally come up with a result. In this case an output would contain significant error. The factual data collected on friction used and slip, as well as the EFF learning features matching environmental sensor inputs with experienced friction potential, still provide short-duration estimation.
Effects on collision mitigation by braking	Low-validity friction information is not likely to be used. The systems' performance would be the same as without friction estimation.
Effects on collision avoidance	A collision avoidance system might still benefit from knowing the estimates and choosing a careful strategy according to system defaults. It would be difficult to provide reliable assistance for a driver.

8. Results and Discussion

This study consisted of two parts: 1) development of sensor data fusion methods to estimate tyre–road friction potential and to determine road conditions, 2) then applying this information in collision avoidance and collision mitigation algorithm design to review the advantages. The requirements of collision avoidance and the perceived benefits in different collision avoidance and mitigation strategies were analysed using simulations and examples. In addition, the impacts the friction estimation could have on other vehicle safety systems were briefly discussed in Chapter 2.

8.1 Estimation of friction potential

New environmental sensors to detect ice, snow and water on the road can provide valuable information on slippery road conditions. Combining these measurements with existing methods that estimate tyre–road friction potential based on vehicle dynamics, for example from accelerations and wheel slip, is a promising new topic for sensor data fusion research. While the friction estimation from vehicle dynamics usually requires at least moderate accelerations, in this study 0.3 *g* or higher, environmental sensing has the potential to provide an estimate nearly continuously and also give advance information before arriving on the surface.

This study discussed a friction estimation process consisting of several feature extraction and decision fusion steps. First the friction-related features were extracted in three feature fusion modules; environmental, vehicle and tyre feature fusion. The detected features and initial estimates for friction potential were used as an input for the decision fusion module calculating the final estimates and their validity.

The main emphasis in environmental sensing was on estimating probabilities for ice, snow and water just in front of the vehicle by using light absorption and polarization properties. These probabilities were then used in classifying and detecting road conditions.

The classification was limited in the sense that the sensor systems used in the study were not designed to detect loose gravel, wet leaves, road paintings or e.g. pit cover plates, which can also be slippery when compared to dry asphalt. Currently it is difficult even to classify different types of ice, as several conditions such as sunshine or polishing caused by previous braking affect the friction potential. Future work is suggested for modelling in detail the effect of different environmental variables on friction potential. Rough classifications for friction potential can already be achieved, covering mainly icy, snowy, wet and dry asphalt.

The environmental sensors used in this study – Road Eye, IcOR, Ibeo LUX and two temperature sensors – were able to provide friction-related measurements from 1–25 meters in front of the vehicle. The IcOR polarization camera is able to detect black ice from longer distances, but this capability was not tested in the sensor data fusion. In separate sensor-specific tests, the classification success rate of IcOR and Road Eye has varied between 70–95%, depending on road conditions, sensor calibration and ambient light. When the outputs were combined, and by reviewing the performance on the collected databank during the study, the environmental feature fusion was able to produce an estimate approximately 90% of driving time, in daylight conditions on test tracks.

As environmental sensing can provide a near-continuous classification for the tested surfaces, it easily ends up dominating the sensor data fusion. However, environmental sensors cannot truly test the friction potential, as it exists only between the tyre and the road.

A learning feature was used to improve the environmental-sensor-based initial estimates for friction potential. This method required a variety of environmental sensor data to be collected; raw sensor data for temperature, light absorption, and polarization. Friction used values experienced during high tyre slip were recorded in a database with matching environmental sensor readings. A minimum of 8% slip ratio (with tyres that peaked at 10%) was used for triggering learning. This approach was effectively used to replace literature-based values for average friction potentials on e.g. ice or snow. The database can also capture the effect different tyres have on friction. Compensating for the role of tyres has importance e.g. in future co-operative systems, where cars exchange information on slippery road segments.

The friction estimation system carefully checked sensor data validity as well as changes in road conditions and driving manoeuvres to provide friction potential also during low acceleration and low use of friction; while no estimate could be made based on vehicle dynamics alone. As the main principle, the friction processing was using environmental sensing to search for changes in road conditions that happen after a recent accurate estimate originating from vehicle dynamics sensors. Using this method, the vehicle-dynamics-based friction potential estimate was considered valid for a while longer, but as the vehicle moved further, the validity of the output dropped quickly while the estimation had to rely only on environmental sensor information.

During a minute of normal driving on dry asphalt in an urban area, accelerating and braking with 0.2–0.4 *g*, algorithms using vehicle dynamics, sensors were able to provide an estimate for friction potential approximately 5% of the time. On winter-time slippery conditions this value grows due to more frequent tyre slip, and smooth ice can be detected with 0.1–0.15 *g* acceleration.

The friction estimation system predicts friction potential much like a human does; based on cumulated experience and by testing the friction levels during hard acceleration, cornering and other situations where the potential can be accurately estimated. During hard manoeuvres on surfaces where friction potential does not vary a lot, e.g. when cornering on wet asphalt, the system could even exceed human performance in estimating the limits set by friction. Especially inexperienced and inattentive drivers might benefit from the support. However, during constantly alternating road conditions the environmental sensing and friction estimation fail to match human understanding of the situation, as the following example shows:

The large variation of friction potential even in a small area causes a great difficulty in friction estimation for vehicle safety system calculations. In winter-time, a road may have clear asphalt tracks, but outside of these tracks one often finds snow (Figure 72). Driver warning systems as well as collision mitigation systems would have to take into account the likely changes within centimetres, and the possibilities to keep the vehicle on the track. Constant warnings about low friction potential would irritate drivers. The system detects consecutive large changes in friction and an application has to decide how to use this information.

Figure 72. Varying surface type and friction potential cause difficulties in modelling the road – snowy road with clear asphalt tracks.

The friction estimation system has been tested on dry, wet, icy and snowy asphalt, a few times on slushy asphalt, but not on dirt roads or gravel. When driving in test areas *the system was able to provide friction potential estimates with an error mostly within 0.2*, compared to reference values measured in peak braking tests. The EFF classification success rate sets the upper limits for estimation availability, in the tests at approximately 90%, even though the VFF (and TFF) can provide short-duration estimates independently.

The system also provides several other outputs, with accuracy depending e.g. on whether the tyre sensors were in use. The current friction used by the vehicle was measured with acceleration sensors for the whole vehicle, error sources being e.g. an unknown wind speed, road bumps and the vehicle pitch and roll angles. Alternatively experimental tyre sensors provided the use of friction at the tyre level. The tyre sensors can also capture the effect of wind, as it affects tyre deformations.

The system detects sudden changes, classifies road conditions and driving manoeuvres, and with tyre sensors, it provides information on stages of aquaplaning. The environmental sensors are used to provide a prediction for friction potential in front of the vehicle.

This study gives the impression that friction potential can be estimated only using a large set of sensors. However, the definition of friction used (Chapter 4.3.1) as roughly equivalent to the acceleration of the vehicle, also suggests statistical ways to collect friction information. Even with current mobile phones that have an integrated acceleration sensor, the maximum accelerations could be

collected for a road segment by a large group of users: The highest accelerations could indicate friction categories, assuming different curve speeds and braking at intersections. To benefit from the algorithms developed for vehicle IMUs, first the orientation of a fixed mobile phone must be estimated, i.e. the direction of gravity measured for example by averaging values over time. Secondly, the travel mode is of interest: driving, walking, bicycle riding etc.

8.2 Collision avoidance and mitigation

The friction potential is a key unknown in collision mitigation / automatic emergency braking systems. The recent prototypes of the APALACI and COMPOSE projects used a fixed value for friction potential, decided based on ordinary driving conditions. Using a high default value causes the systems to lose some of their safety potential on low friction surfaces. Using a low or medium default value would on the other hand cause the safety systems to activate too early in high friction conditions, taking the driver "out of the loop" possibly unnecessarily. The default value of 1.0, near the practical maximum deceleration, was selected in this study as a likely basis for comparing CMS performance with or without friction estimation.

The maximum benefits from friction estimation were examined in simulations, where a car driving on a surface with a friction potential of 0.4, approximating snow, collides with a stationary car directly in front. According to the results presented in Table 12, when the CMS incorrectly assumed a friction potential of 1.0, it lost on average 43% of its capability to reduce collision energy with different speeds.

On the snow-like surface the safety potential of collision mitigation was slightly reduced even with correct friction estimation, as deceleration is lower and the calculated growth in distance for starting the braking does not fully compensate for this. This calculation assumed that the braking is initiated at the moment the collision becomes unavoidable. The likely positive effects from being able to warn the driver earlier than on high friction, were not simulated.

In practice, a CMS with imperfect environmental sensing might also decide to use a slightly higher value for friction potential than the recent estimates indicate, to ensure that a collision indeed is unavoidable even if the friction would change within the braking distance. The main flaw of the presented friction estimation system from collision avoidance and mitigation perspectives is not necessarily being able to give reliable information for the full braking distance

ahead. The braking distance and therefore the difficulty of predicting upcoming friction with environmental sensors further increase on slippery surfaces. Therefore, even if the friction estimation system would classify a road as icy, the system still might not start full braking e.g. 200 meters before an obstacle based simply on braking distances on ice.

On the other hand, collisions can often be avoided until very late by making a steering manoeuvre. The required minimum range for detecting changes in friction potential varies from case to case.

The simulations additionally show that collision mitigation systems lose some of their safety potential with increasing initial speed, when colliding with static obstacles: at high speeds an avoidance manoeuvre would have a higher safety impact than plain braking does. This is evident especially in collisions that involve only a small part of the vehicle's front (Figure 71). The vehicle has until the very last moment a possibility to avoid the collision and the CMS (as defined for these simulations) does not activate.

The benefits of friction estimation in collision avoidance are rather small when the system has been designed to change trajectory as early as obstacles are detected to safely avoid collisions. These types of strategies use low to average friction during avoidance manoeuvres. The potential movement of dynamic obstacles could, however, be estimated based on friction information, and a safe driving speed could be selected.

When a near-miss strategy was used in collision avoidance design, the simulation results showed clear differences between friction levels (Figure 70). The effects are comparable to changes in collision mitigation timing; near-miss avoidance begins only slightly earlier. An incorrect high friction estimate could result in a dangerous collision, while a low estimate would start the avoidance manoeuvre early. In near-miss avoidance the friction use is likely to be high enough to produce new friction potential estimates during the avoidance manoeuvre. These new estimates could be used to update plans for evasive actions.

In the context of the simulations, this work introduced a new calculation method to assist collision avoidance and mitigation. The method was named T-CVM according to its principle of assessing safe trajectory options based on their *target curvature and velocity*. The T-CVM has its origins in the popular curvature-velocity method (CVM). The presented variant adds support for different friction potentials, dynamic obstacles, obstacle classification (obstacle types can be either excluded or included in the calculation), accurate vehicle dimensions and partially also dynamics.

The T-CVM is based on large pre-calculated look-up tables, where even millions of possible trajectories are simulated beforehand. Each simulation starts with an initial curvature and velocity for how the vehicle enters the scene. In a selected maximum time, the vehicle attempts to reach new target values for curvature and velocity. The size of the look-up table generated for tests was over 2 GB.

When an obstacle is detected and mapped to a grid around the vehicle, a list of trajectories that lead to a collision can be instantly read from the look-up tables. The method provides a table of time-to-collision values attempting to cover most optional curvatures and velocities in the current situation.

Even though the number of memory operations can be large, using look-up tables ensures high update rates, generally above 100 Hz, for collision calculations. The benefits of the T-CVM are seen especially in high-speed, close-range collision calculations involving several obstacles with speculated movement.

As the calculation method basically provides a table of options to select new curvature and velocity from, it needs to work together with some higher level software components that make the final selection on how to drive. Many parameters may be involved in selecting from safe steering options, such as the preferable safety margins, highest acceleration and jerk, shape of the road, and in autonomous vehicles, also goal direction.

9. Conclusion

The role of sensor systems is growing in future vehicles. This is already evident from current research projects for developing driver assistance systems. Several sensors are used to monitor the driver, vehicle and their surroundings. Double-checking driver actions with sensor systems and warning when risks are high is seen as a way to improve traffic safety.

Sensor data fusion in its several forms has become an actual topic in the automotive industry. It plays an important part also in attempts to obtain the maximal benefit from a minimum number of sensors, which naturally add extra cost. Fusion is often application-specific and no single toolset exists.

This work discussed the estimation of the maximum tyre–road friction coefficient, friction potential, to be used in upcoming preventive safety systems. The requirements and assumed benefits of friction estimation to different systems were collected, and collision mitigation and collision avoidance applications were selected for more detailed analysis.

The reliability of friction estimation – knowing to what degree the information can be trusted, was viewed as important as the actual resolution of the estimation. Even a resolution of a few main classes for friction potential can benefit a number of driver assistance and co-operative safety applications. The capability to predict friction potential continuously and not only during a few driving manoeuvres, as in previous studies, is a necessary requirement. Also being able to predict maximum friction before arriving on the surface is valuable for driver warning, safe distance and braking calculations.

A modular sensor data fusion architecture was examined, consisting of

- Data Gateway, adapted to the vehicle
- Vehicle Feature Fusion (VFF) module estimating friction potential based on vehicle dynamics sensors

- Environmental Feature Fusion (EFF) module estimating friction potential and road conditions using a number of environmental sensors
- Tyre Feature Fusion (TFF) refining information from experimental tyre sensors
- Decision Fusion processing the input from three feature fusion modules.

The EFF and TFF are optional modules, though they considerably improve the system performance. The Data Gateway, Decision Fusion and VFF are always required.

The architecture used an almost classical division into feature extraction and decision fusion. While much of the FRICTI@N project, which was the framework for this thesis, concentrated on the feature extraction, this work covered the fusion steps and the process of combining environmental measurements with vehicle dynamics data.

Environmental sensors can be used to estimate friction potential in situations that would be almost impossible with vehicle dynamics sensors alone, such as when the vehicle is driving straight with constant speed. They can also be used to predict friction potential ahead of the vehicle. Large variations in the friction potential can, however, cause a difficulty in mapping the surroundings of the vehicle and using this information in safety applications.

The tested environmental sensors can provide information on ice, snow and water on the road, based on changes in light polarization and infrared light absorption. This already enables a rough classification of road conditions into dry, wet, snowy and icy, and possibly also slushy. Future research is needed to further improve the classification of road surfaces and to systematically model the effect of different environmental variables on tyre–road friction potential.

This study used machine learning to match environmental sensor data with actual measured friction levels. Gradual learning by building a database was shown to improve on rough classifications found in the literature for an average tyre in different road conditions.

Sensors measuring vehicle dynamics can be used to estimate friction potential especially during high acceleration or large wheel slip. In this study the estimation was successful starting from an acceleration of 0.3 g or a wheel slip ratio of approximately 5%. Vehicle dynamics sensors also constantly measure used friction, which is factual information for data fusion and applications.

Experimental tyre sensors show potential in measuring friction directly from tyre carcass deformations. Due to sensor durability and manufacturing issues,

this potential cannot yet be fully utilized. The role of the tyre sensors in this study was to provide data on friction used and aquaplaning only.

The friction estimation system has not yet been tested extensively on different surfaces – it has been tested mainly on dry, wet, snowy and icy asphalt test track. During the test drives the system provided estimates mostly within 0.2 of the actual friction potential. The estimate was available 90% of the time, but with changing validity depending on how often a reliable estimate could be calculated from vehicle dynamics. The environmental sensors after all cannot directly measure friction, as it exists only between the tyre and the road.

The output from various sensor types for data fusion provides options to evaluate the plausibility of single sensor readings. Through data fusion, valid estimates for friction potential can also be provided during low acceleration, e.g. by maintaining previous vehicle dynamics based estimates while environmental readings stay the same.

This study tested a hypothesis that e*nvironmental sensing combined with information from existing vehicle dynamics sensors – and optionally from a tyre sensor – enables the estimation of tyre–road friction potential with an accuracy and reliability high enough to enhance collision mitigation and avoidance.* The advantages of friction estimation were simulated for different collision mitigation and collision avoidance strategies. Furthermore, the relevance of common estimation errors to practical application design was analysed.

A new method presented for calculating collisions was able to incorporate friction estimates in trajectory approximation. The method is based on pre-calculating millions of possible vehicle trajectories to quickly assess the available options during driving.

The simulations confirmed that collision mitigation systems without friction estimation, designed to brake when a collision becomes unavoidable, lose much of their safety potential on slippery surfaces: When a car is about to hit a static obstacle of the same size directly in front, and the system starts braking based on an incorrect default value 1.0 for friction potential, while the potential is actually 0.4, the simulated system lost on average 43% of its capability to reduce collision energy. The reduction of collision energy varies by the initial velocity.

Alternative strategies for collision avoidance were discussed, some taking early action to safely avoid collisions and thereby avoiding also high accelerations and use of friction. The benefits of friction estimation to these approaches come mostly from reducing or suggesting that the driver reduce speed on slip-

pery surfaces, and being able to better estimate the limits for potential movement of other road users.

The near-miss strategies for collision avoidance on the other hand are highly dependent on friction estimation, much like collision mitigation. The near-miss strategies begin their avoidance only slightly earlier than collision mitigation would start braking. However, as the friction estimation cannot generally provide reliable information for a long braking distance ahead, the estimates cannot be fully used without a separate logic to decide a safe strategy.

The collision mitigation strategies discussed in this work do not apply the brakes while the driver still has a chance to avoid a collision. This suggests to use even the highest value of the estimated friction potential range. Collision avoidance should rather act based on the low range, at least in autonomous systems, but interaction with drivers in uncertain cases is an open topic in safety system development.

The discussed collision mitigation and collision avoidance strategies all seem to benefit from friction estimation by improving the timing of their warnings for the driver in high-risk situations.

Future friction research should focus especially on environmental sensor development, so as to improve the detection range, spatial detail and classification of road conditions.

In the near future, co-operative safety systems that will communicate with other vehicles and infrastructure will provide early information on changing road conditions.

Collision avoidance and mitigation benefit from detailed modelling of the environment to address a list of unknowns in their calculations. The key issues to be addressed include the intentions and likely movement of other road users, traffic rules and 3D road geometry, reliable classification of small objects and their weight – and again, friction.

As a conclusion, this study highlighted the importance of friction in new vehicle safety systems supporting drivers. The proposed friction estimation methods provide the vehicle with an initial estimate of friction potential, bridging some of the gap between the driver's and the vehicle's capabilities in perceiving the environment.

References

[1] Commission of the European Communities. Transport – White Paper European Transport Policy for 2010. 2001. http://ec.europa.eu/transport/white_paper/documents/index_en.htm.

[2] Koskinen, S., Peussa, P. ed. 2009. FRICTI@N project final report. Deliverable 13 for the European Commission. Tampere, Finland.

[3] Mäkinen, T. et al. 2005. APOLLO Final Report including Technical Implementation Plan. Deliverable 22/23 for the European Commission. Tampere, Finland. Available online at: www.vtt.fi/apollo (7.7.2008).

[4] Saastamoinen, K. 1993. Kelin vaikutus ajokäyttäytymiseen ja liikennevirran ominaisuuksiin ('Effect of road conditions on driving behaviour and properties of the traffic flow'). Finnish Road Administration 80/1993.

[5] Sihvola, N. and Rämä, P. 2008. Drivers' opinions about road weather conditions and road weather information – interviews during winter conditions. Finnish Road Administration 16/2008. 62 pp. + app. 10 pp. ISSN 1457-9871, ISBN 978-952-221-069-2, TIEH 3201096. http://alk.tiehallinto.fi/julkaisut/pdf2/3201096-v-kuljett_kasityk_kelista.pdf.

[6] Peltola, H. et al. 2004. Speeds during wintertime and heavy vehicles. Report, Ministry of Transport and Communications Finland. http://www.lvm.fi/fileserver/Julkaisuja%2067_2004.pdf (20.11.2008).

[7] Sarjamo, S. et al. 2004. Wintertime traffic safety in Finland and Sweden. Research report, LINTU Research Programme. http://www.lintu.info/SUORUO_FIN.pdf (20.11.2008).

[8] Roine, M. 1999. Accident risks of car drivers in wintertime traffic. VTT publications 401, thesis. http://www.vtt.fi/inf/pdf/publications/1999/P401.pdf (20.11.2008).

[9] Clarke, D. et al. 2007. Fatal Vehicle-occupant Collisions: An In-depth Study. Road Safety Research Report No. 75. Department for Transport, London. http://www.dft.gov.uk/pgr/roadsafety/research/rsrr/theme5/fatalvehicleoccupant75.pdf (20.11.2008).

[10] Van der Steen, R. 2007. Tyre/road friction modelling. Literature survey. Eindhoven University of Technology. http://www.mate.tue.nl/mate/pdfs/8147.pdf (5.12.08).

[11] Ekdahl, M. et al. FRICTI@N, Deliverable D4, User needs, application scenarios and system requirements. Information Society Technologies (IST) Programme. Brussels, 2006.

[12] Liukkula, M. 2006. Tyre Characterisation on Summer and Winter Surfaces. Presentation in Tire Technology Expo 2006, 3rd International Colloquium on Vehicle–Tyre–Road Interaction. Nokian Tyres. http://www.vertec.hut.fi/P05_Tire_tests.pdf (26.1.09).

[13] Wong, J.Y. 2008. Theory of Ground Vehicles. Fourth Edition. Published by John Wiley & Sonds, Inc., Hoboken, New Jersey. 560 pp.

[14] Li, L. Wang, F. and Zhou, Q. 2006. Integrated Longitudinal and Lateral Tire/Road Friction Modeling and Monitoring for Vehicle Motion Control. IEEE Transactions on Intelligent Transportation Systems, vol. 7, no. 1, March 2006.

[15] Velenis, E. et al. 2005. Dynamic tyre friction models for combined longitudinal and lateral vehicle motion. Vehicle system dynamics. Vol. 43, No. 1, January 2005.

[16] H. B. Pacejka and E. Bakker, "The magic formula tyre model," in Proc. 1st Int. Colloq. Tyre Models Vehicle Dynamics Analysis Delft, The Netherlands, 1991, pp. 1–18.

[17] Burton, D. et al. 2004. Effectiveness of ABS and Vehicle Stability Control Systems. 2004. Research report 00/04. Royal Automotive Club of Victoria Ltd. http://monash.edu.au/muarc/reports/Other/RACV%20ABS%20braking%20system%20effectiveness.pdf (13.12.2008).

[18] eSafety Compendium. 2006. Produced by eSafety Support. http://esafetysupport.org/download/eSafety_Activities/1.pdf (15.12.08).

[19] Scholliers, J. et al. 2008. Project final report and recommendations for future assessments. Final Report of PReVENT IP subproject PReVAL. http://www.prevent-p.org/en/public_documents/deliverables/d164_preval_final_report.htm (10.12.08).

[20] Malone, K. et al. 2008. Final Report and Integration of Results and Perspectives for Market Introduction of IVSS. Final Report of eImpact EU project. http://www.eimpact.info/download/eIMPACT_D9_D10_v2.0.pdf (19.1.09).

[21] Ress, C. et al. 2006. Electronic horizon – support ADAS applications with predictive map data. 13th World Congress & Exhibition on Intelligent Transport Systems and Services. ExCel London, United Kingdom.

[22] Official IEEE 802.11 Working Group Project Timelines – 12/15/08. http://grouper.ieee.org/groups/802/11/Reports/802.11_Timelines.htm (19.1.09).

[23] SAFESPOT Integrated Project Home Page. http://www.safespot-eu.org/ (6.8.09).

[24] Vaisala Remote Road Surface State Sensor DSC111. Product specifications. http://www.vaisala.com/weather/products/weatherinstruments/surfacesensors/surfacestatesensor (23.12.08).

[25] Home page for Destia's Varo service (road condition warnings). In Finnish. http://www.varopalvelu.fi (1.1.09)

[26] Myllylä J. and Pilli-Sihvola, Y. 2002. Floating Car Road Weather Monitoring. 11th International Road Weather Conference, Sapporo. 8 pp.

[27] Kytö, M., Erkkilä, K and Nylund, N. 2009. Heavy-duty vehicles: Safety, environmental impacts and new technology, RASTU. Summary report 2006–2008. VTT Project Report, 2 June 2009. http://www.motiva.fi/files/2279/RASTU_Summary_Report_2006-2008.pdf (18.9.2009).

[28] Elman, U. 2008. Novel cost-effective IR-based remote ice detection system allows extensive deployment. Transport Research Arena Europe 2008, Ljubljana.

[29] Yamada, M., Ueda, K., Horiba, I. and Sugie, N. 2001. Discrimination of the Road Condition Toward Understanding of Vehicle Driving Environments. IEEE Transactions on Instrumentation and Measurement, Vol. 2, No. 1, March 2001.

[30] Gustafsson, F. 1998. Estimation and change detection of tire-road friction using the wheel slip. IEEE Control System Magazine, 18(4):42–49, 1998.

[31] Andersson, M., Bruzelius, F., Casselgren, J., Gäfvert, M., Hjort, M., Hultén, J., Håbring, F., Klomp, M., Olsson, G., Sjödahl, M., Svendenius, J., Woxneryd, S. and Wälivaara, B. 2007. Road Friction Estimation. IVSS Project Report.

[32] Canudas-de-Wit, C., Petersen, M. L. and Shiriaev, A. 2003. A new nonlinear observer for tire/road distributed contact friction. Proceedings of the 42nd IEEE Conference on Decision and Control, Manui, Hawaii USA, December, 2003, pp. 2246–2251.

[33] Umeno, T. 2003. Estimation of Tyre–road Friction by Tyre Rotational Vibration Model. R&D Reviews of Toyota CRDL, Vol. 37, No.3 2003.

[34] Continental Corporation. 1999. The ”Intelligent” Tire Press Release. http://www.conti-online.com/generator/www/com/en/continental/portal/themes/press_services/press_releases/products/automotive_systems/brakesystems/pr_1999_09_10_6_en.html (29.12.08).

[35] Brandt, M., Bachmann, V., Vogt, A., Fach, M., Mayer, K., Breuer, B. and Hartnagel, H.L. 1998. Highly sensitive AlGaAs/GaAs position sensors for measurement of tyre tread deformation. IEEE Electronics Letters, Volume 34, Issue 8.

[36] Pohl, A., Steindl, R. and Reindl, L. 1999. "The 'Intelligent Tire' Utilizing Passive SAW Sensors – Measurement of Tire Friction," IEEE Trans. Instrum. Meas., vol. 48, pp. 1041–1046, Dec. 1999.

[37] AudiWorld web site. Audi allroad Quattro concept. 2005. http://www.audiworld.com/news/05/naias/aaqc/content5.shtml (9.2.2009).

[38] Viikari, V., Varpula, T. and Kantanen, M. Road condition recognition using 24 GHz automotive radar. 2009. IEEE Transactions on Intelligent Transportation Systems. In press. Vol. 10 (2009) No: 2.

[39] J. Casselgren. 2007. Road surface classification using near infrared spectroscopy. Licentiate thesis. Dept. Appl. Physics and Mech. Eng., Luleå Univ. of Tech, Luleå, Sweden.

[40] Casselgren, J., Kutila, M. and Jokela, M. 2009. Road surface classification using methods of polarised light. IEEE Transaction on Intelligent Transportantion Systems, Special Issue on ITS and Road Safety. Revised on 27 Oct. 2009.

[41] Ibeo LUX technical data. http://www.ibeo-as.com/english/products_ibeolux.asp (19.1.09).

[42] Schulz, R. and Fürstenberg, K. 2006. Laserscanner for Multiple Applications in Passenger Cars and Trucks. AMAA 2006, 10th International Conference on Advanced Microsystems for Automotive Applications, Berlin.

[43] Ibeo. 2009. Bad weather performance with Ibeo laserscanners. http://www.ibeo-as.com/english/technology_d_badweather.asp (28.8.2009).

[44] Hecht, E. 1998. Optics. Addison Wesley, U.S.A.

[45] Jokela, M., Kutila, M. and Le, L. 2009. Road Condition Monitoring System Based on a Stereo Camera. Proceedings of the 2009 IEEE 5th International Conference on Intelligent Computer Communication and Processing (IEEE ICCP). Cluj-Napoca, Romania. 27–29 Aug. 2009. pp. 423–428.

[46] Tuononen, A. 2009. Optical Position Detection to Measure Tyre Carcass Deflections and Implementation for Vehicle State Estimation. Dissertation, Helsinki University of Technology. http://lib.tkk.fi/Diss/2009/isbn9789522482501 (19.1.2010).

[47] Tuononen, A. and Hartikainen L. 2008. Optical Position Detection Sensor to Measure Tyre Carcass Deflections in Aquaplaning. International Journal of Vehicle Systems Modelling and Testing 2008, Vol. 3, No. 3 pp. 189–197. Inderscience.

[48] Hall, D. 1992. Mathematical Techniques in Multisensor Data Fusion, Artech House, Inc., Norwood.

[49] Park, S. 2007. Final report of ProFusion2 project. PReVENT subproject deliverable D15.12.

[50] Wedin, O. et al. 2009. Data Fusion - Road Weather. ROADIDEA EU project deliverable 3.3. Available online at http://www.roadidea.eu/documents/Knowledge%20Base/ROADIDEA%20D3.3%20Data%20fusion%20-%20road%20weather%20V1.pdf (19.12.2009).

[51] W.R. Pasterkamp. 1997. The Tyre as Sensor to Estimate Friction. Ph.D. Thesis. Delft University Press.

[52] Gustafsson, F. 2009. Automotive Safety Systems. IEEE Signal Processing Magazine, July 2009.

[53] H. B. Pacejka. 2006. Tyre and vehicle dynamics. Second edition. ISBN-13: 980-0-7506-6918-4.

[54] Mäkinen, T. ed. 2008. Final Report of PReVENT subproject APALACI. http://www.prevent-ip.org/en/public_documents/deliverables/d5010_b_-_apalaci_final_report.htm (8.4.09).

[55] Volvo cars press release 5 September 2008. Volvo City Safety cuts insurance premiums. http://www.volvoclub.org.uk/press/releases/2008/city_safe.shtml (15.1.09).

[56] Walessa, M. ed. 2008. COMPOSE project final report. PReVENT SP deliverable D51.11. http://www.prevent-ip.org/download/deliverables/COMPOSE/PR-51110-SPD-080213-v11-D51.11.pdf (14.2.09).

[57] DARPA Grand Challenge home page. http://www.darpa.mil/grandchallenge/index.asp (16.3.09).

[58] Koren, Y. & Borenstein, J. 1991. Potential Field Methods and Their Inherent Limitations for Mobile Robot Navigation. Proceedings of the IEEE International Conference on Robotics and Automation Sacramento, California, April 7–12. pp. 1398–1404. http://www-personal.umich.edu/~johannb/Papers/paper27.pdf (22.2.09).

[59] Kelly, A. 1995. An Intelligent Predictive Control Approach to the High Speed Cross Country Autonomous Navigation Problem. Dissertation. The Robotics Institute, Carnegie Mellon University.

[60] Simmons, R. 1996. The Curvature-Velocity Method for Local Obstacle Avoidance. Proceedings of the IEEE International Conference on Robotics and Automation, pp. 3375–3382, Minneapolis MN, April 1996.

[61] Koskinen, S. 2000. Route tracking for service robots using natural landmarks. Proceedings of EUREL European Advanced Robotics Systems Masterclass and Conference – Robotics 2000. University of Salford. Vol. 2 (2000), 8 pp.

[62] Virtanen, A., Koskinen, S. and Peussa, P. 2001. Navigation system using natural landmarks FSR2001. 3rd International Conference on Field and Service Robotics. Espoo, FI, 11–13 June 2001. Finnish Society of Automation; Helsinki University of Technology.

[63] Kämpchen, N. 2007. Feature-Level Fusion of Laser Scanner and Video Data for Advanced Driver Assistance Systems. Dissertation, Ulm University.

[64] Seiler, P., Song, B. and Hedrick, J. 1998. Development of a Collision Avoidance System. University of California-Berkeley. Society of Automotive Engineers. http://vehicle.me.berkeley.edu/Publications/AVC/pseil_sae98.pdf (17.3.09).

[65] Naik, A. 2005. Arc Path Collision Avoidance Algorithm for Autonomous Ground Vehicles. Master's thesis, Virginia Polytechnic Institute and State University. http://scholar.lib.vt.edu/theses/available/etd-01162006-112326/unrestricted/AnkurThesis.pdf (22.3.09).

Sami Koskinen. Sensor Data Fusion Based Estimation of Tyre. Road Friction to Enhance Collision Avoidance. VTT Publications 730.

Errata

p. 17: Electronic control systems like ABS and ESC participate in the vehicle control only when ~~the maximum friction is exceeded~~ *there is already large slip*.

p. 48, a clarification due to a vague referral to a project report: “Figure 9 shows an exemplar *classification by VTEC (Johan Casselgren)* from a test track measurement with four road conditions: dry asphalt, water, ice and snow. *A VTEC’s classifier was also used in the final sensor fusion sofware implementation of this study.*”

p. 55, repeating a reference: “In addition to vehicle and tyre state estimation, the optical sensor can be used in validating tyre models *(see [46]).*”

p. 62, background: To achieve this, a modular architecture was used.
A modular structure was an early decision together by the FRICTI@N project partners to cluster the sensors and also to distribute work between partners based on the sensors they were working with. In the beginning of the project, VDO (Thomas Haas) named the modules “subsystems” and suggested a data flow based on friction outputs. Later, as the author continued with the overall and environmental–vehicle fusion development, the final architecture, its data flow and naming was revised according to the presented fusion implementation and methods.

p. 65, clarification on input data: Figure 20. MATLAB Simulink top level view of implemented software. The data acquisition *from the development vehicle sensors* on the left, *provided by IKA, and author’s* friction processing in the middle, running 100 Hz.

p. 72. Table 6. Some required system parameters, *revised from project’s original input list.*

p. 100. The vehicle features, *as informed by IKA*, are summarised below:

p. 175, clarification on tests: The friction estimation ~~system has~~ *methods have* been tested *using the FRICTI@N project databank from* ~~on~~ dry, wet icy and snowy asphalt, *also once on an artificial slippery surface* ~~a few times on slushy asphalt~~, but not on dirt roads or gravel. *There have been environmental sensor changes during the collection of the databank. Therefore the work claims fusion methods while the collected performance results are indicative.* ~~When driving in test areas~~ *In test data and driving tests* the system provided friction potential estimates with an error mostly within 0.2, compared to reference values measured in peak braking tests.

Appendix A

The following MATLAB code was used as an example in Chapter 7, Collision Avoidance and Mitigation. It calculates the collision avoidance database for defined values of initial speed, initial curvature and friction potential.

```
% Collision avoidance database generation

plot_trajectory = 0; % for tests and plotting
plot_car = 0; % for tests and plotting
% vehicle parameters
Vehicle_width = 2.03; % with mirrors
Vehicle_length = 4.92;
Vehicle_L = 2.84; % wheelbase
Vehicle_rear = -1.09; % from rear axle
Vehicle_front = Vehicle_length-1.09; % from rear axle
Vehicle_inertia = 3585; % kgm^2
Vehicle_mass = 2188; % kg
g = 9.81;
CvA = 2.2 * 0.3; % estimate, drag coefficient * area
pii = 3.14159265;
pii_half = 1.57079632; % intentionally not exaxt
Vehicle_max_acceleration = 4; % forward acceleration simplified: 7 seconds
from 0 to 100 km/h
Vehice_longitudinal_force_delay = 100; % quick implementation of brak-
ing/acceleration delay, reaches any value in 0.1 sec or under; max pro-
duced longitudinal acceleration change / sec
Vehice_lateral_force_delay = 100; % quick implementation of steering de-
lays, reaches any value in 0.1 sec or under; max produced lateral accel-
eration change / sec
simulation_upper_speed_limit = 130; % km/h
simulation_lower_speed_limit = -20;
velocity = [simulation_lower_speed_limit:10:simulation_upper_speed_limit];
% must have several (now size 16), as start speed otherwise has an error
velocity_ms = velocity./3.6;
min_turning_radius = 11.00/2-Vehicle_width/2; % calculated from outer
wheel curb to curb value
steering_angle_max = 0.5645; % radians, results in min_turning_radius
% Initial virtual steering angles to represent curvatures. Avoid having
too many (now size 33). Should be non-linear: more angles near 0.
initial_steering_angles = [0.5645 0.5081 0.4516 0.3952 0.3387 0.2823
0.2258 0.1694 0.1129 0.0988 0.0847 0.0706 0.0565 0.0423 0.0282 0.0141 0 -
0.0141 -0.0282 -0.0423 -0.0565 -0.0706 -0.0847 -0.0988 -0.1129 -0.1694 -
0.2258 -0.2823 -0.3387 -0.3952 -0.4516 -0.5081 -0.5645];
turning_radiuses = Vehicle_L.*tan(pii_half-initial_steering_angles);

% x,y grid where collisions are checked.
x_up_near = [-28:0.3:28]+0.1; % +0.1 to move grid so that straight driving
can be checked better
y_up_near = [Vehicle_front+0.16:0.3:34.59];
x_up_far = [-28:2:28];
y_up_far = [34.59+1:2:75.59];
y_down_near = [Vehicle_rear-0.26:-0.5:-14.35];
x_down_near = [-28:0.5:28];
y_left_near = [Vehicle_rear-0.03:0.3:3.68];
```

```
y_right_near = y_left_near;
x_left_near = [-27.575:0.3:-1.175];
x_right_near = [1.175:0.3:27.575];

% ------------ TABLE INIT --------------
dt = 0.005; % step size for trajectory calculation [s], default 0.005
time = 0;

% ********* TABLE INDEX VALUES (the 3 key values to identify the table.
For each set we need to calculate a new table)
friction_potential_acc = 1*g; % [m/s^2] friction potential as acceleration
[0.1:0.1:1]
initial_velocity = velocity_ms(9); % the velocity which we use to enter
the situation
index_entry_angle = 17; % 17 middle
% *********

entry_angle = pi/2+initial_steering_angles(index_entry_angle); en-
try_radius = turning_radiuses(index_entry_angle); % first radius

% target values, fixed amount of angles and varying size of target veloci-
ties
% 2 second braking or acceleration is max during this simulation, in the
calculation max change ~100 km/h, 5 km/h steps with high friction
reachable_velocity_min = max((simulation_lower_speed_limit-5)/3.6, ini-
tial_velocity-2*friction_potential_acc);
if (reachable_velocity_min < 0 && initial_velocity > 0)
 time_to_0 = initial_velocity/friction_potential_acc;
 reachable_velocity_min = max((simulation_lower_speed_limit-5)/3.6,
 0-(2-time_to_0)*Vehicle_max_acceleration);
elseif (reachable_velocity_min < 0 && initial_velocity <= 0)
 reachable_velocity_min = max((simulation_lower_speed_limit-5)/3.6,
 initial_velocity-2*Vehicle_max_acceleration);
end;
reachable_velocity_max = min((simulation_upper_speed_limit+5)/3.6, ini-
tial_velocity+2*min(Vehicle_max_acceleration,friction_potential_acc));
if (reachable_velocity_max > 0 && initial_velocity < 0)
 time_to_0 = abs(initial_velocity/friction_potential_acc);
 reachable_velocity_max = min((simulation_upper_speed_limit+5)/3.6,
 0+(2-time_to_0)*min(Vehicle_max_acceleration,friction_potential_acc));
end;

% scaled number of target velocities, initial velocity as the starting
% point
target_velocities = sort([[initial_velocity:-5/3.6:reachable_velocity_min]
[initial_velocity+5/3.6:5/3.6:reachable_velocity_max]]);
if (length(target_velocities) > 15)
 target_velocities = sort([[initial_velocity:
 -6/3.6:reachable_velocity_min]
 [initial_velocity+6/3.6:6/3.6:reachable_velocity_max]]);
end;
if (length(target_velocities) < 10)
 target_velocities = sort([[initial_velocity:
 -4/3.6:reachable_velocity_min]
 [initial_velocity+4/3.6:4/3.6:reachable_velocity_max]]);
end;
reachable_velocity_min = target_velocities(1);
reachable_velocity_max = target_velocities(length(target_velocities));

% scaled number of targeted steering angles (curvatures), based on fric-
tion use and minimum reachable speed
```

```
max_steering_radius_based_on_friction=reachable_velocity_min^2/friction_po
tential_acc;
max_steering_angle_based_on_friction=
abs(atan(max_steering_radius_based_on_friction/Vehicle_L)-pii_half);

target_steering_angles = [steering_angle_max:-steering_angle_max/13:
-steering_angle_max]; % Target steering angle initialization. The more,
the better.
% reshaping steering angles, more angles required near 0
target_steering_angles = [target_steering_angles(1,1:8) tar-
get_steering_angles(1,9):-steering_angle_max/26: tar-
get_steering_angles(1,27-8) target_steering_angles(1,27-7:
length(target_steering_angles)) ];
% reshaping steering angles if maximum allowed steering angle is smaller
% due to low friction or high speed
if (max_steering_angle_based_on_friction < 0.45 && reachable_velocity_min
> 0)
 target_steering_angles = [max_steering_angle_based_on_friction:
 -max_steering_angle_based_on_friction/13:
 -max_steering_angle_based_on_friction];
 if max_steering_angle_based_on_friction > 0.08 % otherwise enough
  target_steering_angles = [target_steering_angles(1,1:8)
  target_steering_angles(1,9):
  -max_steering_angle_based_on_friction/26:target_steering_angles(1,27-8)
  target_steering_angles(1,27-7:length(target_steering_angles)) ];
 end;
elseif initial_velocity >= (60/3.6) % check if high speed (and high fric-
tion)
 target_steering_angles = [steering_angle_max:-steering_angle_max/10:
 -steering_angle_max];
 target_steering_angles = [target_steering_angles(1,1:7)
 target_steering_angles(1,8):-steering_angle_max/40:
 target_steering_angles(1,21-7) target_steering_angles(1,21-6:
 length(target_steering_angles)) ];
end;

% TO BE SAVED AFTER CALCULATION:
% x-y index for data. The index contains a number for each x,y pair. The
number is of format location_in_data*1000+size
% data file is a 4*n table consisting of several
% [index for target_steering, index for target_speed, ttc1, ttc2]
index_up_far = zeros(length(x_up_far),length(y_up_far));
data_up_far = zeros(4,1); % init
index_up_near = zeros(length(x_up_near),length(y_up_near));
data_up_near = zeros(4,1); % init
index_left_near = zeros(length(x_left_near),length(y_left_near));
data_left_near = zeros(4,1); % init
index_right_near = zeros(length(x_right_near),length(y_right_near));
data_right_near = zeros(4,1); % init
index_down_near = zeros(length(x_down_near),length(y_down_near));
data_down_near = zeros(4,1); % init
% ttc index which shows the target_steering, target_velocity pairs not
% reachable
ttc_index =
2*ones(length(target_steering_angles),length(target_velocities));

% algorithm internal check for invalid inputs, also radius must not be 0
entry_friction = abs((initial_velocity*initial_velocity)/entry_radius)
if entry_friction > 10
 error = entry_friction
end;
```

```
% otherwise, allow even some potential slip in the beginning
% ------------ TABLE INIT END --------------

% plotting handles only one trajectory at a time (not the loop)
if plot_trajectory == 1
 incr_x = [0]; incr_y = [0];
 plot(0,0,'x');
 hold;
end;

% ------------ LOOP BEGIN ------------------
for index_velocity = 1:length(target_velocities)
 for index_steering_angle = 1:length(target_steering_angles)
  progress = [index_velocity length(target_velocities)
  index_steering_angle length(target_steering_angles)] % output
  if (plot_trajectory > 0)
   index_velocity = 11; %
   index_steering_angle = 20; % 19 middle
   target_steering_angle = target_steering_angles(index_steering_angle)
   if (plot_trajectory == 2)
    return;
   end;
   plot_trajectory = 2;
  end;

  % INIT
  prev_velocity = initial_velocity;
  start_friction = entry_friction;
  prev_angle = pi/2;
  prev_radius = entry_radius;

  prev_longitudinal_acceleration = 0; % init for delay calculation
  prev_lateral_acceleration = 0; % init for delay calculation, does not
  include centrifugal force

  target_velocity = target_velocities(index_velocity); % for all v
  % for all angles
  target_steering_angle = target_steering_angles(index_steering_angle);
  target_radius = Vehicle_L*tan(pii_half-target_steering_angle);

  Air_resistance_target = 0.5 * 1.2 * CvA * target_velocity *
  target_velocity;
  Air_deceleration_target = (abs(Air_resistance_target)) / (Vehicle_mass *
  g);
  target_friction_acc = sqrt(Air_deceleration_target^2 +
  abs((target_velocity*target_velocity)/target_radius)^2)

  % handle trajectory as incremental
  incremental_trajectory_x = 0;
  incremental_trajectory_y = 0;

  if target_friction_acc > friction_potential_acc+0.1
   % cannot be reached, skip calculating this combination
   ttc_index(index_steering_angle,index_velocity)=0; % mark not reachable
   continue;
  end;

  % loop while time < 2 seconds
  for time = 1:(2/dt)
   lat_friction_centrifugal =
   abs((prev_velocity*prev_velocity)/prev_radius);
```

```
if (lat_friction_centrifugal > friction_potential_acc && start_friction
< friction_potential_acc) % increment overshoot
 lat_friction_centrifugal = friction_potential_acc;
end;

Air_resistance = 0.5 * 1.2 * CvA * prev_velocity * prev_velocity;
Air_deceleration = (abs(Air_resistance)) / (Vehicle_mass * g);
if (prev_velocity < 0) % different direction when reversing
 Air_deceleration =  -Air_deceleration;
end;

w_target = pii*(prev_velocity/(pii*target_radius));
w_curr = pii*(prev_velocity/(pii*prev_radius)); % yaw rate
w_diff = w_target-w_curr;
% rotational energy, keeping also sign
Er_target = 1/2*Vehicle_inertia*(w_target*w_target)*sign(w_target);
Er_curr = 1/2*Vehicle_inertia*(w_curr*w_curr)*sign(w_curr);

velocity_diff = target_velocity - prev_velocity;
max_long_acceleration = 0; % init
lat_acceleration = 0; % init

if (target_velocity < 0 && prev_velocity > 0) || (target_velocity > 0
&& prev_velocity < 0)
 % Different velocity signs. Strategy: first brake without turning.
 curr_radius = prev_radius;
 if velocity_diff > 0
  max_long_acceleration = sqrt(friction_potential_acc^2 -
  lat_friction_centrifugal^2); % full friction use
  if (lat_friction_centrifugal > friction_potential_acc) % sliding
  approximation
   max_long_acceleration = 1;
  end;
  if (abs(max_long_acceleration - prev_longitudinal_acceleration)/dt) >
  Vehice_longitudinal_force_delay % braking/acceleration delay
  implementation
   max_long_acceleration = sign(max_long_acceleration -
   prev_longitudinal_acceleration)*Vehice_longitudinal_force_delay*dt +
   prev_longitudinal_acceleration;
  end;
  curr_velocity = prev_velocity - Air_deceleration*dt +
  max_long_acceleration*dt;
 elseif velocity_diff < 0
  max_long_acceleration = sqrt(friction_potential_acc^2 -
  lat_friction_centrifugal^2); % full friction use
  if (lat_friction_centrifugal > friction_potential_acc) % sliding
  approximation
   max_long_acceleration = 1;
  end;
  if (abs(max_long_acceleration - prev_longitudinal_acceleration)/dt) >
  Vehice_longitudinal_force_delay % braking/acceleration delay
  implementation
   max_long_acceleration = sign(max_long_acceleration -
   prev_longitudinal_acceleration)*Vehice_longitudinal_force_delay*dt +
   prev_longitudinal_acceleration;
  end;
  curr_velocity = prev_velocity - Air_deceleration*dt -
  max_long_acceleration*dt;
 else
  max_long_acceleration = Air_deceleration;
  curr_velocity = prev_velocity; % assumes Air_deceleration always
```

```
 below friction potential
end;
w_new = pii*(curr_velocity/(pii*prev_radius));
else
% strategy: friction potential shared half between longitudinal and
lateral, as long as final curvature and speed have not been reached
temp_prevent_lateral_acceleration = 0;
if velocity_diff > 0
 if (lat_friction_centrifugal > friction_potential_acc) % sliding
  max_long_acceleration = 0;
 else
  if (w_diff > 0 || w_diff < 0)
   % remaining friction shared half (pot^2 = (centrif+x)^2+x^2), but
   taking vehicle perfomance into account. This can be unoptimal at
   times, starting to turn too early.
   temp_a = (2*lat_friction_centrifugal + sqrt(
   (2*lat_friction_centrifugal)^2 + 8*(friction_potential_acc^2-
   lat_friction_centrifugal^2) )) / -4;
   temp_b = (2*lat_friction_centrifugal - sqrt(
   (2*lat_friction_centrifugal)^2 + 8*(friction_potential_acc^2-
   lat_friction_centrifugal^2) )) / -4;
   temp_c = max(temp_a,temp_b);
   max_long_acceleration = min(Vehicle_max_acceleration, temp_c);
  else
   max_long_acceleration = min(Vehicle_max_acceleration,
   % full friction use
   sqrt(friction_potential_acc^2 - lat_friction_centrifugal^2));
  end;
  if (abs(max_long_acceleration - prev_longitudinal_acceleration)/dt)
  > Vehice_longitudinal_force_delay % braking/acceleration delay
  implementation
   max_long_acceleration = sign(max_long_acceleration -
   prev_longitudinal_acceleration)*Vehice_longitudinal_force_delay*dt
   + prev_longitudinal_acceleration;
  end;
 end;
 curr_velocity = prev_velocity - Air_deceleration*dt +
 max_long_acceleration*dt;
elseif velocity_diff < 0
 if (lat_friction_centrifugal > friction_potential_acc)
  max_long_acceleration = 1;
 else
  if (w_diff > 0 || w_diff < 0)
   if (sign(w_target) == sign(w_curr)) && (abs(w_target) >
   abs(w_curr))
    % Steering angle should increase while braking - this could lead
    into too high friction use and unable to reach target
    % First the vehicle should just brake
    if (sqrt(Air_deceleration_target^2 +
    abs((prev_velocity*prev_velocity)/target_radius)^2)) >
    (friction_potential_acc-0.05)
     max_long_acceleration = sqrt(friction_potential_acc^2 -
     lat_friction_centrifugal^2); % full braking while friction
     potential would be exceeded
     temp_prevent_lateral_acceleration = 1;
    else % brake more than turn, pot^2 = (0.5y + centrif)^2 + y^2
     temp_a = (lat_friction_centrifugal + sqrt(
     lat_friction_centrifugal^2 + 5*(friction_potential_acc^2-
     lat_friction_centrifugal^2) )) / -2.5;
     temp_b = (lat_friction_centrifugal - sqrt(
     lat_friction_centrifugal^2 + 5*(friction_potential_acc^2-
```

```
     lat_friction_centrifugal^2) )) / -2.5;
     max_long_acceleration = max(temp_a,temp_b);
    end;
   else
    % Remaining friction shared half. May start turning too early.
    temp_a = (2*lat_friction_centrifugal + sqrt(
    (2*lat_friction_centrifugal)^2 + 8*(friction_potential_acc^2-
    lat_friction_centrifugal^2) )) / -4;
    temp_b = (2*lat_friction_centrifugal - sqrt(
    (2*lat_friction_centrifugal)^2 + 8*(friction_potential_acc^2-
    lat_friction_centrifugal^2) )) / -4;
    max_long_acceleration = max(temp_a,temp_b);
   end;
  else
   max_long_acceleration = sqrt(friction_potential_acc^2 -
   lat_friction_centrifugal^2); % full friction use
  end;
  if (abs(max_long_acceleration - prev_longitudinal_acceleration)/dt)
  > Vehice_longitudinal_force_delay % braking/acceleration delay
   max_long_acceleration = sign(max_long_acceleration -
   prev_longitudinal_acceleration)*Vehice_longitudinal_force_delay*dt
   + prev_longitudinal_acceleration;
  end;
 end;
 curr_velocity = prev_velocity - Air_deceleration*dt -
 max_long_acceleration*dt;
else
 max_long_acceleration = Air_deceleration;
 curr_velocity = prev_velocity;
end;

% Uses remaining friction potential for lateral acceleration
if (w_diff > 0 || w_diff < 0)
 if (lat_friction_centrifugal > friction_potential_acc &&
 start_friction > friction_potential_acc) % uses more friction than is
 available
  curr_velocity = prev_velocity - Air_deceleration*dt; % do not
  accelerate/brake after all
  lat_acceleration = 2; % just an approximation for straightening when
  sliding
 else
  start_friction = 0; % not sliding any more
  lat_acceleration = sqrt(friction_potential_acc^2 -
  max_long_acceleration^2) - lat_friction_centrifugal;
  if (abs(lat_acceleration - prev_lateral_acceleration)/dt) >
  Vehice_lateral_force_delay % steering delay implementation
   lat_acceleration = sign(lat_acceleration -
   prev_lateral_acceleration)*Vehice_lateral_force_delay*dt +
   prev_lateral_acceleration;
  end;
 end;
 % reaching new rotational velocity
 if temp_prevent_lateral_acceleration == 0 && (lat_acceleration > 0 ||
 lat_acceleration < 0)
  time_to_new_rotational_velocity = abs(Er_target -
  Er_curr)/(Vehicle_mass*lat_acceleration*Vehicle_L/2); % divided with
  mass*acc*distance
  if (time_to_new_rotational_velocity < dt)
   w_new = w_target; % approximation for velocity since it is not
   changed
   curr_radius = target_radius;
```

```
    else
     w_new = w_curr + dt/time_to_new_rotational_velocity  * w_diff;
     curr_radius= prev_velocity/w_new;
    end;
   else
    w_new = pii*(curr_velocity/(pii*prev_radius));
    curr_radius = prev_radius;
    lat_acceleration = 0;
   end;
  else
   w_new = w_target;
   curr_radius = target_radius;
  end;
end;

% algorithm always needs a radius
if curr_radius == 0
 curr_radius = 9999999999999999999;
end;
curr_angle = prev_angle+w_new*dt;

% prepare for new loop
prev_velocity = curr_velocity;
prev_radius = curr_radius;
prev_angle = curr_angle;
prev_longitudinal_acceleration = max_long_acceleration;
prev_lateral_acceleration = lat_acceleration;

incremental_trajectory_x = incremental_trajectory_x
+dt*curr_velocity*cos(curr_angle);
incremental_trajectory_y = incremental_trajectory_y
+dt*curr_velocity*sin(curr_angle);

% plotting at end of loop, requires only one trajectory at a time
if (plot_trajectory > 0)
 incr_x = [incr_x incremental_trajectory_x]; incr_y = [incr_y
 incremental_trajectory_y];
 plot(incremental_trajectory_x,incremental_trajectory_y,'x');
end;

% calculation for reachable distances and velocities, plus plotting
x_front_left = incremental_trajectory_x + Vehicle_front*cos(curr_angle)
- (Vehicle_width/2)*sin(curr_angle);
x_front_right = incremental_trajectory_x +
Vehicle_front*cos(curr_angle) + (Vehicle_width/2)*sin(curr_angle);
x_rear_left = incremental_trajectory_x + Vehicle_rear*cos(curr_angle) -
(Vehicle_width/2)*sin(curr_angle);
x_rear_right = incremental_trajectory_x + Vehicle_rear*cos(curr_angle)
+ (Vehicle_width/2)*sin(curr_angle);
y_front_left = incremental_trajectory_y + Vehicle_front*sin(curr_angle)
+ (Vehicle_width/2)*cos(curr_angle);
y_front_right = incremental_trajectory_y +
Vehicle_front*sin(curr_angle) - (Vehicle_width/2)*cos(curr_angle);
y_rear_left = incremental_trajectory_y + Vehicle_rear*sin(curr_angle) +
(Vehicle_width/2)*cos(curr_angle);
y_rear_right = incremental_trajectory_y + Vehicle_rear*sin(curr_angle)
- (Vehicle_width/2)*cos(curr_angle);

if (time == (2/dt)) % at the end of simulation, check if target
velocity and steering was reached
 if (abs(velocity_diff) >  2/3.6) || (w_diff > 0.01) % give some extra
```

```
  ttc_index(index_steering_angle,index_velocity)=0; % not reachable
 end;
end;

% plotting at end of loop, requires only one trajectory at a time
if (plot_car == 1)
 plot(x_front_left,y_front_left,'r');
 plot(x_front_right,y_front_right,'r');
 plot(x_rear_right,y_rear_right,'r');
 plot(x_rear_left,y_rear_left,'r');
 continue; % does not calculate collision table
end;


% ---------- COLLISION DETECTION START ---------------
% go through all the grids to calculate which cells are affected

% UP-NEAR
increase_location = 0; % loop assist, changing data index
prev_index = 0; % loop assist
for j = 1:length(x_up_near) % go through all X
 x_temp = x_up_near(j);
 for k = 1:length(y_up_near) % go through all Y
  y_temp = y_up_near(k);
  if index_up_near(j,k) > 0 % previous data exists
   index_up_near(j,k) = index_up_near(j,k)+increase_location*10000;
   prev_index = index_up_near(j,k);
  end;
  % collision check
  if (((incremental_trajectory_x-x_temp)^2 + (incremental_trajectory_y-
  y_temp)^2) < (Vehicle_front^2+0.3^2)) && 1 == collision(x_front_left,
  y_front_left,x_front_right,y_front_right,x_rear_left,
  y_rear_left,x_rear_right,y_rear_right,x_temp,y_temp,0.3) % COLLISION
  CHECK
   % collision has happened
   collision_data = [index_steering_angle, index_velocity, time*dt,
   time*dt]';

   if index_up_near(j,k) == 0 % no previous data exists, give correct
   index, keep the order
    index = floor(prev_index/10000);
    number_of_entries = prev_index-floor(prev_index/10000)*10000;
    index = index+number_of_entries; % new index
    number_of_entries = 0;
    if index == 0 % first
     index = 2;
    end;
    % concatenate data
    sizedata = size(data_up_near);
    if (index+number_of_entries-1) == sizedata(1,2) % already last
     data_up_near = [data_up_near collision_data];
    else % not last
     increase_location = increase_location + 1; % for future rounds
     data_up_near = [data_up_near(:,1:(index+(number_of_entries-1)))
     collision_data data_up_near(:,(index+number_of_entries):
     sizedata(1,2))];
    end;
    number_of_entries = number_of_entries +1;
    index_up_near(j,k) = index*10000+number_of_entries;
    prev_index = index_up_near(j,k);
```

```
      else
       % go through the data to possibly just increase ttc2
       found = 0;
       index = floor(index_up_near(j,k)/10000);
       number_of_entries = index_up_near(j,k)-
       floor(index_up_near(j,k)/10000)*10000;
       for z = index:index+(number_of_entries-1)
        if (data_up_near(1,z) == index_steering_angle && data_up_near(2,z)
        == index_velocity)
         found = 1;
         data_up_near(3,z) = min(data_up_near(3,z),time*dt);
         data_up_near(4,z) = max(data_up_near(3,z),time*dt);
        end;
       end;
       if found == 0 % have to add new data
        % concatenate data
        sizedata = size(data_up_near);
        if (index+number_of_entries-1) == sizedata(1,2) % already last
         data_up_near = [data_up_near collision_data];
        else % not last but in the middle
         increase_location = increase_location + 1; % for future rounds
         data_up_near = [data_up_near(:,1:(index+(number_of_entries-1)))
         collision_data data_up_near(:,(index+number_of_entries):
         sizedata(1,2))];
        end;
        number_of_entries = number_of_entries +1;
        index_up_near(j,k) = index*10000+number_of_entries;
       end;
      end;
     end;
    end;
   end;

   % UP-FAR
   % LEFT-NEAR
   % RIGHT-NEAR
   % DOWN-NEAR
   % code removed since it can be copied from above by updating only the
   table names


   % ---------- COLLISION DETECTION END -----------------

  end;
 end;
end;
% ------------ LOOP ENDS ------------------
```

To use the T-CVM result tables in implementing collision avoidance strategies, the following steps are required:

1. Select the set of look-up tables from memory (the data structure has been presented in Figure) that match the current friction potential, vehicle velocity and curvature (constituting the main index).

2. The T-CVM result table is initialized with a pre-calculated table of reachable velocity and curvature combinations, also retrieved using the main index.

3. For each obstacle co-ordinate (co-ordinates can be optionally filtered to match occupancy grid accuracy), calculate the relative distance and direction to the obstacle from ego vehicle origin. These co-ordinates are next checked against the areas covered by the occupancy grids (e.g. up_near and right_near grids).

4. The location of TTC data is retrieved for the relative co-ordinates of the obstacle, using an index found from the occupancy grid cell, that the obstacle was mapped to:

```
data_location = index_up_near(x,y);
graph_index = floor(data_location/10000);
graph_number_of_entries = data_location-floor(data_location/10000)*10000;
```

5. The TTC data is then added to the current T-CVM result table, possibly overwriting the current values with smaller values. This completes the T-CVM result table for main index used. Several tables can be calculated when analysing steering options with different levels of friction use.

```
for i = graph_index:(graph_index+graph_number_of_entries-1)
   j = data_up_near(1,i);
   ii = data_up_near(2,i);
   if result(j,ii) > 0 % can reach this combination during next 2 seconds
      % Next, compare data_up_near(3,i) and data_up_near(4,i) with the
      % time that the cell is occupied by an obstacle.
      % Static obstacles are always added.
      result(j,ii) = min(result(j,ii), data_up_near(3,i)); % static
   end;
end;
```

6. An initial target curvature and velocity are selected based on navigation goals. The current values or the driving direction before starting an avoidance manoeuvre can also be used. The TTC value for the initial curvature and velocity is read from the T-CVM result table.

7. If the collision avoidance is already performing a manoeuvre, for example the closest non-colliding steering combination to the initial values can be selected as the target. Several preferences and strategies can be involved in selecting the values, i.e. how to avoid the obstacle. The desired values of velocity and curvature will be inputted to separate control algorithms to execute.

   If the avoidance or mitigation has not been initiated, several checks can be performed on the TTC values in the T-CVM result table, for timing the actions. Three different strategies and checks have been presented in Chapter 7.3.2. For example, the avoidance can be activated when the current TTC drops below the maximum value (2 seconds in the example code).

   Advanced strategies require also moving the vehicle co-ordinates forward on its current trajectory e.g. to estimate the moment when collisions become unavoidable.

Series title, number and report code of publication

VTT Publications 730
VTT-PUBS-730

Author(s)
Sami Koskinen

Title

Sensor Data Fusion Based Estimation of Tyre–Road Friction to Enhance Collision Avoidance

Abstract

Vehicle steering, braking and acceleration are subject to friction forces arising from contact of the tyres with the road surface. The contact force is both enabling and limiting. The ratio of the contact friction to the force of the tyres pressing on the road surface is described as the coefficient of friction. The maximum coefficient of friction for different surfaces characterizes the extent of tyre grip.

Collision avoidance and collision mitigation systems require information on tyre grip so as to accurately calculate braking distances and evasive manoeuvres. Estimating road slipperiness (skid resistance) during driving has however proven difficult.

This dissertation discusses estimating the maximum coefficient of friction (herein referred to as the friction potential) together with determining road conditions. Both estimations are based on multi-sensor data fusion; that is, combining data from several sensors. The presented sensor data fusion utilizes various sensors from three main classes: 1) environmental sensors, 2) sensors measuring vehicle dynamics and 3) experimental tyre sensors. This work concentrates particularly on methods for combining measurements of vehicle dynamics with environmental sensor readings; for example, wheel speed signals are linked to readings about ice, snow or water on the road.

The methods were incorporated into a prototype passenger car implementation, where testing yielded a reliable estimate of friction potential for approximately 90% of driving time. The estimate of friction potential was then within 0.2 of reference values measured in braking tests. These results encapsulate a proof of concept on asphalt roads in some wet, snowy, icy and dry road conditions.

The advantages of friction estimation for collision avoidance and collision mitigation systems are analysed using mainly simulations. A correct initial estimate of the friction potential enables the systems to improve traffic safety efficiently also in slippery road conditions. However, the range of available environmental sensors does not cover long braking distances.

Together with the simulations, the work introduces a new method for collision avoidance calculations and timing the activation of collision mitigation. The method is based on a large number of precalculated vehicle trajectories.

ISBN
978-951-38-7382-0 (soft back ed.)
978-951-38-7383-7 (URL: http://www.vtt.fi/publications/index.jsp)

Series title and ISSN	Project number
VTT Publications 1235-0621 (soft back ed.) 1455-0849 (URL: http://www.vtt.fi/publications/index.jsp)	4066

Date	Language	Pages
February 2010	English, Finnish abstr.	188 p. + app. 12 p.

Name of project	Commissioned by
FRICTI@N (FP6-IST-2004-4-027006)	European Commission

Keywords	Publisher
Friction, sensor, data fusion, collision avoidance, collision mitigation, environmental sensing, tyre, road, conditions, trajectory, curvature-velocity, ADAS	VTT Technical Research Centre of Finland P. O. Box 1000, FI-02044 VTT, Finland Phone internat. +358 20 722 4520 Fax +358 20 722 4374

Julkaisun sarja, numero ja raporttikoodi

VTT Publications 730
VTT-PUBS-730

Tekijä(t)
Sami Koskinen

Nimeke

Anturidatafuusioon perustuva renkaan ja tien välisen kitkan estimointi ja tulosten hyödyntäminen törmäyksenestossa

Tiivistelmä

Renkaiden ja tien välinen liikettä vastustava voima, kitka, asettaa rajat ajoneuvon ohjaukselle, jarrutukselle ja kiihdytykselle. Se on samalla sekä mahdollistava että rajoittava kontaktivoima. Kitkan ja renkaita tietä vasten puristavan voiman suhde ilmaistaan kitkakertoimella. Kitkakertoimen maksimiarvo eri pinnoilla kuvaa renkaiden pitävyyttä.

Kehitteillä oleviin törmäyksiä estäviin ja törmäysenergiaa lieventäviin kuljettajan tukijärjestelmiin tarvitaan tietoa renkaiden pitävyydestä, jotta jarrutusmatkoja ja väistömahdollisuuksia voidaan arvioida entistä tarkemmin. Tien liukkauden määrittäminen ennalta ajon aikana, ilman renkaiden selkeää luistoa, on kuitenkin osoittautunut hankalaksi.

Tämä väitöstyö käsittelee kitkakertoimen maksimiarvon, tässä kitkapotentiaalin, ja kelitietojen määrittämistä. Tutkimuksessa hyödynnetään anturidatafuusiota eli useiden antureiden tuottamien tietojen yhdistämistä. Anturidatafuusiossa käytetyt anturit edustavat kolmea päätyyppiä: 1) ympäristöä havainnoivat anturit, 2) auton liiketilaa mittaavat anturit ja 3) rengasantureiden prototyypit. Työssä keskitytään erityisesti menetelmiin, joilla voidaan yhdistää ajoneuvon liiketilan mittaustietoja ympäristöä havainnoivien antureiden tuottamiin tietoihin. Esimerkiksi renkaiden pyörimisnopeuksista saatuja tietoja yhdistetään tietoihin tiellä olevasta jäästä, lumesta tai vedestä.

Esitellyillä menetelmillä ja henkilöautoon toteutetulla prototyyppijärjestelmällä on testeissä kyetty arvioimaan kitkapotentiaalia luotettavasti noin 90 prosenttia ajoajasta. Tällöin kitkapotentiaalin arvio poikkeaa enintään 0,2 jarrutustesteillä mitatuista referenssiarvoista. Järjestelmää on testattu asfalttiteillä. Menetelmien toimivuus on todennettu joukolla märkiä, lumisia, jäisiä ja kuivia kelejä.

Kitka-arvion hyötyjä on analysoitu törmäyksiä estävissä ja törmäysenergiaa lieventävissä järjestelmissä pääasiassa simulaatiotuloksia käyttäen. Arvio kitkapotentiaalista auttaa näitä järjestelmiä parantamaan liikenneturvallisuutta tehokkaasti myös liukkailla keleillä. Kuitenkaan saatavilla olevien keliantureiden mittauskantama ei vielä kata pitkiä jarrutusmatkoja.

Tämä työ esittelee simulaatioiden yhteydessä uuden, lukuisiin ennalta laskettuihin liikeratoihin perustuvan nopean laskentamenetelmän törmäystilanteiden arviointiin ja esteiden väistöön.

ISBN
978-951-38-7382-0 (nid.)
978-951-38-7383-7 (URL: http://www.vtt.fi/publications/index.jsp)

Avainnimeke ja ISSN	Projektinumero
VTT Publications 1235-0621 (nid.) 1455-0849 (URL: http://www.vtt.fi/publications/index.jsp)	4066

Julkaisuaika	Kieli	Sivuja
Helmikuu 2010	Englanti, suom. tiiv.	188 s. + liitt. 12 s.

Projektin nimi	Toimeksiantaja(t)
FRICTI@N (FP6-IST-2004-4-027006)	Euroopan komissio

Avainsanat	Julkaisija
Friction, sensor, data fusion, collision avoidance, collision mitigation, environmental sensing, tyre, road, conditions, trajectory, curvature-velocity, ADAS	VTT PL 1000, 02044 VTT Puh. 020 722 4520 Faksi 020 722 4374

This dissertation discusses the estimation of maximum coefficients of friction between tyres and a road surface, together with the determination of road conditions. The estimation is based on sensor data fusion, combining data from three classes of sensors: environmental sensors, sensors measuring vehicle dynamics and experimental tyre sensors.

Upcoming collision avoidance and collision mitigation systems need information on tyre grip to further improve their calculations for braking distances and evasive manoeuvres. The advantages of friction estimation for collision avoidance and collision mitigation systems are analysed using simulations. A correct initial estimate of the maximum coefficient of friction supports the systems to efficiently improve traffic safety also in slippery road conditions.

ISBN 978-951-38-7382-0 (soft back ed.)
ISSN 1235-0621 (soft back ed.)

ISBN 978-951-38-7383-7 (URL: http://www.vtt.fi/publications/index.jsp)
ISSN 1455-0849 (URL: http://www.vtt.fi/publications/index.jsp)